

This is to certify that the

dissertation entitled

OXYGEN-LIGATED FE-S AND MO-FE-S CLUSTERS AS POSSIBLE MODELS OF NITROGENASE

presented by

Miriam Elaine Rogers

has been accepted towards fulfillment of the requirements for

Ph.D. degree in Chemistry

Date June 26, 1986

MSU is an Affirmative Action/Equal Opportunity Institution

0-12771



RETURNING MATERIALS:
Place in book drop to remove this checkout from your record. FINES will be charged if book is returned after the date stamped below.

4.

the water

OXYGEN-LIGATED FE-S AND MO-FE-S CLUSTERS AS POSSIBLE MODELS FOR NITROGENASE

Ву

Miriam Blaine Rogers

A DISSERTATION

Submitted to

Michigan State University

in partial fulfillment of the requirements

for the degree of

DOCTOR OF PHILOSOPHY

Department of Chemistry

ABSTRACT

OXYGEN-LIGATED FE-S AND MO-FE-S CLUSTERS AS POSSIBLE MODELS OF NITROGENASE

Ву

Miriam Elaine Rogers

A tridentate ligand, 1,8,13-tris[(N-4-hydroxyphenyl)carboxamido]triptycene ((HO)₃-tripod), was designed and synthesized. Complexation
of the ligand with a tetrameric iron-sulfur cluster was examined in
order to prepare an oxygen-ligated mixed-ligand Fe₄S₄ cluster as a
possible model for the P-clusters of nitrogenase. The basal portion of
the ligand is a 1,8,13-trisubstituted triptycene, prepared from the
Diels-Alder reaction of a 1,8-disubstituted anthracene with an
ortho-substituted benzyne. In the process of synthesizing this
macrocyclic ligand, an investigation of the factors governing the
regioselectivity of the cycloaddition reaction was conducted.
Twenty-one new trisubstituted triptycene derivatives and a new
synthetically useful benzyne precursor, 2-amino-6-methoxycarbonyl
benzoic acid, were prepared and characterized by ¹H NMR, ¹³C NMR and
IR spectroscopies, as well as mass spectrometry.

Proton nuclear magnetic resonance studies of the reaction between [Pr₄N]₂[Fe₄S₄(SEt)₄] and the (OH)₃-tripod ligand or between [Et₄N]₂[Fe₄S₄Cl₄] and the trisodium salt of the (HO)₃-tripod ligand were conducted. Analysis of the isotropically shifted peaks, by comparison with reported chemical shifts of related iron-sulfur clusters, indicates a mixture of tetrameric (Fe₄S₄) and hexameric (Fe₆S₆) forms of the ligated cluster is generated in solution.

An oxygen-ligated linear Mo-Fe-S cluster, $[Et_4N]_2[S_2MoS_2Fe(OAc)_2]$, was prepared as a possible model for the FeMo-cofactor of nitrogenase. Tetraethylammonium tetrathiomolybdate was reacted with anhydrous ferrous acetate in acetonitrile to yield the acetate-ligated dimer. The optical features are similiar to other dimers that have an FeS₄Mo core. Variable temperature ¹H NMR and magnetic susceptibility measurements show paramagnetism that follows Curie Law behavior. An observed $\mu_{eff} = 4.9$ BM is consistent with an S = 2 ground state and indicates an Fe(II)-Mo(VI) description of this complex.

To my parents:

Mr. and Mrs. R. Rogers

ACKNOWLEDGMENTS

I would like to acknowledge D. A. Holtman for assistance in obtaining temperature-dependent magnetic susceptibility data on [Et₄N]₂[S₂MoS₂Fe(OAc)₂] and Dr. D. Herold for providing high resolution mass spectra on several trisubstituted triptycenes.

I would like to thank Drs. Brian Ward, J. Michael Williams and Vijay
Kumar for their helpful discussions and suggestions concerning
synthetic problems.

I am appreciative that Professors Pinnavaia, Eick, Chang, LeGoff, Hart and Averill have served on my Committee. Special thanks to Dr. Hart, for allowing me to work in his labs for a year; to Dr. Chang for his patience and understanding on many long-distance phone calls concerning problems of working in absentia; to Dr. P. for assuming Chairmanship of my Committee at the last minute; and to Dr. Eick for serving as second reader.

I am grateful to Michigan State University, the University of Virginia and Dr. Averill for financial support during my graduate studies. I thank the Department of Chemistry at M.S.U. for permitting me to complete my research at U.Va.

I would like to thank my coworkers: Paul Lamberty, Gay Lilley, Elise Ponzetto, Susan Hefler, Charles Hulse, William Frazier (my running coach), Teresa Zirino (my fellow cohooter) and Douglas Holtman (Krossword King (oops, I spelled it wrong)) for making the lab a more pleasant place to be. In addition, I would like to thank my "bosses" in the NMR lab: Dr. J. Scott Sawyer (fearless leader of the F-team) and

Dr. Jeffrey Ellena (NMR Czar) for interesting times around the magnet.

More than thanks are owed to Mr. Michael Hoard, whose guidance and enduring friendship throughout the past eight years has meant a great deal to me (and may have changed my life); to Dr. Susan Kauzlarich for her constant encouragement, advice and friendship; and to my parents, for believing in me.

TABLE OF CONTENTS

Cnapte	r					Page
LIST O	F TABLES			•	•	vii
LIST O	F FIGURES			•	•	viii
LIST O	F ABBREVIATIONS			•		хi
I. INT	RODUCTION	• •		•	•	1
A.	Nitrogenase and its relevance			•	•	1
В.	Synthetic models of nitrogenase	• •		•	•	9
c.	Design of oxygen-ligated models of nitr	ogenas	e	•	•	18
II. R	ESULTS AND DISCUSSION			•	•	24
۸.	(HO) ₃ -Tripod ligand	• •		•	•	24
	1. Synthesis	• •		•	•	24
	2. Physical properties			•	•	40
В.	Binding study of the (HO)3-tripod ligan	d				
	to an Fe ₄ S ₄ core	• •		•	•	45
	1. Synthetic approach			•	•	45
	2. Proton nuclear magnetic resonance	studie	3	•	•	46
c.	$[Et_4N]_2[S_2MoS_2Fe(OAc)_2]$			•	•	67
	l. Synthesis			•	•	67
	2. Physical properties			•		68
	a. Optical			•	•	68
	b. Proton nuclear magnetic reson	ance.		•	٠.	71
	c. Magnetic susceptibility			•	•	74
III.	EXPERIMENTAL			•	•	78
A.	Materials			•	•	78
R	Physical methods.	_		_	_	79

Chapte	er	Page
c.	Preparation of 1,8-disubstituted anthraquinones	80
D.	Preparation of 1,8-disubstituted anthracenes	81
E.	Preparation of o-methoxycarbonylbenzyne precursor	83
F.	Preparation of 1,8,13- and 1,8,16-trisubstituted triptycenes	84
G.	Preparation of 1,8,13- and 1,8,16-tris[(N-substituted)-carboxamido]triptycenes	95
н.	Reaction of $[Pr_4N]_2[Fe_4S_4(SEt)_4]$ with $(HO)_3$ -tripod ligand	98
I.	Reaction of $[Et_4N]_2[Fe_4S_4Cl_4]$ with $Na_3(0_3-tripod)$	98
	1. Preparation of Na ₃ (O ₃ -tripod)	98
	2. Reaction of chloro tetramer with the trisodium salt of (HO) ₃ -tripod	99
J.	Preparation of [Et ₄ N] ₂ [S ₂ MoS ₂ Fe(OAc) ₂]	99
IV. C	CONCLUSIONS	101
REFERE	INCES	104

.

LIST OF TABLES

Table		Page
I	⁵⁷ Fe Mössbauer isomer shifts and quadrupole	
	splittings of various Fe-S clusters	. 19
II	Ratios of anti to syn isomers of trisubstituted	
	triptycenes	. 36
III	Calculated and observed 13C NMR shifts for aromatic	
	resonances of the (HO) ₃ -tripod ligand	. 44
IV	Isotropic shifts for the ligand protons in	
	$[Fe_4S_4(0_3-tripod)(SEt)]^{2-}$ and $[Fe_6S_6(0_3-tripod)_2]^{3-}$	
	species in Me ₂ SO-d ₄ solution	50
V	Electronic spectral features and molar absorptivities	
	for $[S_2MoS_2Fe(OAc)_2]^{2-}$, $[S_2MoS_2FeCl_2]^{2-}$, and	
	[S ₂ MoS ₂ Fe(OPh) ₂] ²⁻ complexes	. 70
VI	Isotropic proton nuclear magnetic resonance shifts	
	((AH/H) _{iso}) observed for the OAc group of	
	$[\text{Et}_{4}\text{N}]_{2}[\text{S}_{2}\text{MoS}_{2}\text{Fe}(\text{OAc})_{2}]^{2} \dots \dots \dots \dots \dots$	73

LIST OF FIGURES

Figure		Page
1	Schematic drawing of the electron transport chain	
	of nitrogenase	4
2	Schematic drawing of four types of Fe-S centers that	
	occur in proteins	5
3	Schematic drawing of structural models proposed for	
	the FeMo-cofactor	7
4	57Fe Mössbauer spectrum of the MoFe protein, taken at	
	30 K (from ref. 16)	8
5	Schematic drawing of the P-clusters of nitrogenase	
	based on the 57Fe Mössbauer and magnetic properties	
	of the MoFe protein	10
6	Schematic drawing of structurally characterized	
	Mo-Fe-S clusters	12
7	Schematic drawing showing the distortions of the	
	$[Fe_4S_4]^+$ core in: (left) $[Et_3MeN]_3[Fe_4S_4(SPh)_4]$;	
	(right) $[Et_4N]_3[Fe_4S_4(SCH_2Ph)_4]$. From ref. 40b	14
8	Possible models for the P-clusters, involving	
•	oxygen ligation at three vertices of a	
	4Fe-4S core	16
9	Schematic drawing of the transformation of	
	"hexamers" to "tetramers"	17
10	Schematic drawing of [Fe ₄ S ₄ (L)(SR)] ²⁻ ; where L is	
	a tuidentate ligand	21

Figure		Page
11	Schematic drawing of the (HO)3-tripod ligand	22
12	Schematic drawing of a triptycene structure	
	showing the numbering of atoms	25
13	Schematic of a synthetic approach toward	
	the preparation of triptycene	
	1,8,13-tricarboxylic acid	26
14	Schematic of linear versus convergent synthetic	
	approaches	30
15	Schematic of convergent synthesis approach to	
	triptycene 1,8,13-tricarboxylic acid	31
16	Schematic drawing of the synthesis of the	
	(HO) ₃ -tripod ligand	34
17	13C NMR (360 MHz) of the (HO) ₃ -tripod ligand in	
	Me ₂ SO-d ₆	43
18	Schematic showing spin density stabilization at the	
	ortho and para positions of an aromatic ring	49
19	¹ H NMR spectra (360 MHz) of the (HO) ₃ -tripod ligand	
	and its reaction with [Pr ₄ N] ₂ [Fe ₄ S ₄ (SEt) ₄] in	
	Me ₂ SO-d ₆ after a 4 h period and a 12 h period	52
20	¹ H NMR spectra (360 MHz) of Na ₃ (O ₃ -tripod),	
	reaction between Na ₃ (O ₃ -tripod) and	
	[Et ₄ N] ₂ [Fe ₄ S ₄ Cl ₄], and reaction of	
	[Pr ₄ N] ₂ [Fe ₄ S ₄ (SEt) ₄] with (HO) ₃ -tripod and five	
	equivalents of PhSH in Me ₂ SO-d ₆	57

Figure		Page
21	¹ H NMR spectra (360 MHz) of the reaction between	
	$[Bt_4N]_2[Fe_4S_4Cl_4]$ and $Na_3(O_3-tripod)$ in Me_2SO-d_6 .	
	The ratio of cluster to ligand (C:L) used in the	
	reactions is indicated next to each spectrum	61
22	Schematic of possible Fe-S clusters present from	
	interconversions of an $[Fe_4S_4(0_5R)(Cl)]^{2-}$ cluster	
	in solution	63
23	Schematic drawing of two possible coordination	
	modes of the (OH) ₃ -tripod ligand to an Fe ₆ S ₆	
	hexagonal core	65
24	Electronic spectrum of [Et ₄ N] ₂ [S ₂ MoS ₂ Fe(OAc) ₂]	
	in CH ₃ CN	69
25	¹ H NMR spectra (360 MHz) of [Bt ₄ N] ₂ [S ₂ MoS ₂ Fe(OAc) ₂]	
	in CD ₃ CN at various temperatures	72
26	Plot of isotropic shift ((AH/H) _{iso}) versus 1/T	
	for [Et ₄ N] ₂ [S ₂ MoS ₂ Fe(OAc) ₂]	75
27 .	Plot of χ versus T for temperature-dependent	
	magnetic susceptibility data on	
	[Rt.N]_[S-MoS-Fe(OAc)_].	76

LIST OF ABBREVIATIONS

ADP = adenosine 5'-diphosphate

Ar = arene

ATP = adenosine 5'-triphosphate

BM = Bohr magneton

t-Bu = tertiary-butyl

Bu₄N⁺ = tetrabutylammonium

cat = catechol

CPK = Corey-Pauling-Koltun

DEAE = diethylaminoethyl

DMA = N,N-dimethylacetamide

DME = dimethoxyethane

dtc = dithiocarbamate

EPR = electron paramagnetic resonance

Et = ethyl

Et₂N = triethylamine

Et₄N⁺ = tetraethylammonium

EtOAc = ethylacetate

EtOH = ethanol

EtSH = ethanethiol

EXAFS = extended X-ray absorption fine structure

FeMo-co = iron-molybdenum cofactor

GC = gas chromatography

glu = glutamate

(HO)₃-tripod = 1,8,13-Tris[(N-4-hydroxyphenyl)carboxamido]triptycene

HPLC = high-pressure liquid chromatography

IR = infrared

m = meta

MCD = magnetic circular dichroism

Me = methyl

MeOH = methanol

Me₂SO = dimethylsulfoxide

MS = mass spectrometry

 $Na_3(O_3-tripod) = trisodium salt of (HO)_3-tripod$

NBS = N-bromosuccinimide

NMR = nuclear magnetic resonance

 $O_3R = -O_3$ -tripod

o = ortho

o-xylS₂ = ortho-xylyldithiolate

p = para

P_i = inorganic phosphate

Ph = phenyl

Pr₄N⁺ = tetrapropylammonium

ref. = reference

TLC = thin-layer chromatography

TMS = tetramethylsilane

tyr = tyrosinate

I. INTRODUCTION

A. Nitrogenase and its relevance

Nitrogenase is the metalloenzyme responsible for the catalytic reduction of dinitrogen to ammonia in biological systems¹. The protein is found in prokaryotic microorganisms ranging from strict anaerobes to strict aerobes. The enzyme reduces nitrogen (with concomitant reductive dephosphorylation of ATP to ADP) at room temperature and atmospheric pressure, as shown in equation 1.

$$N_2 + 8H^+ + 8e^- + 12ATP \longrightarrow 2NH_3 + 12ADP + 12P_1 + H_2$$
 (1)

catalyst: nitrogenase

temperature: ambient

pressure: 1 atm.

Industrially, the Haber-Bosch process is used to reduce dinitrogen by reacting three moles of hydrogen with one mole of nitrogen over a catalyst of alumina treated with iron and potassium oxide, as shown in equation 2.

$$3H_2 + N_2 \longrightarrow 2NH_3$$
 (2)

catalyst: Al₂O₃/K₂O/Fe

temperature: 450 °C

pressure: 200-300 atm.

This process, which supplies the most widely used form of nitrogen fertilizer (NH₃), requires a high operating temperature (450 °C) and pressure (200-300 atm.). Nonrenewable fossil fuels, such as natural gas and liquid hydrocarbons, are used as sources of hydrogen, as well as to supply energy to achieve the harsh operating conditions.

Inorganic chemists are trying to duplicate the unique physical and chemical properties of nitrogenase in order to develop synthetic analogues that approximate the catalytic properties of the biomolecule². The long-range goal of this type of research is to synthesize a model that could eventually be developed into an efficient commercial catalyst.

Nitrogenase can be separated into two protein components, the Fe protein and the MoFe protein, by anion exchange (DEAE-cellulose) chromatography. The Fe protein has a molecular weight of 60,000 Daltons and has been shown to contain a single tetranuclear 4Fe-4S cluster³. The Fe protein binds two MgATP units to form an Fe protein (MgATP)₂ complex⁴. The MoFe protein consists of two subcomponents which have a combined molecular weight of 220,000 Daltons. Assays have shown the presence of 32 irons, 32 acid-labile sulfurs and 2 molybdenums per MoFe protein3. An isolatable subcomponent, from the extraction of the MoFe protein with N-methylformamide, contains 1 Mo, 6-8 Fe and 6-10 S= per mole. This subunit is essential for enzymatic activity and has been termed the ironmolybdenum cofactor, or FeMo-co. A mutant strain (UW45) of Azotobacter vinelandii produces an inactive MoFe protein, which lacks the cofactor unit, and consequently the ability to reduce dinitrogen⁵. The other subcomponent of the MoFe protein consists of two tetrameric iron-sulfur clusters which were identified by either cluster

displacement experiments⁶ (1°F NMR detection of substituted fluorinated thiols) or by cluster transfer techniques⁵ (EPR detection of Fe-S clusters transferred into apoproteins). These clusters are a variant of the normal 4Fe-4S clusters and have been referred to as P-clusters⁷.

The MoFe and Fe proteins function together as an electron transport chain. A schematic representation of the nitrogenase system is shown in Figure 18. Electrons are transferred from an initial electron donor such as a reduced ferredoxin to the Fe protein (MgATP)₂ complex⁹. The binding of MgATP to the iron protein may serve to make electron transfer more efficient by causing a conformational change in the protein structure¹⁰. Electrons are then shuttled (via the P-clusters, which may act as electron reservoirs) to the MoFe cofactor. This is the site of the actual reduction process. For every two electrons transferred to substrate, four to five moles of ATP are hydrolysed to ADP⁴. Substrates that can be reduced (besides dinitrogen) are azide, alkynes and isonitriles, while carbon monoxide inhibits activity.

A great deal of research has been aimed at deducing the exact structure of the metal centers in the MoFe protein^{8,11}. Four different types of clusters, shown in Figure 2, have been found in various other iron-sulfur proteins by X-ray crystallography. The extreme oxygen sensitivity of nitrogenase and its high molecular weight have limited the amount of structural information obtainable by X-ray crystallography. The technique of EXAFS (extended X-ray absorption fine structure) spectroscopy has been employed to study the immediate environment of the Mo and Fe atoms in the protein. Mo K-edge scattering has been analyzed as arising from 4 S atoms at 2.35 Å, 2-3

Figure 1. Schematic drawing of the electron transport chain of nitrogenase.

Figure 2. Schematic drawing of four types of Fe-S centers that occur in proteins.

Fe atoms at 2.72 Å and 1-2 additional S atoms at 2.5 Å from $Mo^{12,13}$. The Fe K-edge EXAFS data on the MoFe protein suggest 1.3 ± 1.0 O (or N) atoms at 1.8 Å, 3.4 ± 1.6 S atoms at 2.25 Å, 2.3 ± 0.9 Fe atoms at 2.66 Å and 0.4 ± 0.1 Mo at 2.76 Å from Fe¹⁴. Low temperature (8-25 K) EPR spectra of the MoFe protein display g values near 4.32, 3.65 and 2.01^{15} . This is quite different from a normal tetranuclear cluster which has g values near or below g = 2.0. Several structures, shown in Figure 3, have been proposed for FeMo-co based on the physical data obtained⁸.

The 57Fe Mössbauer spectrum of the MoFe protein, shown in Figure 4, consists of four quadrupole doublets, referred to as "M", "S", "D" and "Fe²⁺" components¹⁶. Least squares fitting of doublet "S" indicates that it accounts for only two iron atoms per holoenzyme, and it is uncertain whether this is due to a persistent impurity or if this iron is an integral part of the MoFe protein. Component "M" is assigned to the metal cluster of FeMo-co, while components "D" and "Fe2+" are assigned to the P-clusters. Mössbauer spectra taken in strong magnetic fields show that the P-clusters are diamagnetic (S = 0) in the resting enzyme. The ratio of intensities of the D:Fe²⁺ doublets is 3:1. Analysis of isomer shifts ($\delta = 0.69 \text{ mm/s}$) and quadrupole splitting ($\Delta E_{Q} = 3.02 \text{ mm/s}$) indicates that the Fe²⁺ doublet represents high-spin iron(II) coordinated tetrahedrally to sulfur. The more intense doublet (D) has an isomer shift $\delta = 0.64$ mm/s, (which is in the range of Fe²⁺ shifts), but has an unusually small quadrupole splitting (AE_Q = 0.81 mm/s). It is concluded that the Fe²⁺ and D components make up a set of spin-coupled Fe₄S₄ clusters (P-clusters), with each cluster containing one Fe2+ and three D ferrous atoms as illustrated in

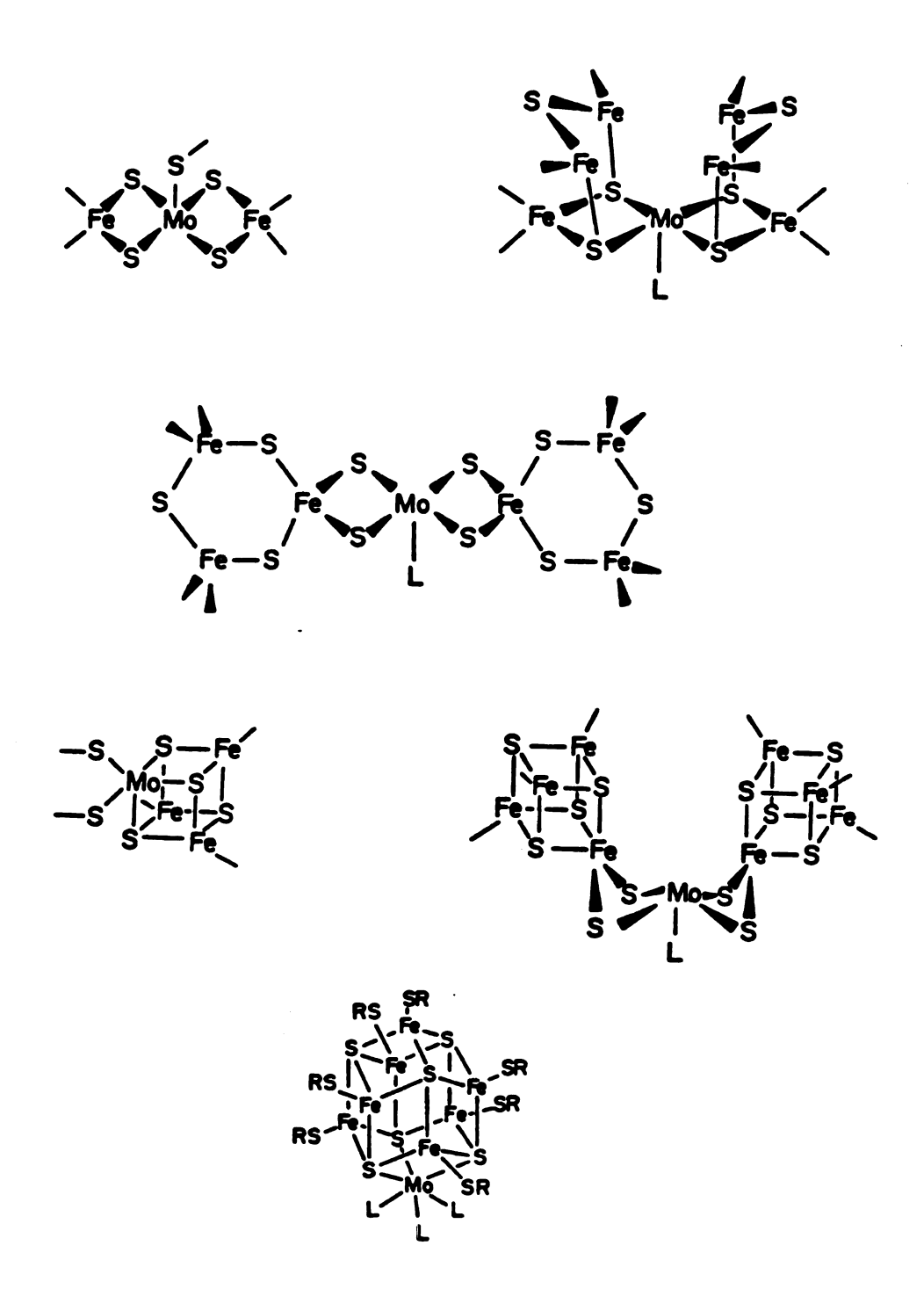


Figure 3. Schematic drawing of structural models proposed for the FeMo-cofactor.

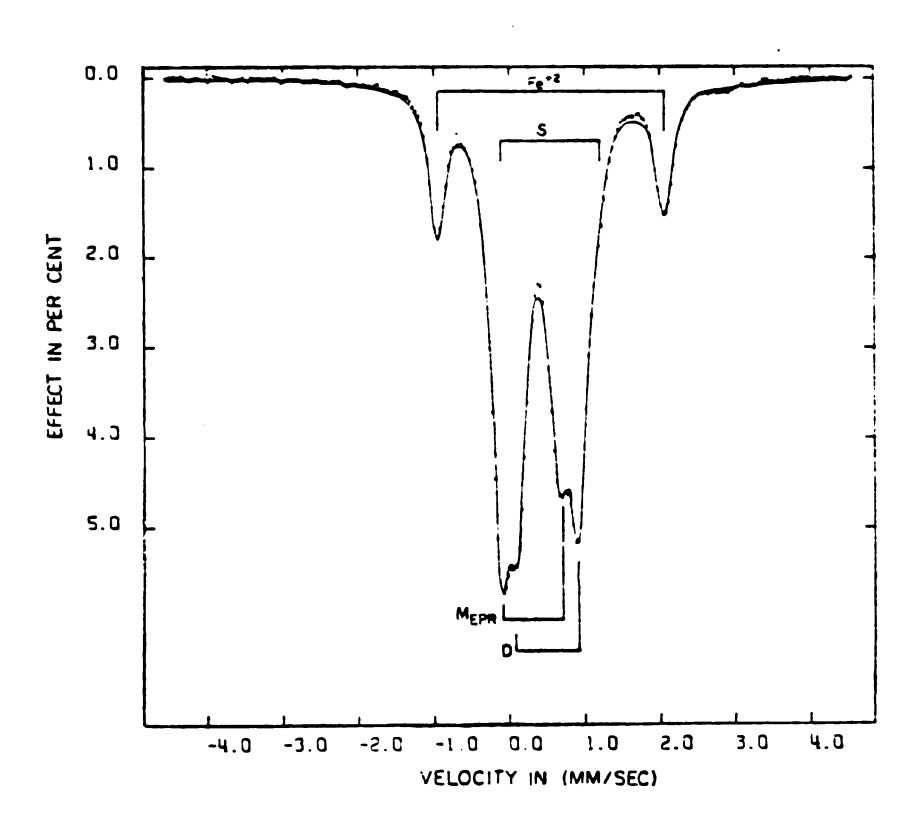


Figure 4. ⁵⁷Fe Mössbauer spectrum of the MoFe protein, taken at 30 K (from ref. 16.).

Figure 5. Additional studies with combined EPR, Mössbauer and MCD spectroscopies 17 indicate that the oxidation state of the Fe₄S₄ core in the native enzyme (P^N) is probably zero (4 ferrous atoms), while magnetic suseptibility measurements 18 of the oxidized MoFe protein show an S = 5 /2 spin state for the oxidized P-clusters (P^{OX}).

B. Synthetic models of nitrogenase

Many experimentalists have tried to mimic the composition and spectroscopic properties of the structurally unique metal cluster of FeMo-co. Three classes of Mo-Fe-S clusters have been prepared and characterized. Structural examples are shown in Figure 6. The first class of models contains an MoS2Fe unit, and are referred to as "linear" clusters. Various linear arrays of metal atoms include binuclear metallic clusters such as [S₂MoS₂FeL₂]²⁻ (L = SAr¹⁹, Cl²⁰, OAr^{21} , OAc^{22} , NO^{23} ; $L_2 = S_s^{24}$, $o-xylS_2^{25}$) (I), trinuclear clusters such as $[Cl_2FeS_2MoS_2FeCl_2]^{2-26}$ (II), $[S_2MoS_2FeS_2Fe(SAr)_2]^{3-21b,27}$ (III), $[S_2MoS_2FeS_2MoS_2]^{3-28}$ (IV) and $[(RS)_2MoS_3FeS_3Mo(SR)_2]^{3-29}$ (V), as well as a new type of hexanuclear cluster [MoOFe₅S₄(CO)₁₂]²⁻³⁰ (VI). A second class of synthetic clusters contains the MoFe₃S₄ cubane core. Examples include linked double cubane structures such as $[Mo_2Fe_4S_9(SEt)_a]^{3-31}$ (VII), $[Mo_2Fe_4S_8(SRt)_9]^{3-31,32}$ (VIII), $[Mo_2Fe_6S_e(SEt)_3(OPh)_6]^{3-33}$, $[Mo_2Fe_7S_e(SEt)_{12}]^{4-34}$ (IX), $[Mo_2Fe_4S_8(OMe)_3(SR)_4]^{3-35}$ (X) and $[Mo_2Fe_4S_8(SR)_4(cat)_2]^{4-36}$ (XI); and single cubanes such as $[MoFe_4S_4(SEt)_3(cat)_3]^{3-37}$ (XII) and [MoFe₃S₄(SR)₃(cat)(L)]³⁻³⁸ (L = solvent) (XIII). A new class of hexameric Fe-S clusters was reported in 1985. The first example of

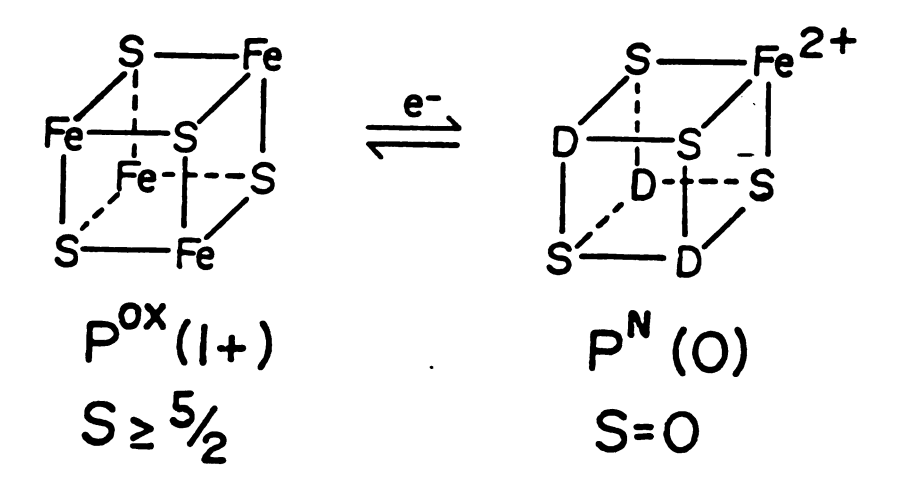


Figure 5. Schematic drawing of the P-clusters of nitrogenase based on the ⁵⁷Fe Mössbauer and magnetic properties of the MoFe protein.

Figure 6. Schematic drawing of structurally characterized Mo-Fe-S clusters.

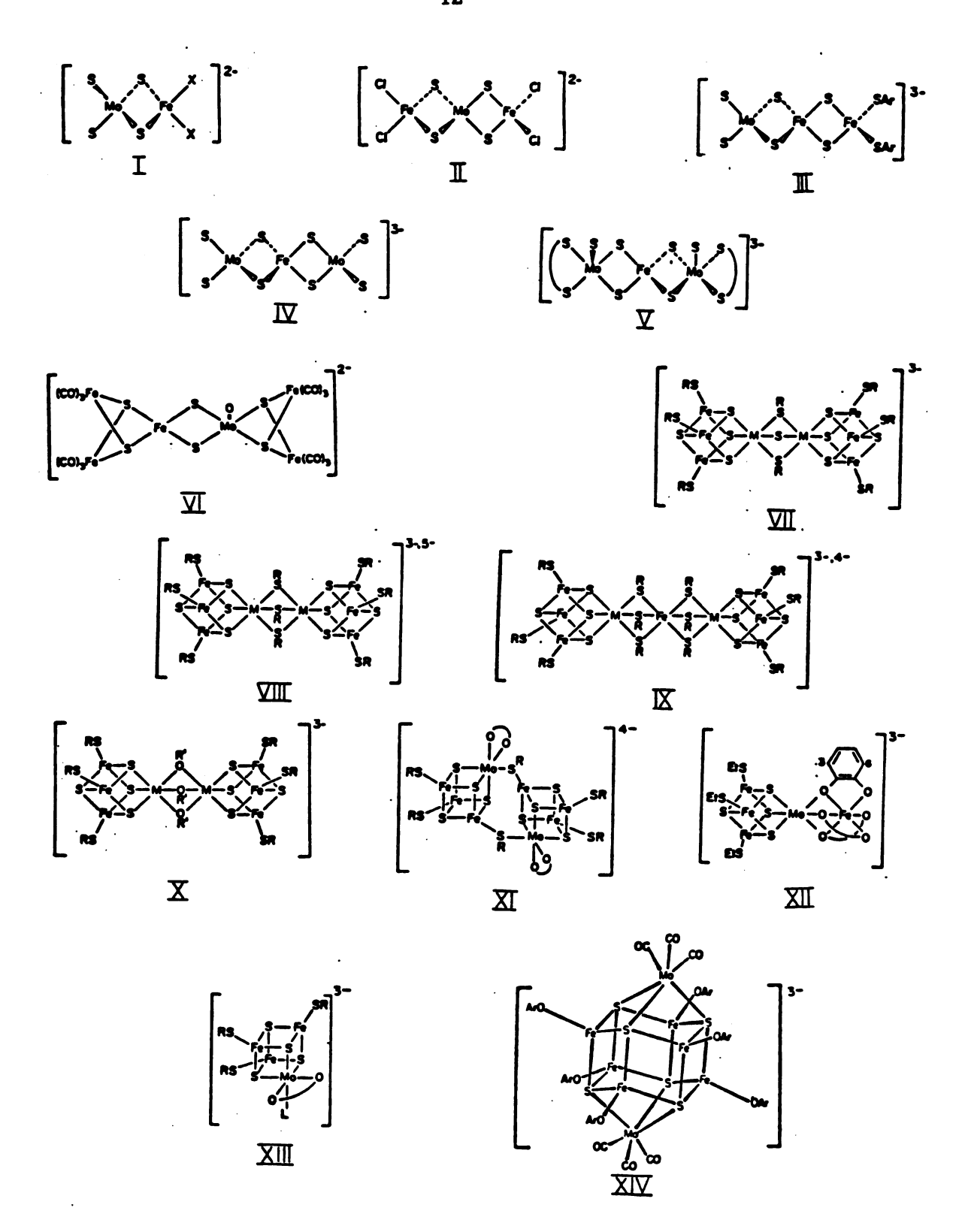


Figure 6

this class of cluster to incorporate Mo is $[Fe_6S_6(OAr)_6(Mo(CO)_3)_2]^{3-39}$ (XIV). Although some of these clusters have similar properties to FeMo-co, none serves as an appropriate analogue.

Synthetic efforts towards modelling P-clusters have been less intense, owing to the limited data available. The ⁵⁷Fe Mössbauer parameters suggest that the P-clusters are a variant of the normal Fe₄S₄ tetrameric cluster. Hypothetical models have been proposed to account for the differentiation of "D" iron atoms from "Fe²⁺" iron atoms, while maintaining a spin-coupled 4Fe-4S structure.

One explanation is that the protein backbone enforces some sort of geometrical distortion on the Fe₄S₄ unit such as to alter its physical properties from a normal cluster. Models of the oxidized state of the P-clusters ([Fe₄S₄]⁺ core) are analogous to synthetic structures that have an [Fe₄S₄(SR)₄]³⁻ formulation. A number of these reduced clusters have been reported (R = CH₂Ph⁴⁰, Ph⁴¹, t-Bu⁴², Et⁴², Me⁴²) and their X-ray structures show a lack of stereochemical regularity of the odd electron Fe₄S₄ core. Two different core structures with distinct electronic properties are found. Figure 740b illustrates that [Fe₄S₄(SPh)₄]³⁻ exhibits a tetragonally elongated cubane core (elongated D_{2d} structure with an idealized 4-fold axis), while [Fe₄S₄(SCH₂Ph)₄]³⁻ exhibits a tetragonally compressed core (imposed 2-fold axis). Magnetic studies and EPR spectra^{40b} show that $[Fe_4S_4(SPh)_4]^{3-}$ has an $S = \frac{1}{2}$ ground state, while $[Fe_4S_4(SCH_2Ph)_4]^{3-}$ has an S = 3/2 ground state. This suggests that a protein-imposed distortion on an Fe₄S₄ core could result in an S = $\frac{5}{2}$ ground state (as observed in the oxidized P-clusters). A threefold distortion could differentiate three of the iron sites from the fourth and may explain

Figure 7. Schematic drawing showing the distortions of the [Fe₄S₄]⁺ core in: (left) [Et₃MeN]₃[Fe₄S₄(SPh)₄]; (right) [Et₄N]₃[Fe₄S₄(SCH₂Ph)₄]. From ref. 40b.

the observed physical data.

The second model, shown in Figure 8, has non-thiolate ligation on three of the four iron atoms. Ferrous iron has a low affinity for saturated amine ligands 43 ; therefore, the most reasonable candidates for coordination would be oxygen-containing amino acids such as tyrosine, glutamic acid, or aspartic acid. This would lead to a mixed-ligand cluster with the formulation [Fe₄S₄(OR)₃(SR)]³⁻. The lability of the terminal ligands and the "tendency to yield a statistical distribution of all possible mixed-ligand complexes"8 has hindered synthesis in this area. Mixed-ligand clusters of the type [Fe₄S₄L₂L'₂]²⁻ (L = Cl, L' = SPh^{44} , OPh^{45} ; L = SPh, L' = OPh^{45} , p-tolyl⁴⁵, Br^{45}) have been isolated in the solid state, but solution studies are difficult due to facile redistribution of terminal ligands. Recently, synthetic models of Fe4S4 cores with all oxygen ligands were prepared. The acetate cluster, [Fe₄S₄(OAc)₄]²⁻, has been generated and examined in solution, but not in the solid state 46. The crystalline phenoxide-ligated cluster, $[Fe_4S_4(OPh)_4]^{2-}$, has been isolated and examined⁴⁷. Phenoxide ligation seems to stabilize a new class of hexameric clusters. The crystal structure of [Fe₆S₆(OC₆H₄-p-CH₃)₆]³⁻⁴⁸ has been recently reported, whereas the thiolate hexamers are usually not observed due to the rapid transformation to tetramers, as shown in Figure 9. If an Fe₆S₆ center were present in an iron-sulfur protein, extrusion by thiophenol would lead to the metastable [Fe₆S₆(SPh)₆]³⁻, followed by rapid conversion to tetrameric [Fe₄S₄(SPh)₄]²⁻.

A third explanation of the physical data would be that each "D" atom is 5-coordinate. Diethyldithiocarbamate has been used as a bidentate ligand on an Fe-S cubane ($[Fe_4S_4L_2L'_2]^{2-}$ ($L = Cl^{49}$, SPh⁵⁰;

Figure 8. Possible models for the P-clusters, involving oxygen ligation at three vertices of a 4Fe-4S core.

Figure 9. Schematic drawing of the transformation of "hexamers" to "tetramers".

L' = $\rm Et_2dtc$), forming a mixed-ligand cluster with monodentate and bidentate ligands. $[\rm Fe_4S_4(SC_6H_4-o-OH)_4]^{2-51}$ is another example of a cluster that contains a 5-coordinate iron atom. The solid state structure shows three conventional tetrahedral FeS₄ sites and one unique FeS₄O site. $[\rm Fe_4S_4(Cl)_3(Et_2dtc)]^{2-49}$ has also been isolated and is the only mixed-ligand cluster with a 3:1 ratio of different ligands.

It is interesting to note the effects of the various substitution patterns of the clusters on the 57 Fe Mössbauer parameters. Table I shows the isomer shifts and quadrupole splitting values for selected samples citied above, and for the P-clusters. Oxygen ligation increases 5 by ~0.04 mm/s and 4 Eq by 0.14 mm/s over that of tetrahedral thiolate coordination. Five-coordination increases 5 ~0.18 mm/s and 4 Eq by ~0.70 mm/s. Clusters in the reduced state, $[Fe_{4}S_{4}(SR)_{4}]^{3-}$, show 4 Eq values that are much higher than those observed for $[Fe_{4}S_{4}(SR)_{4}]^{2-}$ clusters. It appears that a combination of all three explanations would form a more accurate model of P-clusters.

C. Design of oxygen-ligated models of nitrogenase

Interest in further investigating oxygen ligation to metal clusters has led to the design of two models to be discussed in this dissertation. The purpose of the first model was to mimic the properties of P-clusters. It was desirable to make a mixed-ligand Fe_4S_4 cluster that would have three Fe-O bonds and one Fe-S bond and which could be studied in solution as well as in the solid state. The synthetic approach toward an $[Fe_4S_4(O_3R)(SR)]^{2-}$ cluster was to synthesize a tridentate ligand that would bind to three corners of an

Table I. ⁵⁷Fe Mössbauer isomer shifts and quadrupole splittings^a of various Fe-S clusters.

Complex	δ	≜ Eq
[Fe ₄ S ₄ (SPh) ₄] ^{2- b}	0.46	1.07
[Fe ₄ S ₄ Cl ₄] ^{2- b}	0.52	1.09
[Fe4S4Cl2(OPh)2]2-b	0.51	1.01
	0.52	1.28
[Fe4S4(OPh)2(SPh)2]2-b	0.47	0.96
	0.46	1.24
[Fe ₄ S ₄ (OPh) ₄] ^{2- C}	0.50	1.21
$[Fe_4S_4(SC_4H_4-o-OH)_4]^{2-d}$	0.43	0.75
	0.48	1.22
	0.63	1.84
$[Fe_4S_4(SPh)_2(Et_2dtc)_2]^{2-e}$	0.39	1.34
	0.65	1.67
[Fe ₄ S ₄ Cl ₃ (Et ₂ dtc)] ^{2- f}	0.51	1.07
	0.64	2.13
$[Fe_4S_4(SCH_2Ph)_4]^{3-}g$	0.60	1.41
	0.60	0.93
$[Fe_4S_4(SPh)_4]^{3-}g$	0.64	2.04
	0.57	1.13
P-clusters d	0.64	0.81
A. vinelandii	0.69	3.02

aSpectra taken at 4.2 K and referenced to Fe metal at room temperature. bReference 45. cReference 47. dReference 51. eReference 50. fReference 49. Spectum recorded at 77 K. gReference 40a.

Fe₄S₄ cubane, while allowing the fourth corner to have tetrahedral sulfur coordination as shown in Figure 10. This design would prevent ligands from rapidly exchanging in solution as observed with other mixed-ligand clusters 45. Previous attempts to synthesize clusters constrained by large macrocycles used OP(NHC₆H₄-o-SH)₃, OP(NHCH₂C₆H₄-o-SH)₃ and CH₃C(CH₂CO₂CH₂SH)₃52 as ligands. Reactions of these compounds with Fe₄S₄ cubanes were followed by optical and ¹H NMR spectroscopies. Observed shifts in absorption showed that binding had occurred, but the correct coordination was not achieved. It appeared that these ligands were too floppy to tightly bind an Fe₄S₄ cluster, and that polymers were probably formed. A new type of rigid ligand, shown in Figure 11, was designed. The foundation of the ligand is a symmetrically trisubstituted triptycene, with three arms that can attach to the Fe-S cluster. This ligand will be referred to as the (HO)₃-tripod ligand throughout this text. A CPK model indicated that there is less than 1.0 Å distance between iron atoms on the Fe₄S₄ cubane and oxygen atoms on the (HO)3-tripod ligand. The structural rigidity of the triptycene and the ligand bite formed by the phenolates are such that polymer formation is unlikely to occur. Once one phenolate ligand binds to one vertex of an Fe-S cluster, the chelate effect should force coordination of only one Fe₄S₄ cubane per ligand. The synthesis of the (HO)₃-tripod ligand and ¹H NMR studies of its binding to an iron-sulfur center are discussed in this dissertation.

A second investigation of oxygen-ligated clusters involved the synthesis and characterization of a new Mo-Fe-S linear cluster, $[Et_4N]_2[S_2MoS_2Fe(OAc)_2].$ This complex was synthesized before a note on the preparation, by Zhuang, et al.²², appeared in the literature. Only

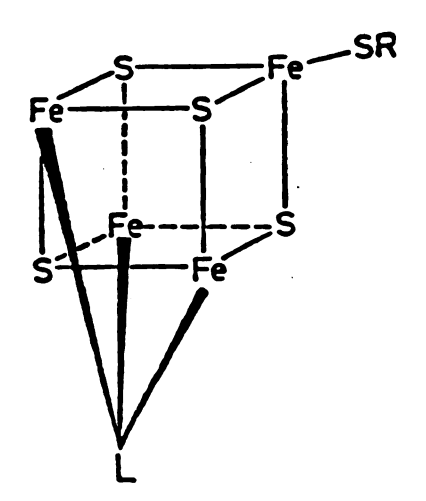


Figure 10. Schematic drawing of $[Fe_4S_4(L)(SR)]^{2-}$; where L is a tridentate ligand.

Figure 11. Schematic drawing of the (HO)3-tripod ligand.

the electronic properties were reported on this compound at that time. The purpose of this model was to mimic the FeMo-cofactor, which is known to be a unique molybdenum-iron-sulfur center. The only oxygen-ligated linear Mo-Fe-S cluster previously reported was $[S_2MoS_2Fe(OPh)_2]^{2-21}$, which was synthesized by a ligand substitution reaction of $[S_2MoS_2FeCl_2]^{2-1}$ and sodium phenoxide. Previous attempts in our laboratory to synthesize the iron-molybdenum-acetate dimer by ligand substitution reaction of $[S_2MoS_2FeCl_2]^{2-1}$ with sodium acetate or from $[S_2MoS_2Fe(SAr)_2]^{2-1}$ (Ar = Ph, p-tolyl) and acetic anhydride failed. A black decomposition product was isolated but not characterized⁵³. This dissertation describes the direct synthesis of the acetate dimer from ferrous acetate (Fe(O₂C₂H₃)₂) and thiomolybdate ([MoS₄]²⁻¹). The optical properties, variable temperature ¹H NMR data and magnetic susceptibility measurements are discussed.

II. RESULTS AND DISCUSSION

A. (HO)3-tripod ligand

1. Synthesis

The (HO)₃-tripod ligand that was synthesized is shown in Figure 11 of chapter 1. The numbering scheme used for the triptycene structures is consistent with the 9,10-dihydro-o-benzenoanthracene nomenclature used by Chemical Abstracts Service and is illustrated in Figure 12. The 1,8,13-trisubstituted structures are referred to as syn and the 1,8,16-trisubstituted structures are referred to as anti.

A preliminary goal was to synthesize a symmetrically trisubstituted triptycene containing carboxyl groups at the 1-, 8- and 13- positions. Friedman and Logullo⁵⁴ initially reported a convenient synthesis of triptycene from the reaction of anthracene with benzyne. The first synthetic approach taken to produce the foundation of the (HO)₃-tripod ligand is shown in Figure 13. The preparation of 1,8-dichloro-anthracene (2) from 1,8-dichloro-anthraquinone (1) was followed as reported in the literature⁵⁵; but its conversion to 1,8-dicyano-anthracene (3)⁵⁶ according to the literature procedure yielded little or no product. The procedure described⁵⁶ for 3 involves reaction of 2 with cuprous cyanide in quinoline for 24 h, followed by digestion of the crude product with nitromethane, and finally recrystallization from acetic acid. This procedure was improved by treating crude 3 with

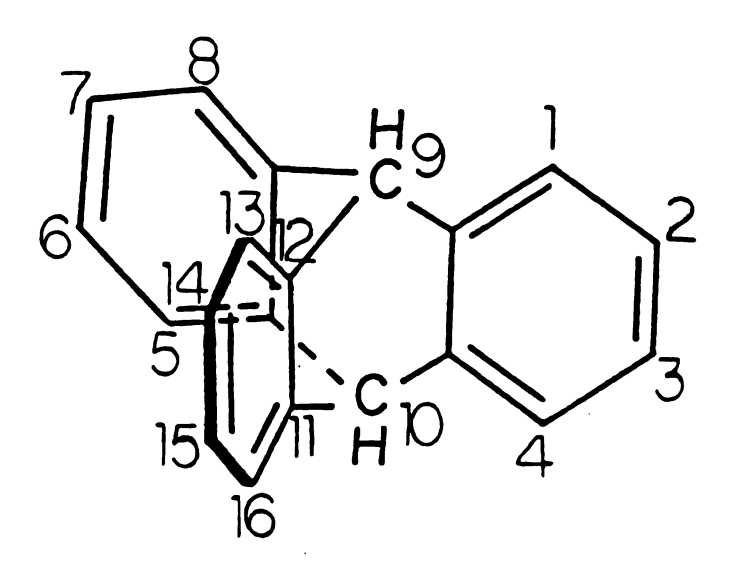


Figure 12. Schematic drawing of a triptycene structure showing the numbering of atoms.

CI O CI
$$\frac{2n}{NH_3}$$
 CI CI $\frac{CN}{CN}$ CN $\frac{CN}{NH_2}$ COOH $\frac{2n}{NH_3}$ COOH $\frac{COOH}{COOH}$ COOH $\frac{COOH}{COOH}$ CN $\frac{CN}{NH_3}$ CN $\frac{CN}{NH_3}$ COOH $\frac{CN}{$

Figure 13. Schematic of a synthetic approach toward the preparation of triptycene 1,8,13-tricarboxylic acid.

aqueous ammonia. This resulted in the decomposition of an organocopper intermediate to give crude 3 and a blue solution of $[Cu(NH_3)_4]^{2+}$. Purification by column chromatography to separate out 1-cyano-8-chloroanthracene and some black tar yielded 3 in 41% yield.

Although numerous substituted triptycenes have been prepared⁵⁷, only one symmetrically trisubstituted compound was known prior to this work. Mori, et al.⁵⁸ had found that the Diels-Alder reaction of 2 with chlorobenzyne led to a mixture of 1,8,13- and 1,8,16-trichlorotriptycenes in 16% combined yield. This type of Diels-Alder addition seemed like the best approach to prepare the basal portion of the (HO)3-tripod ligand, triptycene-1,8,13-tricarboxylic acid (7s). 2-Amino-6methylbenzoic acid (4) was chosen as a convenient benzyne precursor because of its commercial availability. Reaction of 3 with 4 in the presence of isoamyl nitrite in dimethoxyethane (DME)/triethylene glycol dimethyl ether yielded 57% of 1,8-dicyano-13-methyltriptycene (5s) and 1,8-dicyano-16-methyltriptycenes (5a). The nitrile groups on the triptycene caused the mixture of 5a and 5s to be only sparingly soluble in most organic solvents, except extremely polar solvents such as dimethylsulfoxide (Me₂SO) and dimethylacetamide (DMA). The isomers were not separated at this point because the small polarity difference between anti and syn structures made isolation difficult. Conversion of the nitrile groups to carboxylic acids was attempted by reaction with concentrated sulfuric acid⁵⁹, 85% phosphoric acid⁶⁰ and 10% potassium hydroxide/2-methoxyethanol⁵⁶. All of these procedures resulted in recovery of starting material. A clean conversion to 13-methyltriptycene-1,8-dicarboxylic acid (6s) and 16-methyl-triptycene-1,8-dicarboxylic acid (6a) was accomplished by reacting the mixture of

5a and **5s** with KOH in ethylene glycol⁶¹ at 100 °C for four days. The isomeric products 6a and 6s were more insoluble than 5a and 5s, and consequently caused problems in attempts to oxidize the methyl substituent. Oxidation of the methyl group of 6a and 6s using mild reagents such as cerium ammonium nitrate (Ce(NH₄)₂(NO₃)₄) in glacial acetic acid62, chromium oxide (CrO₃) in pyridine63 and tetrabutylammonium permanganate (Bu_4NMnO_4) in pyridine 64, was unsuccessful. When reaction conditions were made severe enough (6a and 6s in Bu4NMnO4/pyridine for 48 h at 100 °C), evidence of oxidation of the triptycene structure to methyl-substituted anthraquinone was observed by 'H NMR spectroscopy. Oxidants have been previously reported to cleave the triptycene system⁶⁵. Attempts to oxidize the methyl group of the isomeric pair of 5a and 5s (which had greater solubility than 6) also met with failure. At this stage, it appeared as if the methyl group could not be converted to a carboxylic acid in one step, and therefore a multiple step approach was tried.

Bromination of a methyl substituent has been known to yield a bromomethyl group⁶⁶, which can subsequently be converted to a primary alcohol, and then oxidized to a carboxylic acid. Due to the low solubility of 6a and 6s, the three additional steps in the synthetic route would have to be clean conversions since purification techniques would be limited. Bromination reactions were conducted with the isomers 1,8-dichloro-13-methyltriptycene (8s) and 1,8-dichloro-16-methyltriptycene (8a) since 6a and 6s were difficult to isolate. Reaction of 8a and 8s with one equivalent N-bromosuccinimide (NBS) and dibenzoyl peroxide led to what appeared to be a bromomethyl substituent.

When 2 equivalents of NBS were reacted with the triptycenes, 1,8-dichloro-13- and -16-dibromomethyltriptycenes (9a and 9a) were isolated. This product, in principle, could be converted to an aldehyde-substituted triptycene and then subsequently oxidized to yield the desired carboxylic acid substituent. At this point, the synthetic problems provoked a reinvestigation into the approach to 7s as outlined in Figure 13. The efficiency of the synthetic plan was reanalyzed, and it was realized that in order to isolate and purify large quantities of 7s, another synthetic route had to be designed.

A linear and a convergent approach to synthesizing a hypothetical molecule A-B-C-D are contrasted in Figure 14⁶⁷. The yields are calculated assuming 90% yield at each step. The linear approach to synthesizing the trisubstituted triptycene (7s) was to perform the Diels-Alder reaction first, and then try to convert the substituents to carboxylic acids. A convergent approach, to the same compound, would convert the substituents on the anthracene and benzyne to carboxylic acids prior to the cycloaddition reaction. This new approach is shown in Figure 15.

The advantages of a convergent approach are increased overall yields of products and simplified purification. The linear synthesis complicates separation and purification problems because the change in physical properties of the compounds diminishes as the synthesis progresses. The only problem envisaged with the convergent approach was that the carboxyl substitutents on the benzyne and anthracene might prefer to orientate to give the anti isomer, due to steric hinderance during the cycloaddition reaction. We were interested in optimizing the yield of syn isomer since the target ligand is

LINEAR:

$$A \xrightarrow{B} A-B \xrightarrow{C} A-B-C \xrightarrow{D} A-B-C-D 73%$$

CONVERGENT:

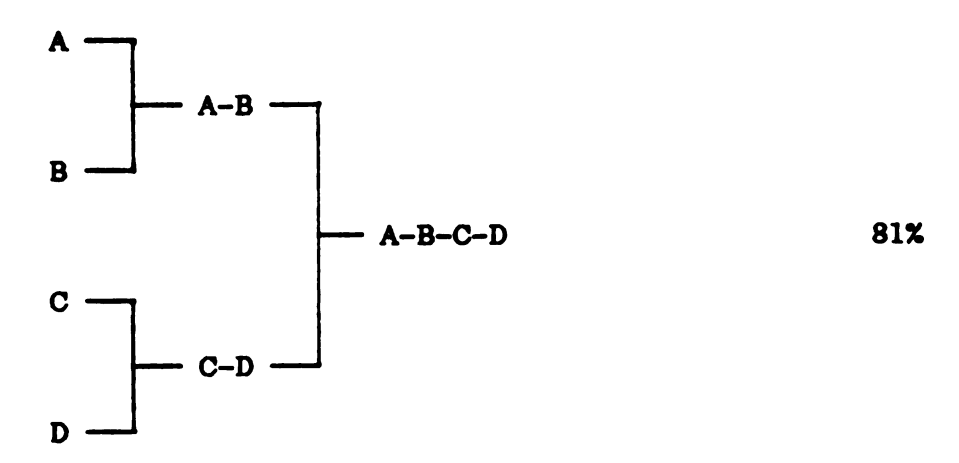


Figure 14. Schematic of linear versus convergent synthetic approaches.

Figure 15. Schematic of convergent synthesis approach to triptycene 1,8,13-tricarboxylic acid.

substituted in this fashion. This dilemma led to an investigation of various factors that are important in controlling the stereochemistry of the Diels-Alder reaction between various benzynes derived from 6-substituted anthranilic acids and 1,8-disubstituted anthracenes. The results are discussed at the end of this section.

The convergent synthesis outlined in Figure 15 shows that 1 was converted to 1,8-dicyanoanthraquinone (10) by reaction with cuprous cyanide in DMA. This is a modification of the original procedure⁶⁸, which uses benzyl cyanide as the solvent. The organocopper intermediate was decomposed with dilute nitric acid to give 10 in 88% yield. Hydrolysis of 10 with H₂SO₄ gave anthraquinone-1,8-dicarboxylic acid (11), which upon reduction with zinc dust in NH₄OH yielded anthracene-1,8-dicarboxylic acid (12). 1,8-Bis(methoxycarbonyl)-anthracene (13) was synthesized as described⁶⁹ by reaction of 12 with acidic methanol (MeOH).

In order for the convergent synthesis approach to work, a new methoxycarbonyl-substituted aryne had to be developed. The two-step synthesis of 2-amino-6-methoxycarbonylbenzoic acid (16) involved selective esterification of 3-nitrophthalic acid (14) to yield 1-methyl-2-hydrogen-3-nitrophthalate (15), which was reduced to the amino benzoic acid 16 (as shown in Figure 15). The literature preparation 70 for 15 reported a 56% yield with a reaction time of 16 h. This procedure was modified to give an increased yield (77%) in a much shorter time (3 h). The hydrogenation of 15 for 8 h in MeOH, using a catalyst of 5% palladium (Pd) on charcoal yielded a gummy yellow solid of 16. Upon standing at room temperature for more than 24 h, this compound undergoes intramolecular condensation reactions to form

amide-linked polymers and MeOH.

Compound 16 was reacted with 13 to yield a 3:1 mixture of 1,8,16-tris(methoxycarbonyl)triptycene (17a) and 1,8,13-tris-(methoxycarbonyl)triptycene (17s). These colorless isomers were separable by column chromatography (silica gel), although radial thin-layer chromatography was used as an efficient way to perform the separation. The radial chromatograph was equipped with a quartz cover which allowed the evolution of bands to be followed using a UV light source. The ester substituents on 17a and 17s provided increased solubility and circumvented many reaction condition problems seen with 5s and 5a or 6s and 6a. Hydrolysis to the triptycene tricarboxylic acids (7a and 7s) in KOH/MeOH was easily performed. The convergent approach shown in Figure 15 provided a practical synthetic route to produce large quantities of the (HO)3-tripod foundation. This was mainly because of the increased solubility of 13 compared to 3 and consequently easier separation and purifications of the subsequent products.

Conversion of 7s to the (HO)₃-tripod ligand is shown schematically in Figure 16. Compound 7s was reacted with thionyl chloride to yield triptycene-1,8,13-tricarboxylchloride (17s). This product was moisture sensitive and therefore immediately reacted with p-aminophenol in the presence of triethylamine, forming the (HO)₃-tripod ligand (19s) in high yield. Four other triptycene amides, 19a, 20a, 21a and 22a, were prepared by reaction of triptycene-1,8,16-tricarboxylchloride (17a) with p-aminophenol, propylamine, p-toluidine and p-aminobenzene p-xylene sulfide, respectively. An alternative preparation of these carboxamido-triptycenes involved reaction of 18s or 18a with seven

Figure 16. Schematic drawing of the synthesis of the (HO)₃-tripod ligand.

equivalents of amine (instead of using Et₃N to scavenge hydrochloric acid).

The reaction of 18s with p-aminothiophenol yielded a mixture of products, some of which appeared to be thioester-linked oligomers. Apparently the difference in pK₈ of phenol (9.9)⁷¹ versus thiophenol (6.4)⁷² causes a difference in reactivity. Solvents and reaction conditions were varied to try to change the amount of product formed, but side-products were always present. Attempts at separation of the product mixture proved to be futile due to solubility problems.

Removal of the S-p-xylene protecting group from 22a, to yield the sulfur analog of the (HO)₃-tripod ligand, was also unsuccessful due to the insoluble nature of this compound.

In the process of preparing the (HO)₃-tripod ligand, a series of new trisubstituted triptycenes was synthesized which gave some insight into the selectivity of the Diels-Alder cycloadditon between disubstituted anthracenes and monosubstituted benzynes. The synthesis and properties of the isomers were examined. The various 1,8-disubstituted anthracenes used were dichloro-, dicyano-, and bis-(methoxycarbonyl)anthracenes, of which the improved preparations were discussed earlier in this section. The three substituted benzyne precursors used included 2-amino-6-methylbenzoic acid, 2-amino-6-chlorobenzoic acid⁷³ and 2-amino-6-methoxycarbonylbenzoic acid.

The three monosubstituted anthranilic acids were reacted with the three disubstituted anthracenes to yield eight pairs of isomeric substituted triptycenes, shown in Table II. The ninth possible pair of isomers (X = CN, Y = Cl) could not be prepared. Monosubstituted benzynes were generated in situ, by slow addition of a DME solution of

Table II. Ratios of anti to syn isomers of trisubstituted triptycenes.

	Č	COOH NH ₂	T E		
•	X =	Y =	ANTI	SYN	YIELD a
8	Cl	CH3	25%	75%	74%
5	CN	CH3	28%	72% ·	57%
23	COOCH ₃	CH3	31%	69%	58%
24	Cl	Cl	77%	23%	27%
25	COOCH,	Cl	73%	27%	20%
26	Cl	COOCH ₃	44%	56%	47%
27	CN	COOCH3	99%	1%	38%
17	COOCH,	COOCH3	76%	24%	62%

^a Yield is crude yield of both isomers prior to chromatography, based on anthracene starting material. Isomer ratios were obtained by integration of the ¹H NMR spectra of the crude triptycene mixture.

monosubstituted anthranilic acid into a solution of disubstituted anthracene and isoamyl nitrite in the same solvent. A twofold excess of monosubstituted anthranilic acid and isoamyl nitrite was used to insure complete reaction. Treatment of the product with aqueous NaOH neutralized the excess acid in solution and precipitated the product. In a few cases, the parent disubstituted anthracenes were present in the product mixtures. It has been reported that maleic anhydride can be used to scavenge anthracene⁵⁸, but it was found that an easier way to separate the anthracene from the triptycene was by sublimation. The yellow starting materials, which have lower melting points and higher volatility compared to the triptycenes, were sublimed off to yield the white mixture of triptycene isomers.

The lowest yields of triptycenes were obtained using chlorobenzyne as the dienophile. This suggests that yields of triptycenes depend on the ability of the substituted anthranilic acid to produce benzyne. It has been reported⁵⁸ that 3-chlorobenzyne is not easily produced via aprotic diazotization of 3-chloroanthranilic acid, or from the isolated chlorobenzenediazonium-2-carboxylate. Attempts to synthesize 1,8-dicyano-13- or -16-chlorotriptycene failed, presumably due to the difficulties in generating 3-chlorobenzyne combined with the very low solubility of 3. In comparison, the new aryne made from 3-methoxycarbonylbenzoic acid via aprotic diazotization gave triptycene products in 50-60% yields.

Separation of six pairs of structural isomers was carried out by semi-preparative HPLC using a silica gel column. The pairs of isomers formed using o-methoxycarbonylbenzyne were the easiest to separate.

Two sets of isomers could not be separated by HPLC; trichloro-

triptycene and dichloro(methyl)triptycene. 1,8,13- and 1,8,16-Trichloro-triptycene have been reported⁵⁵ to be separable on an alumina column using benzene as the eluent. TLC on alumina plates showed no separation in benzene or other solvents. No separation was observed using HPLC conditions similiar to those used with other pairs of isomers. 1,8-Dichloro-13-methyltriptycene was, however, separated from the anti isomer by slow evaporation of an ethyl acetate (EtOAc) solution of the mixture of compounds, whereupon the syn isomer selectively crystallized. Recrystallization from EtOAc gave the syn isomer in 95% isomeric purity.

The ratio of syn to anti isomers was determined by integration of the ¹H NMR spectra of the crude triptycene product (from at least two separate reactions). Table II shows the ratios obtained along with combined yields for compounds 5, 8, 17, 23-27. It is clear from Table II that the substituent on the benzyne (Y) is more important in dictating the observed regiochemistry than the substitutents on the anthracene (X). When $Y = CH_3$, the syn isomer is formed in a 2 or 3 to 1 ratio relative to the anti, regardless of the anthracene substituent X. Conversely, when Y = Cl, the anti isomer is preferred over the syn structure. Only when $Y = CO_2CH_3$, does the anti to syn ratio depend noticeably on X.

These ratios are interpreted as resulting from electronic effects of the substituents on the polarity of the orbitals of the benzyne with respect to the anthracene⁷⁴. All three anthracenes examined have electron withdrawing substituents at the 1- and 8-positions, which are expected to stabilize a partial negative charge at the 9-position and a partial positive charge at the 10-position, with the stabilization being

in the order $CN > CO_2CH_3 > Cl$. This prediction of stabilization is based on the relative electron withdrawing effect of the substituents (Hammett σ_p parameters⁷⁵). Because the bonding orbital of the benzyne is the π -bond orthogonal to the aromatic system of the benzyne ring, the more important effect of substituents is an inductive one via the σ network, rather than a resonance effect. Qualitatively, an electron-releasing substituent will generate a partial negative charge at the substituted carbon (C-3) of the benzyne, thus stabilizing a polarization of the benzyne as δ + at C-2 and δ - at C-1. An electron-withdrawing substituent will cause exactly the opposite polarization of the benzyne. Simple electrostatic matching of the polarized benzyne and anthracene satisfactorily accounts for the preferred regiochemistry in 5, 8, 23-25.

For 17, 26, 27 the observed regiochemistry depends on the anthracene substituents X. This is rationalized by the recognition that the substituent-induced polarization ($\sigma_{\rm I}$) of the benzyne π electrons by the methoxycarbonyl group ($\sigma_{\rm I}$ = 0.20) is intermediate between those of the methyl and chloro groups ($\sigma_{\rm I}$ = -0.04 and 0.46, respectively)⁷⁶. Consequently, an increased sensitivity to subtle changes in the electronic structure of the anthracene would be expected. For Y = ${\rm CO_2CH_3}$, the anti preference correlates with the ability of the anthracene to stabilize negative charge at C-9 and positive charge at C-10. For X = Cl, the resonance effect ($\sigma_{\rm R}$) is opposite in sign to $\sigma_{\rm p}$. It appears as if the resonance effect, which places a partial negative charge at C-10, dominates, giving a slight excess of the syn isomer. The almost exclusive formation of the anti isomer for X = CN is readily explained by the stronger combined $\sigma_{\rm p}$ and $\sigma_{\rm R}$ effects of CN versus

CO₂CH₃. Alternatively, the favorable alignment of opposed dipoles in the transition state may be significant in determining the final orientation of substituents. For example, the lowest energy arrangement of dipoles⁷⁷ of the benzyne and anthracene to produce 27 yields the anti isomer, and may account for the virtually exclusive formation of the isomer. None of the results suggests that steric effects are significant with the substituents examined.

2. Physical Properties

The melting points of the trisubstituted triptycenes are high, usually above 300 °C. The (HO)₃-tripod ligand melts at 420-424 °C with decomposition. Melting points of syn structures are higher than their anti analogs. The extraordinarily low solubility of many of these triptycenes in common organic solvents made it difficult to obtain analytically pure samples; preparative HPLC runs typically produced 4 1 mg/run. Several elemental analyses were somewhat low in carbon, apparently due to occlusion of methylene chloride in the triptycene lattice. The presence of CH₂Cl₂ was verified by ¹H NMR; integration gave stoichiometries consistent with the elemental analyses. Heating the compounds at 125 °C under a vacuum of 0.07 torr for 64 h did not remove all the chlorinated solvent present, as evidenced by a positive chloride test (sodium fusion method). Electron impact (direct exposure probe) mass spectra showed the molecular ion (M+) peak and usually, peaks due to the loss of substituents on the triptycene structure. High resolution mass spectra were obtained on triptycenes that analyzed low in carbon to confirm the exact mass.

The most effective way to differentiate the isomeric pairs of triptycenes was by their ¹H NMR spectra. The triptycene structure shows a characteristic pattern composed of four doublets, two doublet of doublets, and two singlets. The singlets are due to the bridgehead protons, and their shifts vary depending upon the substituents on the aromatic rings. The 'H NMR of triptycene was studied by Kidd, et al. 78, with the conclusion that chemical shifts are due to ring currents, bond anisotropies, and electron density contributions on the rigid structure. The data obtained confirm these results; the triptycenes with polar substituents show the largest 46 for the bridgehead protons. In each case, the syn isomer bridgehead proton signals show larger 45 than those for the anti isomer. The ABC spin system on each aromatic ring, shows $J_{AB} = J_{BC}$, and $J_{AC} = 0$. In some instances, the overlap of peaks made it necessary to decouple protons selectively in order to assign coupling constants. For 8a, 8s, 24a, 24s and 21a, 2-dimensional homonuclear chemical shift correlation (COSY) spectra were recorded in addition to 1-dimensional 1H NMR to determine coupling constants. Characterization of 17s, 7s and 19s was simplified, owing to the three-fold symmetry and the resulting magnetic equivalence of the identically substituted aromatic rings. The 'H NMR of the (HO)_s-tripod ligand looked like a cross between the spectra of 17s and p-aminophenol. The proton resonances of the OH and NH groups appeared as sharp singlets at 10.2 and 9.3 ppm, respectively. The bridgehead hydrogens appeared at 7.5 and 5.9 ppm, showing a large downfield shift from the bridgehead proton signal observed at 5.2 ppm for triptycene⁷⁸. Two sets of sharp doublets due to the ortho and meta protons on the phenolate ring occur at 7.4 and 6.6 ppm,

respectively. The resonance at 7.6 ppm (doublet) arises from protons at the 3, 6 and 15 positions of the triptycene; at 7.3 ppm (doublet) from the 4, 5, 16 positions; and at 7.2 ppm (doublet of doublet) from the 2, 7, 14 positions.

The 13C NMR spectra of the trisubstituted triptycenes typically showed two signals in the region of 43.3-54.7 ppm due to the bridgehead carbons, four signals between 147.8-141.4 ppm due to the carbons next to the bridgeheads, and eight aromatic ring signals at ~ 126 ppm. For some trisubstituted triptycenes, fewer signals were observed than predicted, presumably due to coincidental overlap of chemical shifts. Most of the 13C resonances observed for the (HO)3-tripod ligand can be tentatively assigned. The 13C NMR spectrum for the (HO)3-tripod ligand is shown in Figure 17. The aldehyde carbons are observed at 165.9 ppm. The shifts of the carbons on the free aromatic rings can be estimated by applying the principle of substituent additivity to incremental shifts reported for monosubstituted benzene rings⁷⁹. The incremental shifts are added to the shift observed for benzene carbon atoms (128.5 ppm), to give the calculated shifts shown in Table III. The remainder of the peaks are due to the carbons of the triptycene aromatic rings. The furthest downfield aromatic peak at 146.5 ppm is most likely due to the carbon atoms at the 1, 8 and 13 positions, since these are closest to the aldehyde group. The resonance at 141.2 ppm is probably due to the carbons next to the bridgehead carbon (on the same side as the substituents), and the peak at 129.9 ppm is assigned to carbons at the 3, 6 and 15 positions. The remainder of the resonances at ~ 125 ppm are not separated by more than 1 ppm and are difficult to assign.

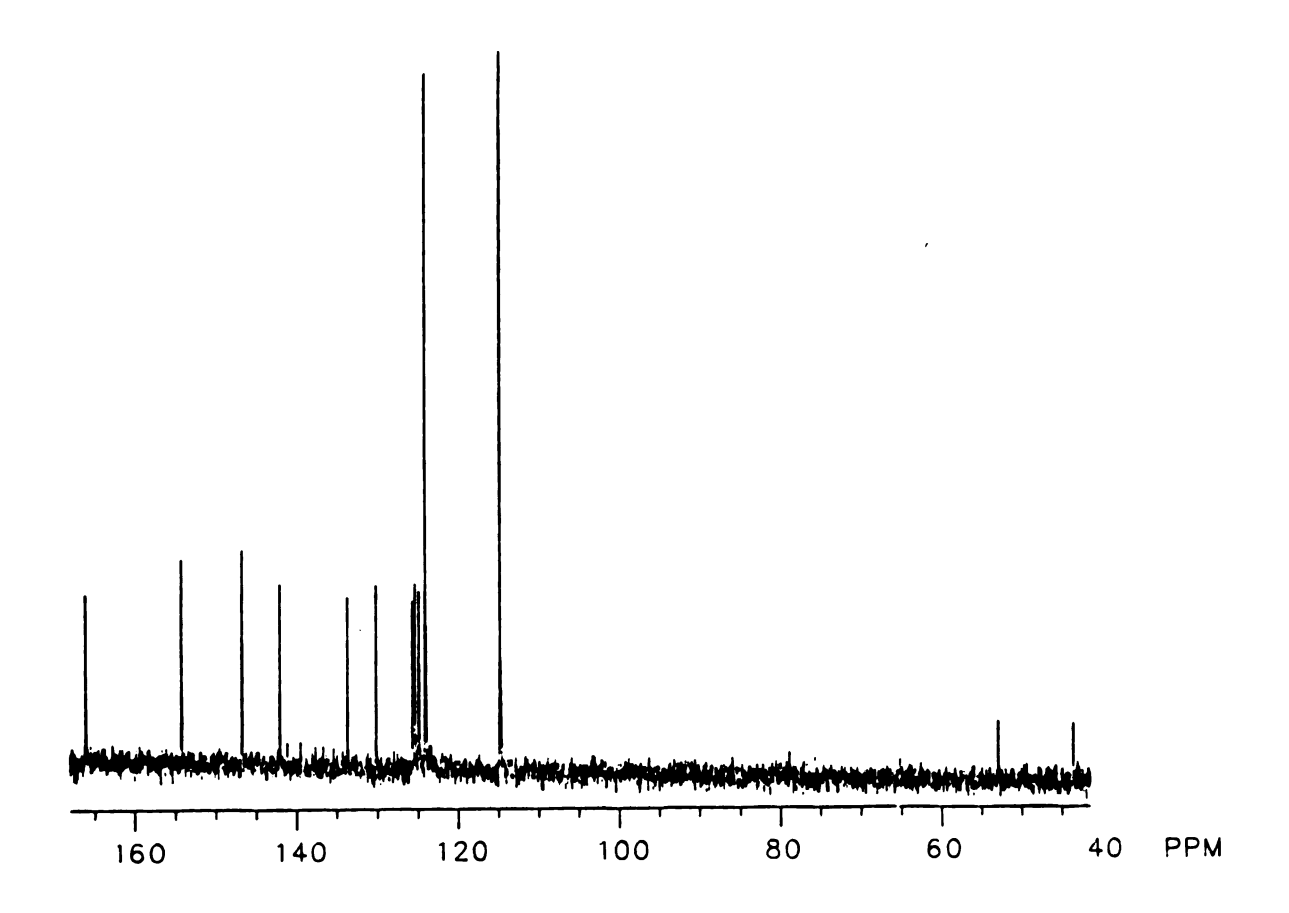


Figure 17. ¹³C NMR (360 MHz) of the (HO)₃-tripod ligand in Me₂SO-d₆.

Table III. Calculated and observed 13C NMR shifts for aromatic resonances of the (HO)3-tripod ligand.

	CH ₃ C=0	·	
2	NH 11 2		
0H	4 3		

	C atom	C atom	Calculated shift	Observed shift
1.	- 7.3	+ 11.1	132.3	133.4
2.	+ 1.4	- 9.9	120.0	123.8
3.	+ 12.7	+ 0.2	116.0	114.6
4.	+ 26.9	- 5.6	149.8	154.0

abased on incremental shifts of aromatic carbon atoms of monosubstituted benzenes (benzene at 128.5 ppm).

bvs TMS in Me₂SO (ppm).

B. Binding study of the (HO)3-tripod ligand to an Fe4S4 core

1. Synthetic approach

Two routes to preparing an oxygen-ligated iron-sulfur tetramer were employed. The first method utilized the fact that an equilibrium exists in the reaction of thiolate-ligated clusters and mercaptans, as shown in equation 3. It has been shown that when R is an alkyl group

it can be replaced by an R'SH group, where SR' is an aromatic thiol⁸⁰. The ligand replacement can be correlated to the acidity of the SR' group. The more acidic aromatic thiols will displace aliphatic thiols which have higher pK_B values. Kinetics data⁸¹ suggest a mechanism in which the rate determining step is protonation of the coordinated ligand followed by rapid separation of the alkylthiol and coordination of the arylthiolate. In the case of phenolates, an equilibrium exists where a small fraction of thiolate is displaced as shown in equation 4.

The reaction can be driven to the right by removing volatile thiol (R = Et, t-Bu) in vacuo. The tridentate ligand should replace three of the thiolates to produce the proposed model for the P-clusters.

The (HO)₃-tripod ligand was reacted with [Pr₄N]₂[Fe₄S₄(SEt)₄] in

Me₂SO-d₆ under a dynamic vacuum (to remove EtSH) for 12 h. The color of the solution changed from dark brown to red-brown. A red coloration is usually indicative of complexation by an oxygen-containing ligand⁸². The ¹H NMR spectrum of this reaction mixture was recorded and is discussed in the next section.

An alternative method of attaching the (HO)₃-tripod ligand employed a ligand exchange reaction between the tetraethylammonium salt of [Fe₄S₄Cl₄]²⁻ and the trisodium salt of the (HO)₃-tripod ligand in Me₂SO-d₄, as shown in equation 5. This method makes use of the

$$[Fe_4S_4Cl_4]^{2-} + Na_3(O_3-tripod) \longrightarrow [Fe_4S_4(O_3R)(Cl)]^{2-} + 3 NaCl + (5)$$

precipitation of NaCl as a driving force for complete substitution. The trisodium salt of the ligand was synthesized by dissolving the (HO)₃-tripod in DMA and reacting it with a solution of sodium methoxide (NaOMe) in MeOH. The DMA and MeOH were removed from the reaction mixture in vacuo, and the resultant solid was reacted with [Et₄N]₂[Fe₄S₄Cl₄] in Me₂SO-d₆. The results of the ¹H NMR studies are discussed below.

2. Proton nuclear magnetic resonance studies

The 'H NMR spectra of the solutions of (HO)₃-tripod ligand and Fe₄S₄ cluster show paramagnetically (isotropically) shifted peaks.

Paramagnetic shifts are the difference in shift between the observed frequency and the analogous diamagnetic reference frequency. Shifts downfield from the internal standard were assigned positive values.

Isotropic shifts were calculated using equation 683.

$$(\Delta H/H)_{iso} = (\Delta H/H)_{obs} - (\Delta H/H)_{dis}$$
 (6)

Because the interpretation of the NMR data depends upon existing theory of paramagnetic shifts, a brief outline of important factors is discussed. Isotropic shifts are due to two components, pseudocontact shifts and scalar shifts, as illustrated in equation 783. Pseudocontact

$$^{\Delta\nu}iso = ^{\Delta\nu}scalar + ^{\Delta\nu}pseudocontact$$
 (7)

or dipolar shifts are observed in the presence of a paramagnetic atom. These shifts are due to a through-space contribution to the observed field which arises from the proton spin orientation with respect to the paramagnetic center (in the magnetic field). Scalar or contact shifts are due to the change in observed field when an unpaired electron spin is delocalized onto a proton nucleus.

A series of $[Fe_4S_4(SR_4)]^{2-}$ clusters has been studied by ¹H NMR spectroscopy⁸⁴, and it has been shown that the dipolar contribution to shift is negligible compared to the contact contribution. Contact shifts observed for an alkyl ligand show that the ligand σ molecular orbitals are involved in the spin delocalization. A characteristic σ delocalization pattern shows a decrease in intensity of the observed signals as the distance from the paramagnetic center increases. In addition, all shifts are downfield from their diamagnetic references. This σ mechanism is consistent with what is observed for $[Fe_4S_4(SR)_4]^{2-}$ when $R = alkyl^{84}$.

Unpaired spin can also delocalize into the π system of an aromatic

ligand. This phenomenon is evidenced by the fact that shifts tend to alternate in sign between adjacent protons. In addition, the magnitude of the shift varies randomly as the distance increases between the resonating proton and the coordination site. For $[Fe_4S_4(SR)_4]^{2-}$ (where $R = aryl)^{84}$ and $[Fe_4S_4(OPh)_4]^{2-82}$, spins delocalize through the ligand π system causing a downfield shift of ortho and para protons but an upfield shift of meta protons. Spin density is stabilized at the ortho and para positions of the aromatic ring as seen in the resonance forms of a phenolate substituent shown in Figure 18.

Reported isotropic shifts of the phenyl protons of the $[Fe_4S_4(OPh)_4]^{2-45}$ complex and other arenethiolate analogs⁸⁴ allowed prediction of approximate chemical shifts for the isotropically shifted resonances of an $[Fe_4S_4(O_3R)(SR)]^{2-}$ cluster, as shown in Table IV. The ¹H NMR spectra of the product species from the reaction of $[Fe_4S_4(SEt)_4]^{2-}$ with the $(HO)_3$ -tripod ligand after 4h and 12h are shown in Figure 19. The spectrum of the free $(HO)_3$ -tripod ligand is shown at the top of Figure 19. The assignments of the diamagnetic resonances are discussed in section II.A.2. The triptycene bridgehead proton resonances are marked as T_B and the peaks due to aromatic protons are marked as T_A . Only the aromatic region is pictured since the peaks upfield from 6 ppm are due only to cation and solvent protons.

The resonances observed for protons bound to the Fe-S cluster show broadened signals due to the fact that paramagnetic ions induce efficient relaxation mechanisms and linewidth is inversely proportional to the efficiency of relaxation. The ortho peak is broader than the meta peak due to the fact that dipolar broadening has an r^{-6}

Figure 18. Schematic drawing showing spin density
stabilization at the ortho and para positions
of an aromatic ring.

Table IV. Isotropic shifts^a for ligand protons in $[Fe_4S_4(O_3-tripod)(SEt)]^{2-} \text{ and } [Fe_4S_6(O_3-tripod)_2]^{3-}$ species in Me₂SO-d₆ solution.

Observed	Diamagnetic	Reported	Predicted ^b	Observed	Observed ^C
proton	shift	Isotropic	shift	shift	Isotropic
		shift			shift
o−H (tet)	7.4d	- 2.3f	5.1	5.5	- 1.9
H (tet)	6.6d	+ 2.2f	8.8	9.1	+ 2.5
o-H (hex)	7.4d	- 5.3g	2.1	_	-
H (hex)	6.6d	+ 5.0g	11.6	11.6	+ 5.0
H ₂ (EtS ⁻)	2.5 ^e	+ 10.0h	12.5	12.5	+ 10.0
H, (EtS-)	1.3 e	+ 1.1h	2.4	2.3	+ 1.2

avs. TMS (ppm).

bdiamagnetic shift + reported shift for similar proton.

cobserved shift - diamagnetic shift.

dshift of free O-tripod ligand.

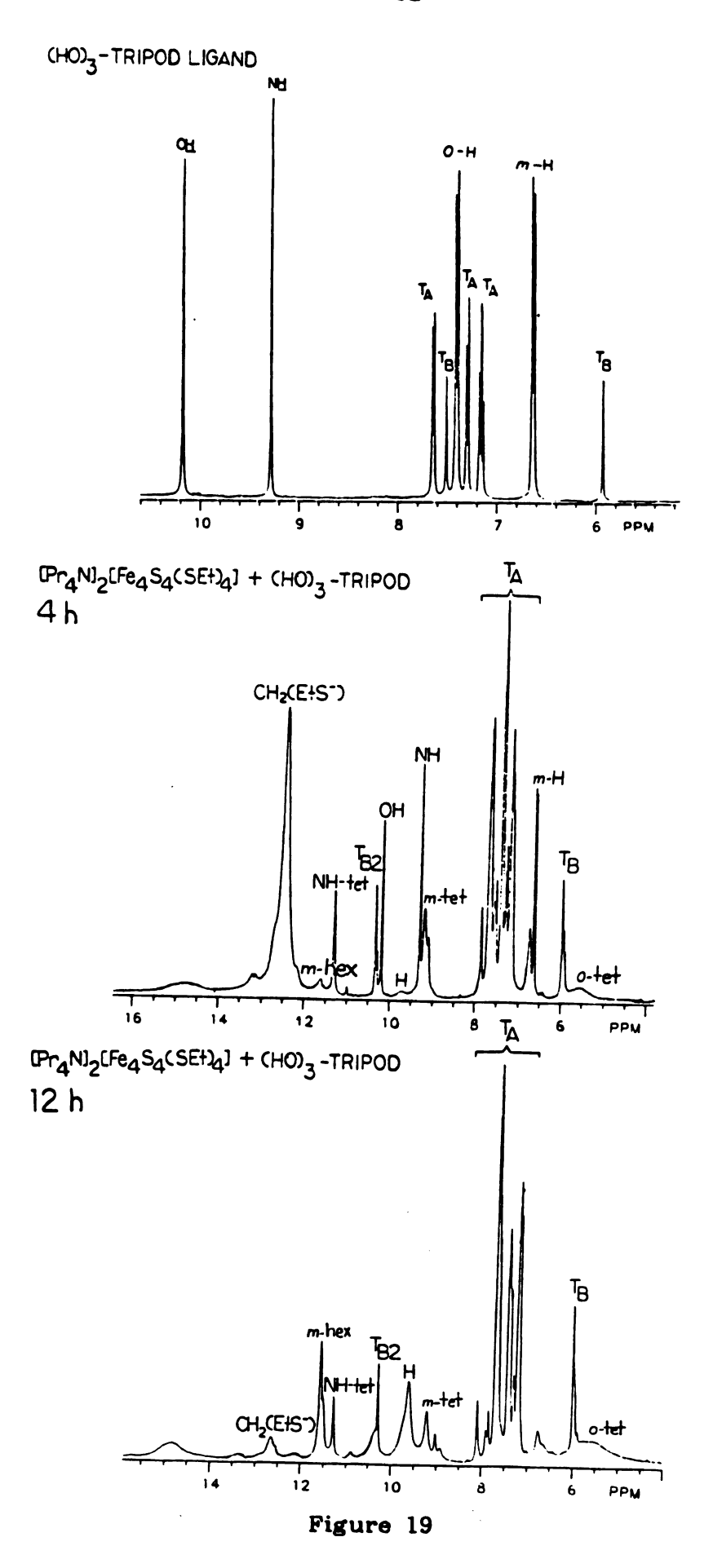
eshift of free ethanethiol (ref. 84)

fisotropic shift of respective protons from [Fe₄S₄(OPh)₄]²⁻ (ref. 47).

Sisotropic shift of respective protons from [Fe₆S₆(OPh)₆]²⁻ (ref. 86).

hisotropic shift of respective protons from [Fe₄S₄(SEt)₄]²⁻ (ref. 84).

Figure 19. ¹H NMR spectra (360 MHz) of the (HO)₃-tripod ligand and its reaction with [Pr₄N]₂[Fe₄S₄(SEt)₄] in Me₂SO-d₆ after a 4 h period and a 12 h period.



dependence⁸⁵. The alternation in signs of the isotropic shifts for the ortho and meta protons and the decrease in intensity of the signal the closer the proton is to the paramagnetic center, are confirmatory signs of dominant contact interaction via a π delocalization mechanism. Table IV shows that the observed isotropic shifts are very close in magnitude and sign to those shifts reported for related compounds.

The spectrum recorded after a 4h reaction period shows peaks at 5.5 ppm and 9.9 ppm which are assigned to the contact shifted ortho and meta protons of the ligand attached to tetramer (noted as o-tet and m-tet). The isotropically shifted resonances of the ethanethiclate group appear at 2.3 ppm (CH₃-EtS⁻) and 12.5 ppm (CH₂-EtS⁻), but the peak intensity is too large for only one EtS⁻ group attached to a cluster.

An analogous ligand substitution reaction between $[Pr_4N]_2[Fe_4S_4(SEt)_4]$ and the $(HO)_3$ -tripod ligand was allowed to run for 12 h. The ¹H NMR spectrum shows no evidence of free ligand and less intense peaks of the ethanethiclate group, indicating that the reaction has gone to completion. Besides the paramagnetically shifted peaks assigned to the tetrameric cluster, peaks that could be assigned to the formation of a hexameric Fe_4S_4 cluster were observed. Hexameric clusters typically show larger isotropic shifts than their tetramer analogs⁸⁶. The meta proton of the $[Fe_4S_4(O_3\text{-tripod})_2]^{3-}$ compound (noted as m-hex) appeared at 11.6 ppm, the ortho proton was expected to appear at 2.1 ppm, but no signal was observed in this region. The ortho proton resonance may be too broad for observation or it may be obscured by the cation resonances in this region.

There are three large signals (at 9.8, 10.4 and 11.3 ppm), that are

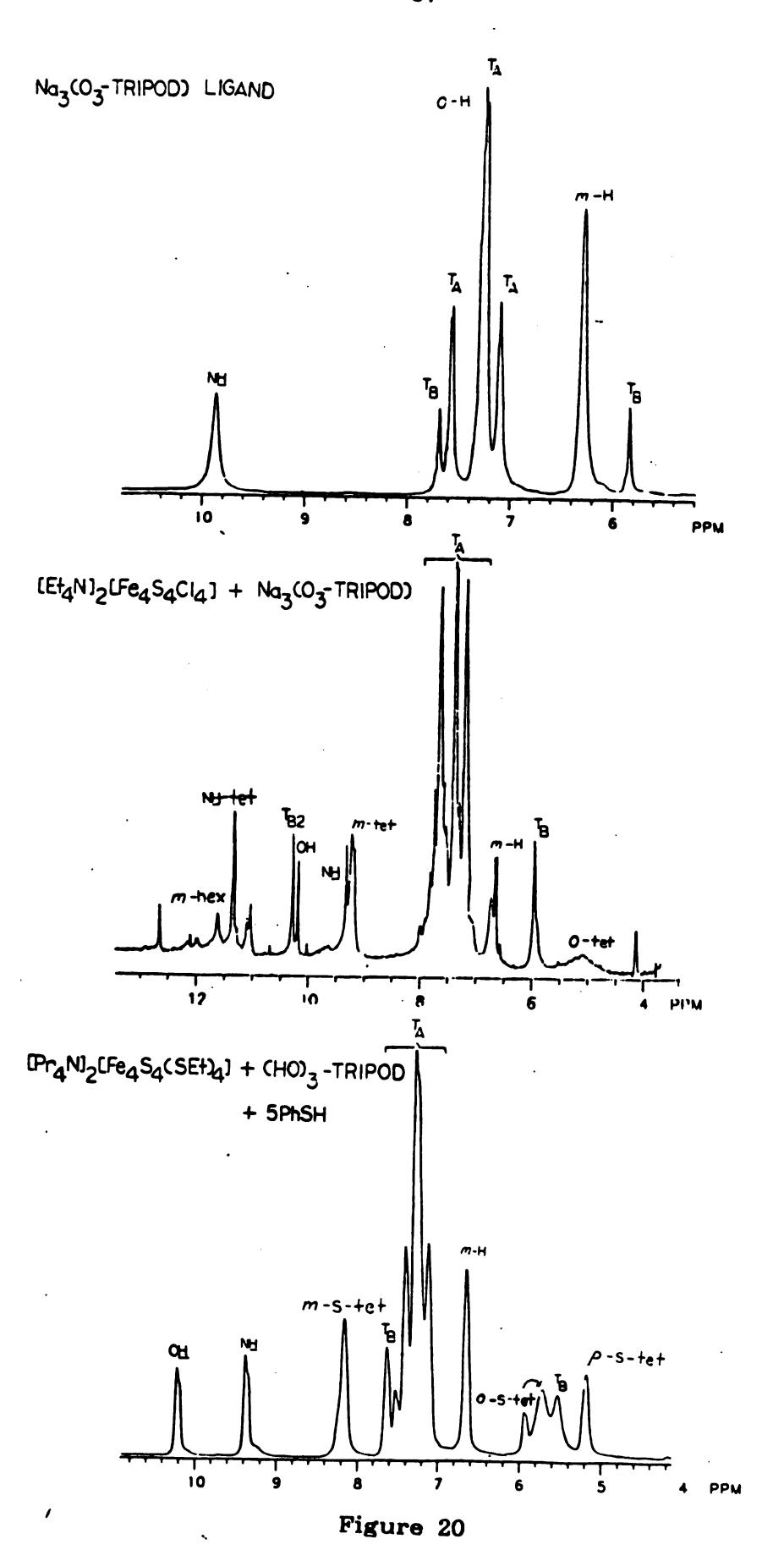
shifted downfield but are not accountable as an ortho or meta resonance of the $[Fe_6S_6(O_3-tripod)_2]^{3-}$ or $[Fe_4S_4(O_3-tripod)]^{2-}$ species. The broad peak at 9.8 ppm (noted as H) increases in intensity as the m-hex peak intensity increases. The peak at 10.4 ppm (noted as T_{B2}) is present even when the reaction has not yet gone to completion and appears too sharp to be contact shifted. This signal (TR2) may be the bridgehead proton of the triptycene (the proton on the same side of the molecule as the substituents). As discussed earlier, the change in shift of the bridgehead protons is extremely sensitive to the nature of the substituents on the aromatic rings. The shift observed upon binding to the cluster could be a through-space interaction due to the unpaired electrons of a sulfur atom on a cubane core being pointed towards the inner bridgehead proton. The intensity of the TB2 peak is the same as the that of peak TB, which is unshifted from its position in the diamagnetic ligand. The third large peak at 11.3 ppm (noted as NH-tet) is assigned to the contact shifted proton of the para NH group on the ligand. Although this peak has a narrow linewidth for an scalar shifted resonance, it is far enough away from the paramagnetic center that any broadening should be minimized. The intensity of the NH-tet peak is half that of the m-tet peak, as would be expected.

Cleland, et al.^{47b} noted certain drawbacks in synthesizing [Fe₄S₄(OPh)₄]²⁻ by removal of volatile thiol; one of which was that a new type of cluster compound with significantly larger isotropic shifts was observed. This new type of cluster was later reported to be phenoxide-ligated hexamer⁸⁶. A second method of ligand exchange reaction between [Fe₄S₄Cl₄]²⁻ and sodium phenoxide was reported to minimize the likelihood of forming a hexameric complex^{47b}. The ligand

substitution method was attempted on the chloro tetramer and the trisodium salt of the tripodal ligand since the first synthesis method was giving a mixture of products. The ¹H NMR spectra of Na₃(O₃-tripod) and the product species from its reaction with $[Fe_4S_4Cl_4]^{2-}$ are shown in Figure 20. The absence of the OH signal in the ¹H NMR spectrum of the Na₃(O₃-tripod) ligand confirms that the salt was formed. The spectrum of Na₃(O₃-tripod) + $[Fe_4S_4Cl_4]^{2-}$ is essentially the same as the spectrum of $(HO)_3$ -tripod + $[Fe_4S_4(SEt)_4]^{2-}$, proving that both methods of ligand substitution are producing a mixture of tetrameric and hexameric cluster species in solution.

The spectrum of [Fe₄S₄Cl₄]²⁻ and Na₃(O₃-tripod) shows the ortho proton peak of the ligand bound to the tetrameric core at 5.1 ppm and the meta proton at 9.2 ppm. The meta proton of the ligand bound to the hexameric cluster was observed at 11.6 ppm. The reactions between the chloro tetramer and the ligand were allowed to stir for 8 h before the NMR was recorded. Several peaks in the spectrum can be assigned to free ligand (OH, NH), but since there is no evidence of free ligand in the spectrum of $Na_3(O_3-tripod)$ another explanation is necessary to account for these resonances. If the reaction mixture is stirred for 24 h the spectrum shows the disappearance of paramagnetically shifted peaks and an increase in free ligand resonances. It is possible that traces of water in the Me₂SO-d₆ (which is exceedingly difficult to dry completely) promoted the generation of free ligand by hydrolysis of the trisodium salt; however, no evidence of free ligand was observed in the 'H NMR spectrum of the Na₃(O₃-tripod) taken in the same solvent as the ligand exchange reactions were performed. It is more probable that the high-coordinating ability of

Figure 20. ¹H NMR spectra (360 MHz) of Na₃(O₃-tripod),
reaction between Na₃(O₃-tripod) and
[Et₄N]₂[Fe₄S₄Cl₄], and reaction of
[Pr₄N]₂[Fe₄S₄(SEt)₄] with (HO)₃-tripod and five
equivalents of PhSH in Me₂SO-d₄.



the Me₂SO-d₆ solvent (in the presence of water) causes partial solvation of the cluster to produce some free (HO)₃-tripod ligand as shown in equation 8. This type of equilibrium reaction has been

$$[Fe_4S_4(O_5R)(Cl)]^{2-} \xrightarrow{Me_2SO} [Fe_4S_4(Me_2SO)_5(Cl)]^+ + (HO)_5-tripod (8)$$

$$H_2O$$

observed for [Fe₄S₄Cl₂(OPh)₂]²⁻⁴⁹, where the ¹H NMR spectrum recorded in Me₂SO-d₆ showed only the presence of free phenol and hence "complete" solvation of the cluster. The lability of coordinated phenoxide ligands has been demonstrated with [Fe₄S₄(OPh)₄]²⁻⁸², and it appears that the (HO)3-tripod is labile enough to result in solvation of the mixed-ligand cluster. It should be noted that the reaction of [Pr₄N]₂[Fe₄S₄(SEt)₄] with the (HO)₃-tripod ligand shows little evidence of free ligand resonances. One explanation for the absence of free ligand could involve the different preparation of the [Fe₄S₄(SEt)₄]²⁻ + $Na_3(O_3$ -tripod) NMR sample compared to that of the chloro tetramer reaction with the Na₃(O₃-tripod) ligand. When [Fe₄S₄(SEt)₄]²⁻ was reacted with the ligand a small aliquot of solvent was injected into the reaction flask and then removed to dryness in vacuo, new solvent was then reinjected and the process repeated for a 12 h time period. The cluster mixture was in contact with the Me₂SO-d₆ for only short periods of time. This short exposure to the solvent limits the possibility of solvation of the cluster. The insolubility of the Na₃(O₃-tripod) ligand made it impossible to carry out the ligand binding reactions in non-coordinating solvents. Attempts to bind the ligand to an Fe-S cluster in CD₃CN, in hopes that the coordinated

cluster would be more soluble in CD₃CN than the individual starting materials, were unsuccessful.

To insure that the (HO)₃-tripod ligand or the Fe₄S₄ unit was not decomposing under the reaction conditions, five equivalents of thiophenol was added to the reaction mixture of [Fe₄S₄(SEt)₄]²⁻ and the (HO)₃-tripod. The resultant spectrum is shown on the bottom of Figure 20. The more acidic thiophenol quantitatively displaces coordinated (HO)₃-tripod ligand to yield [Fe₄S₄(SPh)₄]²⁻ and free ligand. New paramagnetic resonances appear at 5.2 (p-H), 5.7 (o-H) and 8.2 (m-H) ppm, which correspond to the reported thiolate Fe-S cluster shifts⁸⁴. The remaining peaks in the spectrum were due to the diamagnetic ligand.

A series of samples in which the ratio of cluster to ligand was varied, in order to maximize formation of either the tetrameric or hexameric forms of the iron-sulfur clusters, was examined by 'H NMR. Figure 21 shows the spectra that resulted from these experiments and the ratios used. The formation of hexamer should be maximized when the ratio of cluster to ligand is 3:4, since three tetrameric units rearrange to form two hexameric units and each hexameric unit requires two ligands. When the ratio of cluster to ligand is 1:1, the formation of tetrameric cluster should be maximized. The changes in intensities of the o-tet, m-tet, NH-tet, m-hex and H peaks were compared in the stacked plot of spectra. The ratio of ligand to cluster present did effect the amount of tetrameric to hexameric species observed. Irrespective of the ligand to cluster ratio used, the reaction produced a mixture of hexamer and tetramer. The general trend seen in the spectra was that as the peaks H and m-hex grew in intensity,

Figure 21. ¹H NMR spectra (360 MHz) of the reaction between [Et₄N]₂[Fe₄S₄Cl₄] and Na₃(O₃-tripod) in Me₂SO-d₆.

The ratio of cluster to ligand (C:L) used in the reactions is indicated next to each spectrum.

 $[Et_4Nl_2[Fe_4S_4Cl_4] + No_3(O_3-TRIPOD)$

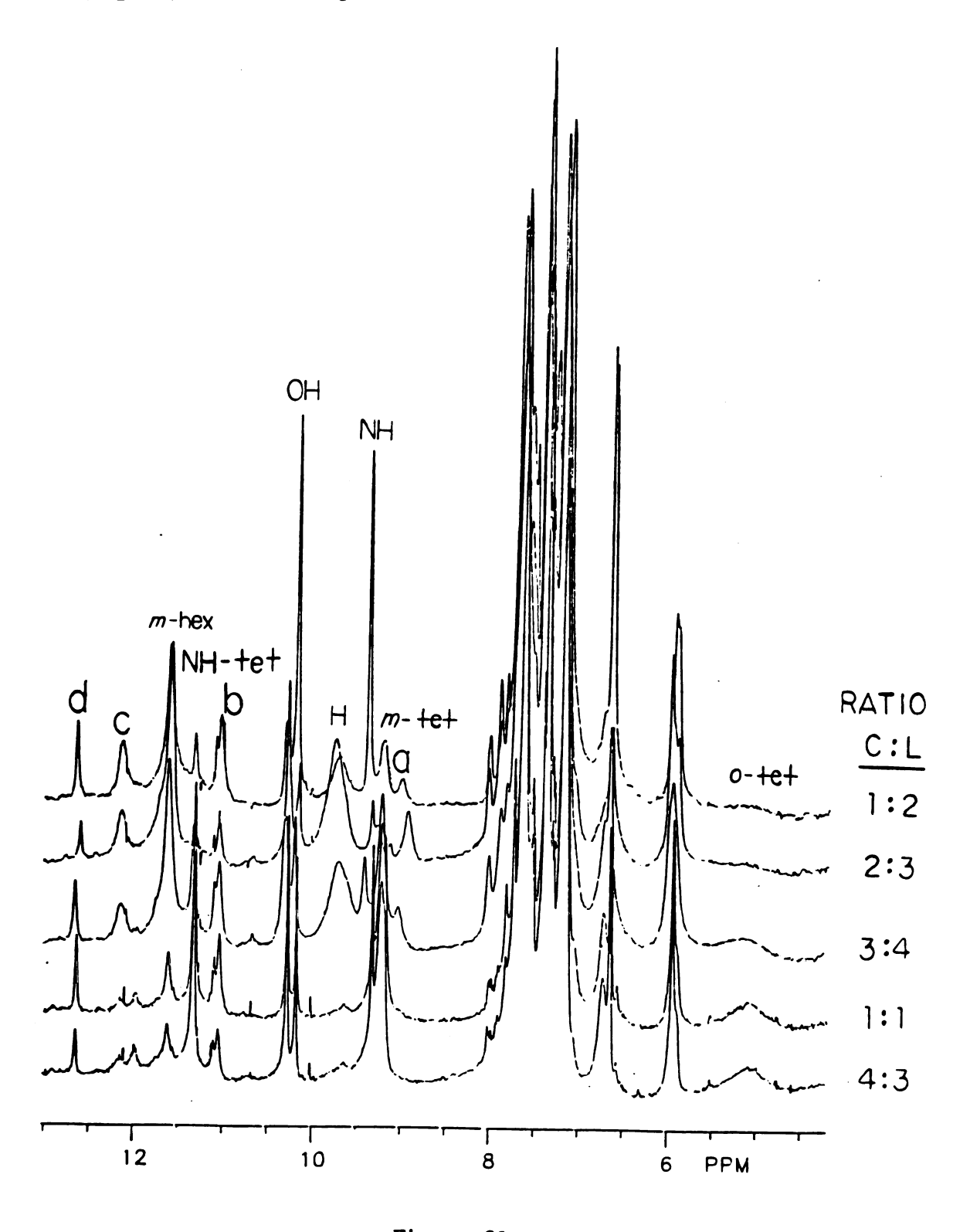


Figure 21

the peaks m-tet, o-tet and NH-tet decreased in intensity. This trend suggests that peak H is associated with a hexameric structure.

Figure 22 shows a schematic of the possible species present in solution which is consistent with the NMR experiments. The (HO)₃-tripod ligand is binding to an Fe₄S₄ core, but in solution the mixed-ligand cluster, [Fe₄S₄(O₃R)(Cl)]²⁻, readily converts to other clusters. When two mixed-ligand tetramers interact, an $[Fe_6S_6(O_3R)_2]^{3-}$ species can be generated in addition to a metastable [Fe₂S₂Cl₂(solvent)₂]²⁻ complex which will rapidly rearrange to form [Fe₄S₄Cl₄]²⁻. The chloro tetramer species can then react with $Na_3(O_3-tripod)$ to give back the original $[Fe_4S_4(O_3R)(Cl)]^{2-}$ complex. When four mixed-ligand complexes interact in solution, a mixture of $[Fe_6S_6(O_3R)_2]^{3-}$ and chloro tetramer will be observed. When three tetrameric mixed-ligand clusters interact, [Fe₆S₆(O₅R)₂]³⁻ can be generated along with a mixed-ligand hexameric cluster, $[Fe_6S_6(O_3R)(Cl)_3]^{3-}$. The H peak is assigned to the meta proton of this mixed-ligand hexameric species. In the presence of excess ligand, the $[Fe_4S_4(O_3R)(Cl)_3]^{3-}$ should, in principle, convert to $[Fe_4S_4(O_3R)_2]^{3-}$. The spectrum taken at a cluster to ligand ratio of 1:2 showed a decrease in peak H intensity while the m-hex peak increased, providing further evidence of the assignment of H. Additional evidence of the existance of a mixed-ligand hexameric species is seen in the reaction between [Pr4N]2[Fe4S4(SEt)4] and (HO)3-tripod. A very broad peak at 14.7 ppm is observed and can be assigned to the CH2 protons of the ethanethiclate group in [Fe₆S₆(O₃-tripod)(SEt)₃]³⁻. The mixture of Fe-S species present in the 'H NMR studies are a result of a complex rearrangement of the mixed-ligand [Fe₄S₄(O₃-tripod)(Cl)]²⁻ cluster in

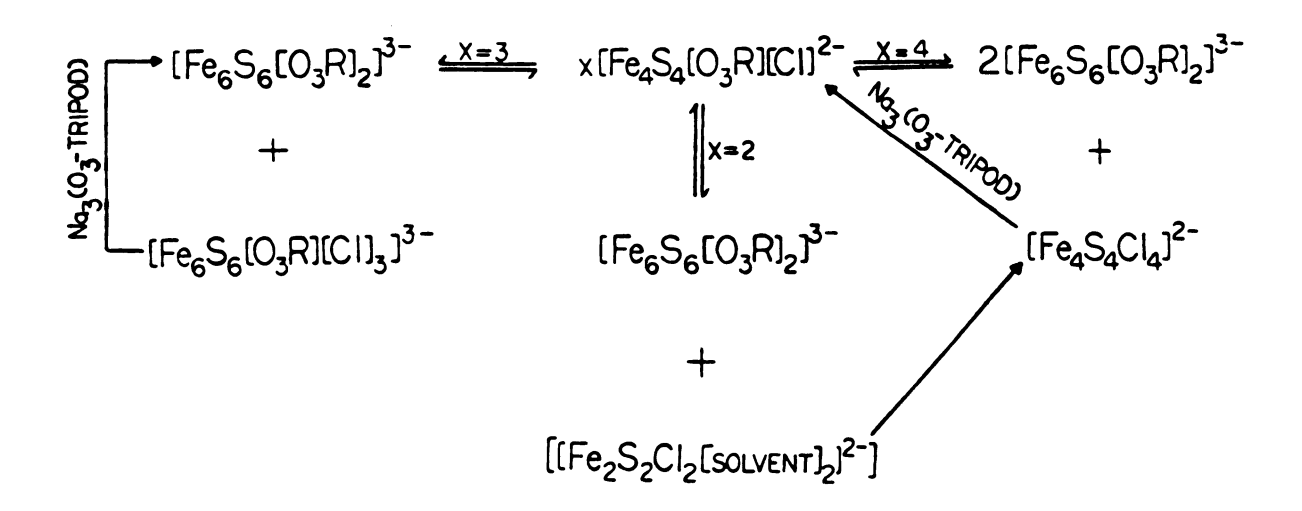


Figure 22. Schematic of possible Fe-S clusters present from interconversions of an $[Fe_4S_4(O_3R)(Cl)]^{2-}$ cluster in solution.

solution. Similarity of solubility properties in polar solvents prevents isolation of either the tetrameric or hexameric species.

The structure of [Fe₆S₆Cl₆]³⁻ 87 has been recently reported to be a distorted hexagonal prism in which two cyclohexane-chair Fe₃S₃ units are eclipsed relative to one another. The distance between iron atoms that lie within a plane perpendicular to the C₃ axis is 3.8 Å, while the distance between iron atoms of the Fe₂S₂ rhombic side units is 2.7 Å. The 2.7 Å distance is identical to the separation of iron atoms in a tetrameric Fe-S core³⁸. The (HO)₃-tripod ligand is designed to span the corners of an Fe₄S₄ cluster, but there are two possible coordination sites in which the ligand can bind to an Fe₆S₆ core. The (HO)₃-tripod ligand can coordinate either to three iron atoms that lie within the hexagonal bases of the prism along the C₃ axis (<u>I</u>), or to iron atoms on different hexagonal bases such that the ligand is bound almost perpendicular to the C₃ axis (<u>II</u>). A schematic of the two possible structures is shown in Figure 23.

Crystallographic data and CPK models were used to estimate the distance necessary for coordination between the terminal oxygen atoms on the ligand and the two possible hexameric structures. The structural parameters for $[Et_4N]_3[Fe_6S_6Cl_6]^{87}$ were used to calculate the distance between terminal Cl atoms and these distances were then corrected for the difference between Fe-Cl and Fe-O bond lengths using simple trigonometric relationships. The results show that there has to be a 6.7 Å distance between oxygen atoms in order for the ligand to bind to iron atoms which lie within a hexagonal base and a 4.9 Å distance to bind to Fe atoms on alternate bases. The O-O distance necessary to span a cubane core is 5.9 Å.

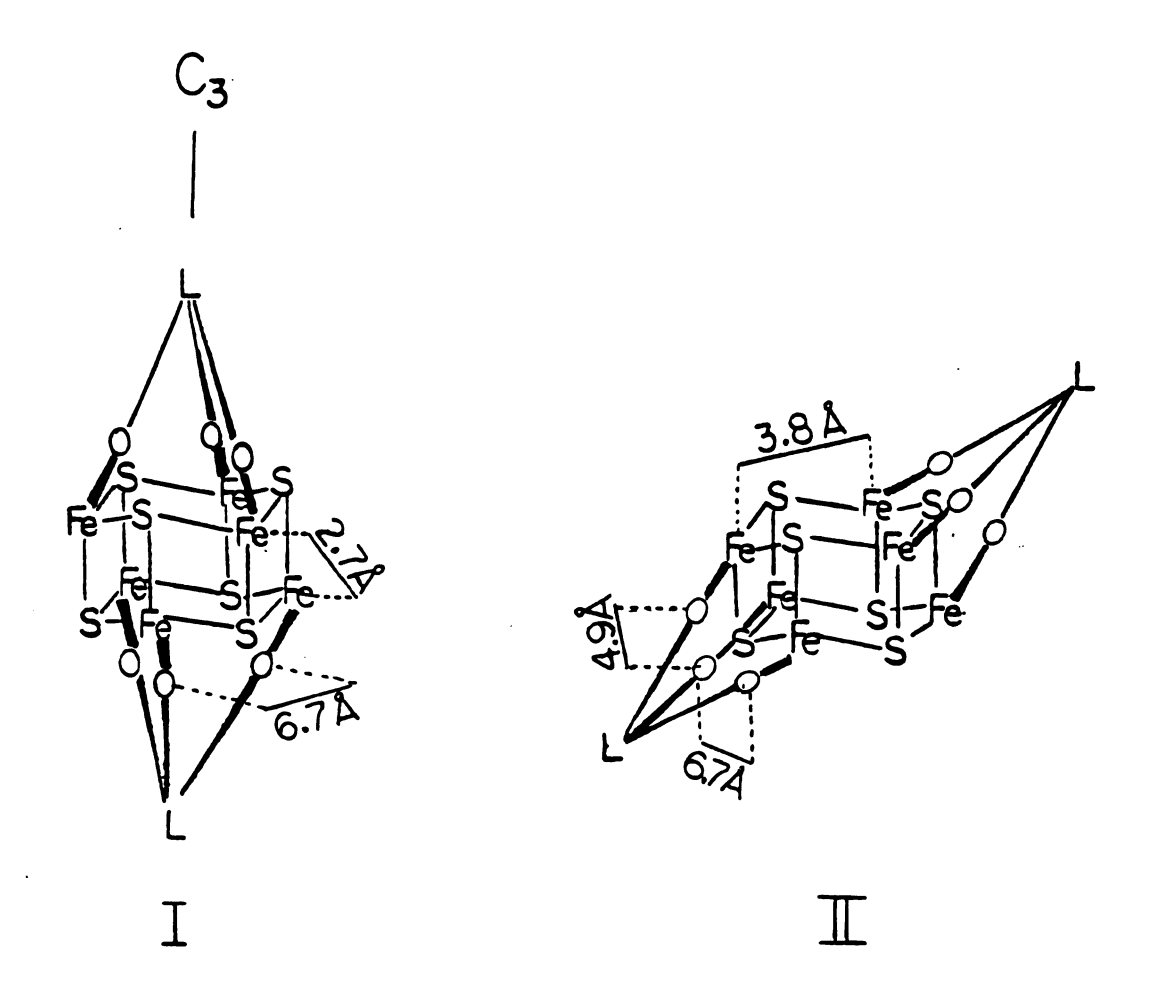


Figure 23. Schematic drawing of two possible coordination modes of the (HO)₃-tripod ligand to an Fe_6S_6 hexagonal core.

Coordination of the ligand as in structure II should result in the loss of 3-fold symmetry of the molecule and consequently an inequivalence of meta proton resonances should be observed. The six meta protons on each ligand would split into two sets of resonances with relative intensities of 2 to 1. The peaks labelled a and c, in the spectra shown in Figure 21, simultaneously increase in intensity along with the meta signals H and m-hex. The a and c resonances could be due to the inequivalent set of protons from the ligand bound to the sides of the hexagonal prism. Qualitatively, it appears as if the more stable hexameric structure is the one where the ligand binds along the C₃ axis. Steric and electronic interactions are minimized in this configuration because the sulfur atom of the cluster is not situated within the ligand cavity and the iron atoms are furthest apart. observed ratio of ~ 4:1 for peaks H:a and m-hex:c suggests that a rapid interconversion between the two modes of binding may be occurring in solution and the more stable structure dominates. The peaks labelled b and d in Figure 21 could be the NH resonances of the $[Fe_6S_6(O_3R)_2]^{3-}$ and the $[Fe_6S_6(O_3R)(Cl)_3]^{3-}$ species. Another set of NH peaks is possibly obscured by other resonances in the region between 11 and 12 ppm. The system is too complicated to definatively assign these resonances.

The accumulated data indicates the possible existance of five Fe-S clusters in solution. The inability of the $(HO)_3$ -tripod ligand to stabilize a 3:1 mixed-ligand Fe₄S₄ cluster in solution has been demonstrated. The Fe-O bonds of tetrameric clusters are known to be covalent in nature and are capable of donating electron density into the $[Fe_4S_4]^{2+}$ core^{47,87}. Conversion to the $[Fe_6S_6]^{3+}$ core probably

allows the spin density to delocalize, as evidenced by the larger contact shifts for the hexameric structures. It is concluded from the NMR experiments that the Fe₆S₆ species are thermodynamically or kinetically stabilized by the terminal oxygen ligation of the (HO)₃-tripod ligand.

C. $[Et_4N]_2[S_2MoS_2Fe(OAc)_2]$

1. Synthesis

Oxygen-ligated molybdenum-iron-sulfur complexes have been synthesized by two methods 19,22 . The first method involved a ligand exchange reaction on a preformed S_2MoS_2Fe cluster. This method was the one used to form $[S_2MoS_2Fe(OAr)_2]^{2-}$ (Ar = Ph, p-tolyl) 21 . The second method involves a direct self-assembly reaction from tetrathiomolybdate and an appropriate iron(II) complex.

Synthesis of $[S_2MoS_2Fe(OAc)_2]^{2-}$ was accomplished using the self-assembly approach. The tetraethylammonium salt of tetrathiomolybdate was reacted with anhydrous ferrous acetate in acetonitrile as shown in equation 9. The resulting dark brown

$$[Et_4N]_2MoS_4 + Fe(O_2CCH_3)_2 \longrightarrow [Et_4N]_2[S_2MoS_2Fe(O_2CCH_3)_2]$$
 (9)

solution was reduced in volume and addition of diethyl ether precipitated a red-brown solid in 75% yield. Attempts to crystallize this compound from acetonitrile or propionitrile resulted in the formation of a black solid, whose optical spectrum in CH₃CN revealed

 $\lambda_{\rm max}$ at 584, 518, 460, 412, 310 and 288 nm, which resembles the spectrum of $[{\rm Et_4N}]_3[{\rm Fe}({\rm MoS_4})_2]^{28}$. This suggests that the bis(tetrathiomolybdate)iron trianion is thermodynamically more stable in solution than the oxygen-ligated dimer. The trianion species may be formed due to the acetate groups dissociating in solution and allowing the iron to reduce the molybdenum.

Synthesis of $[S_2MoS_2Fe(O_2C_2O_2C_6H_5)]^{2-}$ was attempted by ligand substitution reaction of $[S_2MoS_2FeCl_2]^{2-}$ with sodium phthalate $(NaO_2C_2O_2C_6H_5)$. This also resulted in formation of $[Fe(MoS_4)_2]^{3-}$ rather than the desired complex.

2. Physical Properties

a. Optical

The electronic absorption spectrum of $[S_2MoS_2Fe(OAc)_2]^{2-}$ is shown in Figure 24. Peak positions and molar absorptivities are presented in Table V along with those reported for $[S_2MoS_2Fe(OPh)_2]^{2-}$ and $[S_2MoS_2FeCl_2]^{2-}$. The spectrum of the iron-molybdenum-acetate dimer shows intense absorptions between 520 and 400 nm. Both phenoxide-ligated and chloro-ligated dimers show the same type of absorption pattern. Any cluster containing a tetrathiomolybdate unit shows peaks in this region due to sulfur to molybdenum charge transfer transitions⁸⁹, which are observed at $\lambda_{max} = 470$ nm for the free $[MoS_4]^{2-}$. It can be deduced that the band at 464 nm, in the case of the acetate dimer, is a $S \to Mo$ ($\pi \to d$) transition.

The peak at 432 nm of the chloro dimer has been assigned to

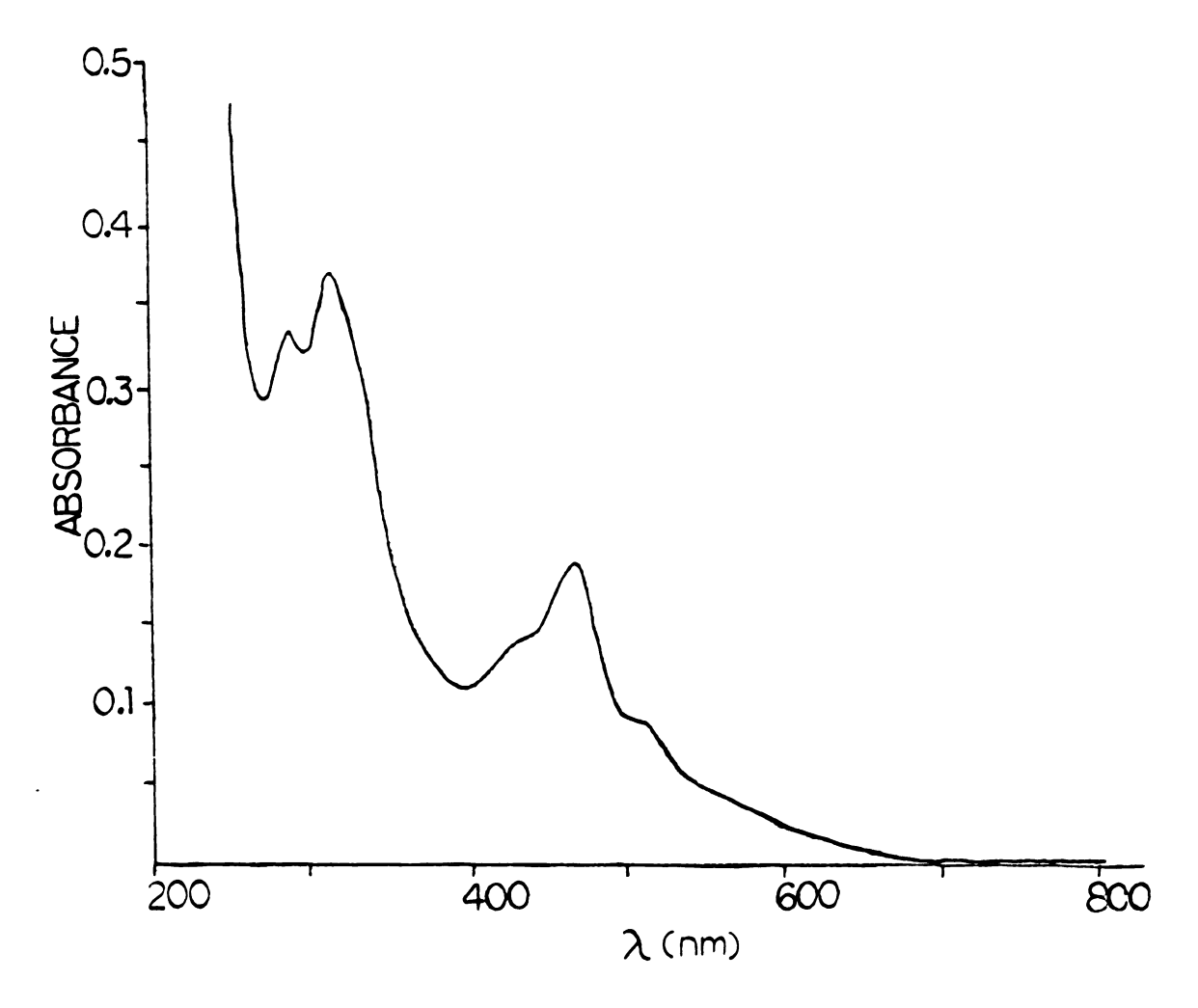


Figure 24. Electronic spectum of $[Et_4N]_2[S_2MoS_2Fe(OAc)_2]$ in CH_3CN .

Table V. Electronic spectral features and molar absorptivities^a for $[S_2MoS_2Fe(OAc)_2]^{2-} \ , \ [S_2MoS_2FeCl_2]^{2-} \ b \ and \\ [S_2MoS_2Fe(OPh)_2]^{2-} \ complexes.$

Complex	λ (10² ε)	
[S ₂ MoS ₂ Fe(OAc) ₂] ²⁻ 286 (78	310 (100) 428	(sh) 464 (53) 516 (sh)
$[S_2MoS_2Fe(OPh)_2]^{2-}$ 232 (19	7) 314 (147) 391	(75) 471 (98) 530 (sh)
$[S_2MoS_2FeCl_2]^{2-}$ 290 (11)	0) 314 (124) 432	(48) 469 (64) 528 (sh)

ain acetonitrile solutions; values in nm, with molar absorptivities in parentheses.

bReference 21.

^CReference 19.

another sulfur to molybdenum charge transfer band which arises from a splitting of degenerate energy levels of the tetrathiomolybdate when the iron binds to the sulfur⁹⁰. Coordination of the iron lowers the symmetry of the [MoS₄]²⁻ unit, and hence two bands are observed. The shoulder peak at 428 nm observed in the acetate dimer may be due to this same phenomenon. The shoulder peak at 516 nm of the acetate dimer can be assigned as a sulfur to iron charge transition since no such low energy absorption is observed in the spectra of [MoS₄]²⁻ anions. The oxygen ligation does not change the spectrum much from that of the chloro-ligated dimer; but the peaks are blue-shifted from other thiolate analogs¹⁹.

b. Proton nuclear magnetic resonance

The variable temperature ¹H NMR spectra of [S₂MoS₂Fe(OAc)₂]²⁻ recorded in the range of -25 °C to 40 °C in CD₃CN are shown in Figure 25. Table VI shows the isotropic shifts based on a diamagnetic shift of 2.01 ppm for free acetic acid. The complex shows one broad peak due to the methyl protons of the acetate group. The resonances due to the tetraethylammonium cation are broadened slightly but remained unshifted with the change in temperature. As the temperature is increased the isotropic shift ((AH/H_{iso})) of the acetate protons is decreased. A decrease in shift as the temperature is increased was observed by Silvis⁹¹ for dominant contact interactions of the thiophenolate and thiotosylate-ligated Fe-Mo-S dimers. By analogy, it can be assumed that the paramagnetic shifts for the acetate dimer are due to dominant contact interactions. The equation for contact

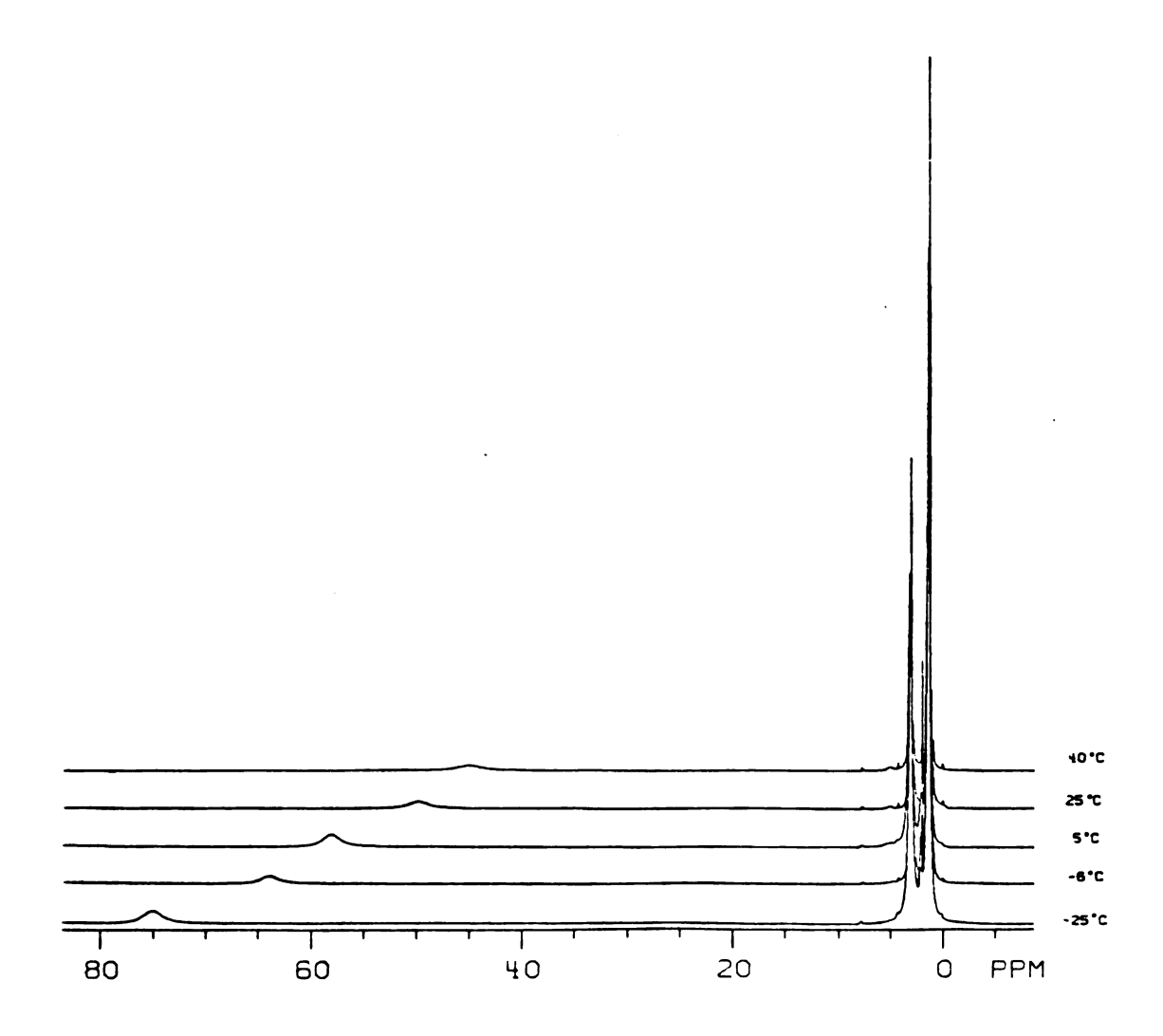


Figure 25. ¹H NMR spectra (360 MHz) of [Et₄N]₂[S₂MoS₂Fe(OAc)₂] in CD₃CN at various temperatures.

Table VI. Isotropic proton nuclear magnetic resonance shifts^a

((AH/H)_{iso}) observed for the OAc group of

[Et₄N]₂[S₂MoS₂Fe(OAc)₂] at various temperatures in

CD₃CN.

Temperature (°C)	(AH/H) _{iso} b (ppm)
- 25	74.96
- 6	63.94
+ 5	57.93
+ 25	49.88
+ 40	45.07

arelative to TMS.

bdiamagnetic resonance of OAc group at 2.01 ppm.

shift $(AH/H)_{iso}$ is usually written as a function of the electron spin-nuclear spin coupling constant, A_i (equation 10)83;

$$(\underline{AH}) = \underline{A\nu} = \underline{Aig_{aV}\beta S(S+1)}$$

$$(10)$$

$$(H)_{iso} \qquad \nu \qquad g_{N}\beta_{N}3kT$$

where ν is the probe frequency and $\Delta\nu$ is the frequency separation of the paramagnetic and diamagnetic shifts in Hz. The magnetic susceptibility for a molecule can be expressed as in equation (11), where

$$\chi = \frac{Ng^2\beta^2S(S+1)}{3kT}$$
 (11)

N is Avogadro's number. It can be seen from comparing equation 10 and 11 that χ is directly proportional to $(\Delta H/H)_{iso}$. A plot of $(\Delta H/H)_{iso}$ versus 1/T should produce a straight line with a slope proportional to A_i if the system obeys Curie Law behavior. A plot of $(\Delta H/H)_{iso}$ versus 1/T for $[S_2MoS_2Fe(OAc)_2]^{2-}$, shown in Figure 26, has a slope $A_i = 2.79 \cdot 10^{-5} \text{ K}^{-1}$, and proves that the complex obeys Curie Law magnetism.

c. Magnetic Susceptibility

The magnetic susceptibility of $[Et_4N]_2[S_2MoS_2Fe(OAc)_2]$ has been measured on a solid sample from 10.9 to 320 K, using a superconducting quantum interference device (SQUID) magnetometer. There are two possible oxidation state combinations for the FeMoS₄ cluster; either a high-spin Fe(III)(d⁵)-Mo(V)(d¹) couple, or high-spin Fe(II)(d⁶)-Mo(VI)(d⁰). A plot of χ versus T is shown in Figure 27. The decaying

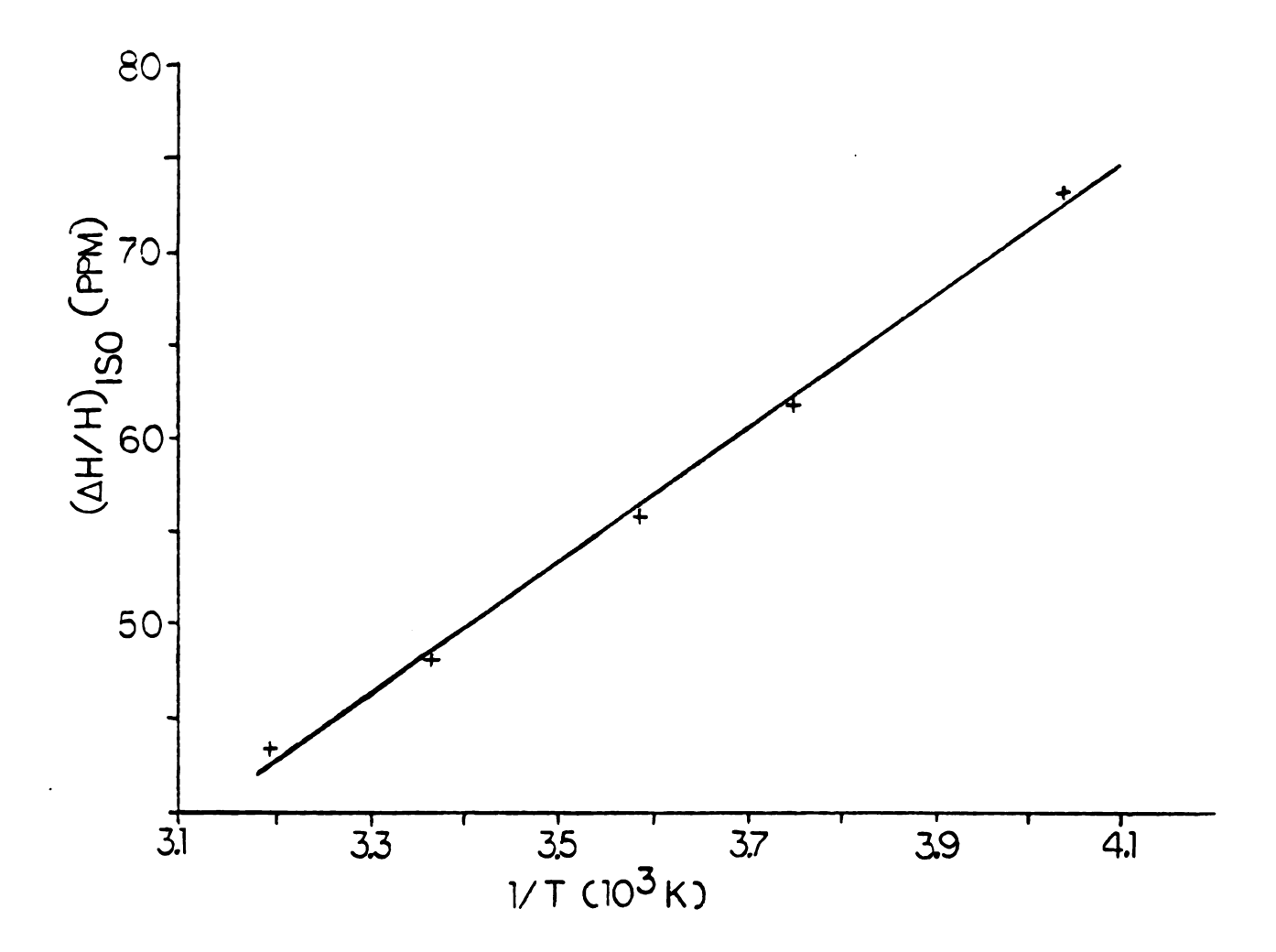


Figure 26. Plot of isotropic shift (($^{AH/H}$)_{iso}) versus 1/T for [Et_4N]₂[S_2MoS_2Fe (OAc)₂].

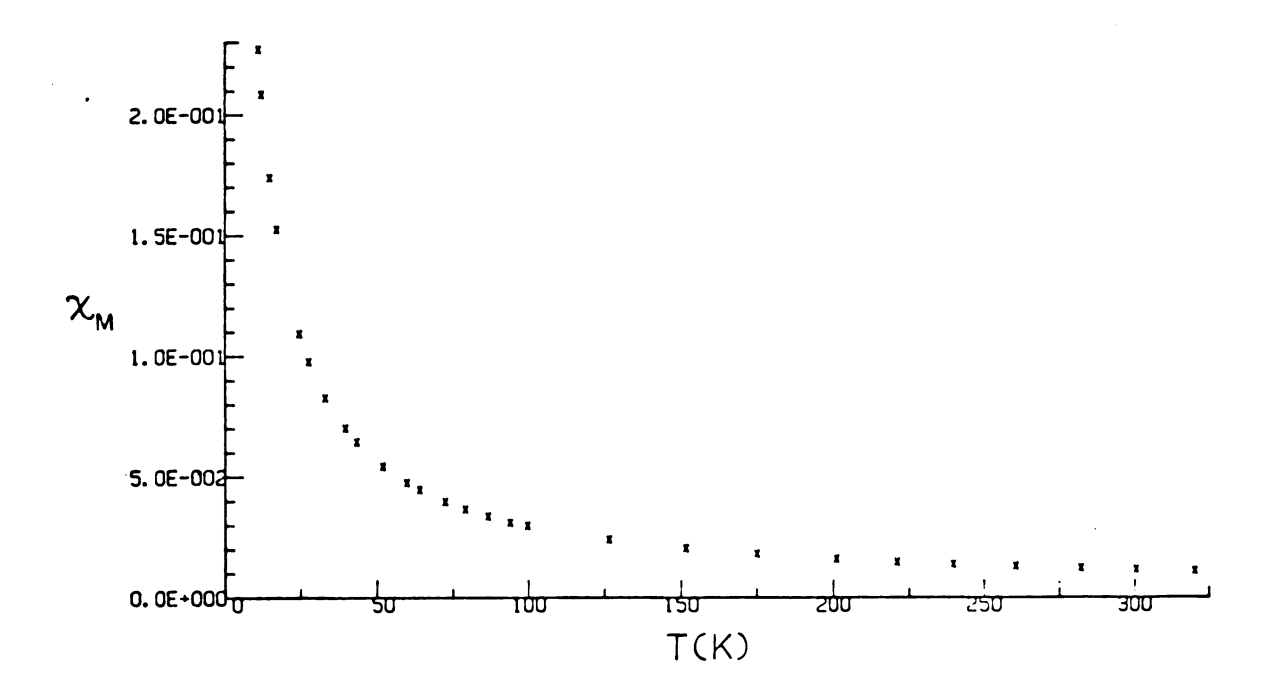


Figure 27. Plot of χ versus T for temperature-dependent magnetic susceptibility data on $[Et_4N]_2[S_2MoS_2Fe(OAc)].$

curve indicates paramagnetism. The effective magnetic moment at room temperature, which has been corrected for diamagnetic contributions of the ligands and cations through the use of Pascal's constants⁸³, is 4.96 $\mu_{\rm R}$. This is consistent with the presence of four unpaired electrons (S = 2) and indicates an Fe(II)-Mo(VI) system. The $\mu_{\rm R}$ value is within the range of monomeric high spin-iron(II) complexes (4.9 -5.5 $\mu_{\rm R})^{92}$. A strongly coupled Fe(III)-Mo(V) system was eliminated as a possible description because this oxidation state couple would show a magnetic susceptibility of S = 2 at low temperatures and S = 3 at high temperatures. No evidence of a transition between S = 2 and S = 3was observed over the temperature range measured. A plot of χ versus 1/T is a straight line from which an effective moment was calculated to be 4.6 $\mu_{\rm B}/{\rm formula}$ unit. The Curie-Weiss formula χ = (C/T + 0) was fitted to susceptibility data above 40 K by a linear least squares routine to give (on a per mole basis) 0 = 9.93 K, C = 3.14 (emu \cdot K)/mol. θ corrects the temperature for the non-zero intercept. The $[S_2MoS_2Fe(SPh)_2]^{2-}$ cluster shows similar values of $\theta = 4.2$ K and $C = 3.19 \text{ (emu } \cdot \text{ K)}^{19}.$

III. EXPERIMENTAL

A. Materials

Manipulations involving air sensitive products (i.e. iron-sulfur clusters) were performed under a dry argon atmosphere. Argon was purified by passage through columns of hot BASF R 3-11 catalyst (copper(II) oxide) and Aquasorb (supported phosphorus pentoxide). MeOH and CH₃CN were purified by distillation under dinitrogen from magnesium methoxide and calcium hydride, respectively. DMA and Me₂SO were allowed to stand over activated 4 Å molecular sieves prior to use. The tetraethylammonium salts of [MoS₄]²⁻³¹ and [Fe₄S₄Cl₄]²⁻⁹² were supplied by Paul E. Lamberty and Walter E. Cleland, respectively. 1.8-Dichloroanthracene⁵⁵, 2-amino-6-chlorobenzoic acid⁷³, p-aminobenzene p-xylene sulfide⁹³ and ferrous acetate⁹⁴ were synthesized by literature procedures. 2-Amino-6-methyl benzoic acid was recrystallized from a 50/50 mixture of EtOH/H₂O. 4-Aminophenol was recrystallized twice from CH₃CN prior to use. All other reagents were obtained from Aldrich Chemical Company, Inc. and were used without further purification, unless otherwise stated. The silica gel used for column chromatography was obtained from Baker and was 230-400 mesh.

B. Physical methods

¹H and ¹³C NMR spectra were recorded on a Nicolet NTC-360 instrument (360 MHz). Chemical shifts are reported in parts per million (δ) relative to internal standard (CH₃)₄Si. Anaerobic NMR samples were prepared in a side-arm flask and transferred via cannulla into a 9 inch NMR tube (which had been degassed and flushed with argon three times). The tubes were either sealed under argon or used with a serum stopper. Low temperature NMR data were obtained by cooling the probe with dinitrogen passed through coils emerged in an isopropanol/dry ice bath. IR spectra were obtained on a Perkin-Elmer model 1430 ratio recording spectrophotometer, using polystyrene for calibration. Optical spectra were obtained on a Cary 219 spectrophotometer, where any solvent absorption was subtracted from the spectra. Mass spectra were measured at 70 eV on a Finnegan MAT model 4600 GC/MS. High resolution mass spectra were obtained on a Finnegan MAT model 8230 GC/MS. Uncorrected melting points were determined either on a Thomas-Hoover capillary apparatus (< 200 °C) or a Laboratory Device Mel-Temp apparatus (> 200 °C). Variable temperature magnetic susceptibility measurements were performed on a S.H.E. Corporation SQUID susceptometer. HPLC analyses, using a Waters Associates μ -Porasil column, were performed with a Waters Associates model M-45 solvent delivery system equipped with a model U6K injector and model 440 absorbance detector. Semi-preparative scale HPLC separations were done using a Whatman Partisil 10 Magnum 9 (50 cm length) silica column. Radial thin-layer chromatography was performed on a 4mm silica plate using a Harrison Research model 7924

Chromatotron. Microanalyses were performed by Atlantic Microlab Inc., Atlanta, Georgia.

C. Preparation of 1.8-disubstituted anthraquinones

1.8-Dicyanoanthraquinone (10): The procedure for synthesis of 1-cyanoanthraquinone from 1-chloroanthraquinone was followed⁹⁵, with 1,8-dichloroanthraquinone as the starting material. 1,8-Dichloroanthraquinone (10.0 g, 36 mmol) and CuCN (9.2 g, 0.10 mol) were slurried in DMA (50 mL) and refluxed under Ar for 3 h. The hot brown solution was poured onto ice (700 g), and the brown-green precipitate was filtered and washed with water. The copper complex was decomposed with 3N HNO₃ (500 mL) at 60 °C for 4 h. The brown solid was filtered, washed with water and air dried. This procedure afforded crude 10 (8.2 g, 88%): mp 402-406 °C (lit.⁶⁸ mp > 390 °C);

¹H NMR (Me₂SO-d₄) δ 8.51 (2H, d, J = 7.92 Hz), 8.44 (2H, d, J = 7.56 Hz), 8.12 (2H, dd, J = 7.74, 7.74 Hz); IR (KBr) 2216 (m, -CN), 1678 (s, -C=O) cm⁻¹; MS (EI) m/e (relative intensity) 258 (M⁺, 100), 230 (55), 211 (82), 175 (44), 149 (11), 101 (31), 87 (13), 75 (41).

Anthraquinone-1,8-dicarboxylic acid (11): The procedure of Waldmann and Oblath⁶⁸ was followed with modifications. Crude 10 (8.2 g, 30 mmol) was refluxed in 70% $\rm H_2SO_4$ (500 mL) for 1 h. The hot solution was poured onto ice (800 g) to precipitate crude 11 as a brown solid (8.2 g, 87%): mp 294-300 °C (lit.⁶⁸ mp 316 °C); ¹H NMR (Me₂SO-d₆) $\rm ^6$ 13.40-13.10 (2H, br, s), 8.28 (2H, d, J = 7.56 Hz), 7.96 (2H, dd, J = 7.92, 7.92 Hz), 7.85 (2H, d, J = 7.20 Hz); IR (KBr) 3400-2750 (s, -OH), 1710-1665 (br, s, -C=0) cm⁻¹; MS (EI) m/e (relative intensity) 296

(M⁺, 0.5), 279 (7), 252 (71), 234 (100), 208 (16), 180 (32), 150 (47), 139 (27), 75(39).

D. Preparation of 1,8-disubstituted anthracenes

1,8-Dicyanoanthracene (3): The procedure of Akiyama, et al.56 was followed with modifications. 1,8-Dichloroanthracene 255 (6.7 g, 30 mmol) and CuCN (8.1 g, 90 mmol) were slurried in distilled quinoline (70 mL) and refluxed for 24 h under Ar. The warm black solution was poured into 1M HCl (600 mL), producing a black solid that was filtered and washed with water. The solid product was partitioned between 1M NH₄OH (300 mL) and CH₂Cl₂ (300 mL) and stirred vigorously for 6 h. The blue aqueous layer was separated and fresh 1M NH₄OH (300 mL) was added to the organic phase and allowed to stir for another 6 h. This procedure was repeated until the aqueous layer was no longer blue. Rotary evaporation of the organic layer left a brown oil which was chromatographed (Re 0.32, silica gel, CH2Cl2) to afford pure 3 as a yellow solid (2.5 g, 41%): mp 300-303 °C (lit. 56 mp 304-306 °C); 'H NMR $(CDCl_3)$ δ 9.16 (1H, s), 8.65 (1H, s), 8.31 (2H, d, J = 10.8 Hz), 8.08 (2H, d, J = 7.2 Hz), 7.63 (2H, dd, J = 10.8, 10.8 Hz); IR (KBr) 2216(s, -CN) cm⁻¹; MS (EI) m/e (relative intensity) 228 (M⁺, 100), 201 (11), 175 (5), 100 (10), 87 (11), 74 (5).

Anthracene-1,8-dicarboxylic acid (12): The procedure of Waldmann and Oblath⁶⁸ was followed with modifications. Crude 11 (8.2 g, 30 mmol) and Zn dust (30 g, 0.5 mol) were refluxed with stirring in 20% NH₄OH (350 mL) for 4 h, during which the color changed from dark red to yellow. The solution was filtered to remove excess Zn, and water

(500 mL) was added to the yellow filtrate. The filtrate was cooled to 0 °C, and 10% HCl was slowly added until a yellow precipitate formed. Filtration of the solid and air drying yielded crude 12 (5.9 g, 79%): mp 345-347 °C (dec.) (lit.68 mp 345 °C (dec.)); ¹H NMR (Me₂SO-d₆) δ 13.30-13.00 (2H, br, s), 10.47 (1H, s), 8.78 (1H, s), 8.34 (2H, d, J = 8.28 Hz), 7.62 (2H, dd, J = 7.74, 7.74 Hz); IR (KBr) 3300-2450 (br, s, -OH), 1712 (s, -C=O) cm⁻¹; MS (EI) m/e (relative intensity) 266 (M⁺, 100), 249 (7), 236 (2), 221 (14), 204 (40), 192 (5), 176 (4), 165 (27), 150 (6), 139 (4), 124 (4), 110 (6), 97 (5), 82 (9), 69 (6).

1,8-Bis(methoxycarbonyl)anthracene (13): The procedure of Akiyama, et al.⁶⁹ was followed with modifications. Compound 12 (2.9 g, 10 mmol) was refluxed in MeOH (400 mL) with concentrated H₂SO₄ (4 mL) for 16 h. Water (100 mL) was added to the warm brown solution, and the product was extracted with CH₂Cl₂ until the organic layer was no longer yellow. Concentration of solvent by rotary evaporation left a brown oil which was chromatographed (R_f 0.57, silica gel, CH₂Cl₂) to yield pure 13 (1.8 g, 61%): mp 101-103 °C (lit.⁶⁹ mp 104-105 °C); ¹H NMR (CDCl₃) δ 10.71 (1H, s), 8.49 (1H, s), 8.28 (2H, d, J = 6.84 Hz), 8.18 (2H, d, J = 8.28 Hz), 7.52 (2H, dd, J = 7.20, 7.20 Hz); ¹³C NMR (CDCl₃) δ 167.35, 133.10, 130.97, 130.89, 129.14, 127.31, 127.10, 123.90, 123.65, 51.95; IR (KBr) 1707 (s, -C=O) cm⁻¹; MS (EI) m/e (relative intensity) 294 (M⁺, 100), 263 (52), 235 (25), 220 (19), 203 (18), 176 (16), 164 (9), 150 (4), 131 (5), 123 (11), 116 (19), 102 (20), 88 (27), 75 (8).

E. Preparation of the o-methoxycarbonylbenzyne precursor

1-Methyl-2-hydrogen-3-nitrophthalate (15): The procedure reported by Nagai, et al. 70 was followed with some modifications. Reagent grade 3-nitrophthalic acid (50 g, 0.24 mol) was dissolved in anhydrous MeOH (200 mL) and was filtered through a fine glass frit to remove small black impurities present in the starting material. The resulting yellowish solution was cooled to 0 °C, and dry HCl gas was bubbled through at a rate of approximately 1 bubble per sec for 20 min. The resulting colorless solution was refluxed for 2-3 h and poured while hot into ice water (900 mL) to precipitate the product 15. The white microcrystals were filtered, washed with cold water, and dried in vacuo at 60 °C. This procedure afforded pure 15 (41.3 g. 77%): mp 162-164 °C (lit. 70 mp 160-162 °C); 'H NMR (Me₂SO-d₄) & 14.10-13.75 (1H, br, s), 8.33 (1H, d, J = 8.17 Hz), 8.22 (1H, d, J = 7.72 Hz), 7.82 (1H, dd, J = 8.01, 8.01 Hz; IR (KBr) 3400-3000 (br, s, -OH), 1766 (s, -C=O ester), 1700 (s, -C=O acid), 1541 (s, -NO₂), 1352 (s, -NO₂) cm^{-1} ; MS (EI) m/e (relative intensity) 225 (M^+ , 2), 208 (68), 194 (100), 181 (37), 164 (22), 151 (79), 136 (46), 119 (36), 104 (63), 92 (41), 75 (68), 63 (30).

2-Amino-6-(methoxycarbonyl) benzoic acid (16): Compound 15 (30.0 g, 0.13 mol) was dissolved in MeOH (125 mL) and placed in a heavy-walled pyrex bottle, to which 5% Pd on charcoal (0.30 g) was added. The rubber stopper used to cover the bottle was lined with Parafilm to insure that sulfur in the stopper would not poison the catalyst. The reaction flask was pressurized to 40 psi with H₂ and allowed to shake on a Parr pressure reaction apparatus for 8 h at room temperature. The resultant bright yellow solution was filtered to

remove the catalyst. Rotary evaporation of the solvent and subsequent drying in vacuo yielded 16 as a gummy solid (23.8 g, 92%): ¹H NMR (Me₂SO-d₆) δ 9.20-8.00 (3H, br, s), 7.21 (1H, dd, J = 7.56, 7.56 Hz), 6.87 (1H, d, J = 8.2 Hz), 6.61 (1H, J = 6.84 Hz), 3.71 (3H, s); ¹³C NMR (CDCl₉) δ 170.64, 170.40, 135.51, 132.55, 119.31, 116.79, 109.96, 52.56; IR (NaCl) 3490 (w, -NH₂), 3380 (w, -NH₂), 1712 (m, -C=O ester), 1615 (m, -C=O acid) cm⁻¹; MS (EI) m/e (relative intensity) 195 (M⁺, 1), 177 (12), 163 (44), 147 (13), 119 (75), 90 (100).

F. Preparation of 1,8,13- and 1,8,16-trisubstituted triptycenes

General procedure for the preparation of 1,8,13- and 1,8,16-trisubstituted triptycenes: The 1,8-disubstituted anthracene (5 mmol) was dissolved in a minimal amount of hot DME (10-300 mL). Isoamyl nitrite (1.3 mL, 10 mmol) was added to the refluxing solution and the substituted anthranilic acid (10 mmol), dissolved in DME (10-20 mL), was added dropwise over a 20-min period. The solution was refluxed 20 min, and another charge of isoamyl nitrite (1.3 mL, 10 mmol) was added. A second aliquot of anthranilic acid (10 mmol), dissolved in DME (10-20 mL), was added over a 20-min period. The solution was refluxed another 40 min, cooled to 0 °C, and 95% EtOH (20 mL) was added. Cold 7.5% NaOH was added until a precipitate formed. The solid was filtered, washed with cold MeOH:H,O (4:1) until there was no brown color in the filtrate, and dried in vacuo at 60 °C. Purification was performed in some cases by subliming off unreacted anthracene. Separation of some isomers by chromatography was performed as indicated.

1,8-Dicyano-13-methyltriptycene (5s) and

1.8-dicyano-16-methyltriptycene (5a): Reaction of 3 (1.1 g) with 2-amino-6-methylbenzoic acid (recrystallized from 95% EtOH), by the general procedure above, yielded 5a and 5s, and some unreacted 1,8-dicyanoanthracene. Sublimation of the mixture separated the lower melting anthracene from the triptycenes to yield an off-white solid of 5a and 5s (0.9 g, 57%). Separation by semi-preparative HPLC afforded pure 5a and pure 5s as white solids.

5a: mp 365-368 °C (dec.), ¹H NMR (CDCl₃) δ 7.59 (2H, d, J = 7.20 Hz), 7.45 (1H, d, J = 7.20 Hz), 7.33 (2H, d, J = 7.92 Hz), 7.14 (2H, dd, J = 7.56, 7.56 Hz), 7.00 (1H, dd, J = 7.56, 7.56 Hz), 6.93 (1H, d, J = 7.56 Hz), 6.26 (1H, s), 5.77 (1H, s), 2.51 (3H, s); ¹³C NMR (CDCl₃) δ 147.54, 145.95, 141.66, 141.53, 132.45, 128.76, 127.96, 127.70, 126.34, 125.93, 122.84, 116.60, 108.83, 50.48, 49.91, 18.49; IR (KBr) 2220 (s, -CN) cm⁻¹; MS (KI) m/e (relative intensity) 318 (M⁺, 72), 303 (100), 288 (6), 275 (8), 158 (5), 151 (9), 144 (8), 138 (10), 130 (9), 124 (7); high resolution mass spectrum, exact mass calcd. for $C_{23}H_{14}N_2$ (M⁺) 318.1157, found 318.1144; HPLC retention time (CH₂Cl₂) 10.8 min, flow rate 8.0 mL/min. Anal. Calcd. for $C_{23}H_{14}N_2$: C, 86.77; H, 4.43; N, 8.80. Found: C, 85.67; H, 4.55; N, 8.65.

5s: mp 408-411 °C (dec.), ¹H NMR (CDCl₃) & 7.50 (2H, d,

J = 7.20 Hz), 7.33 (2H, d, J = 7.92 Hz), 7.26 (1H, d, J = 6.12 Hz), 7.14

(2H, dd, J = 7.56, 7.56 Hz), 6.97 (1H, dd, 7.02, 7.02 Hz), 6.94 (1H, d,

J = 6.12 Hz), 6.58 (1H, s), 5.54 (1H, s), 2.66 (3H, s); ¹³C NMR (CDCl₃) &

147.27, 146.36, 143.52, 140.13, 133.75, 128.55, 127.83, 127.70, 126.38, 125.97,

121.79, 116.59, 108.83, 53.73, 46.58, 18.58; IR (KBr) 2224 cm⁻¹; MS (EI)

m/e (relative intensity) 318 (M⁺, 100), 303 (84), 288 (5), 275 (8), 158 (4),

144 (7), 138 (7), 132 (8), 124 (5); high resolution mass spectrum, exact mass calcd. for $C_{23}H_{14}N_2$ (M⁺) 318.1157, found 318.1144; HPLC retention time (CH₂Cl₂) 9.2 min, flow rate 8.0 mL/min. Anal. Calcd. for $(C_{23}H_{14}N_2)\cdot(CH_2Cl_2)_{1/6}$: C, 84.29; H, 4.36; N, 8.51. Found: C, 83.90; H, 4.74; N, 8.22.

13-Methyl-triptycene 1,8-dicarboxylic acid (6s) and 16-methyl-triptycene 1,8-dicarboxylic acid (6a): A mixture of 5a and 5s (0.75 g, 0.23 mmol) and KOH (6.7 g, 0.12 mol) was dissolved in ethylene glycol (30 mL). The yellow solution was allowed to stir for 4 days at 100 °C and then cooled to room temperature. Water (10 mL) was added to the solution, and HCl (6N) was added dropwise until a white percipitate formed. The solid was collected on a fine glass frit, washed with H₂O, and dried overnight in vacuo to yield 6a and 6s (0.77 g, 93%): mp > 450 °C; ¹H NMR (Me₂SO-d₄) δ 13.20-13.00 (2H, br, s), 8.09 (1H, s), 7.75 (1H, s), 7.65 (2H, d, J = 7.20 Hz), 7.61 (3H, d, J = 7.20 Hz),7.44 (3H, d, J = 7.56 Hz), 7.26 (2H, d, J = 6.84 Hz), 7.21 (1H, d, J = 6.48 Hz), 7.08 (3H, dd, J = 7.56, 7.56 Hz), 6.89 (3H, m), 6.02 (1H, s), 5.77 (1H, s), 3.38 (3H, s), 2.56 (3H, s); MS (EI) m/e (relative intensity) 356 (M⁺, 100), 338 (20), 310 (49), 293 (45), 279 (11), 265 (47), 252 (28), 239 (15), 189 (7), 169 (9), 146 (7), 131 (44), 125 (22), 119 (18), 97 (18), 85 (21).

1.8-Dichloro-13-methyltriptycene (8s) and

1.8-dichloro-16-methyltriptycene (8a): Reaction of 2⁵⁵ (1.2 g) with

2-amino-6-methylbenzoic acid (recrystallized from 95% EtOH), by the
general procedure above, yielded a white solid of 8a and 8s (1.3 g,

74%). Pure 8s was obtained by selective crystallization from EtOAc.

8a and 8s: (Data are reported for a 25:75 mixture of 8a and 8s.)

mp 332-335 °C; ¹H NMR (Me₂SO-d₆) δ 7.51 (2H, d, J = 7.20 Hz), 7.46 (2H, d, J = 7.20 Hz), 7.36 (1H, d, J = 7.20 Hz), 7.35 (1H, dd, J = 6.48, 6.48 Hz), 7.16 (2H, d, J = 7.20 Hz), 7.15 (2H, d, J = 7.20 Hz), 7.08 (2H, dd, J = 7.20, 7.20 Hz), 7.07 (2H, dd, J = 7.20, 7.20 Hz), 6.92 (4H, m), 6.60 (1H, s), 6.28 (1H, s), 6.06 (1H, s), 5.84 (1H, s), 2.49 (3H, s), 2.48 (3H, s); ¹³C NMR (CDCl₂) δ 147.79, 147.34, 144.82, 143.10, 142.97, 142.19, 141.88, 141.81, 133.03, 132.10, 129.91, 129.84, 127.26, 127.13, 126.45, 126.40, 125.97, 125.81, 125.25, 122.36, 122.01, 121.51, 54.67, 50.77, 47.32, 43.39, 18.60, 18.49; MS (EI) m/e (relative intensity) 340 (M⁺ + 4, 4), 338 (M⁺ + 2, 47), 336 (M⁺, 80), 301 (66), 286 (45), 266 (100), 250 (17), 189 (8), 132 (30), 125 (8); high resolution mass spectrum, exact mass calcd. for $C_{21}H_{14}Cl_2$ (M⁺) 336.0473, found 336.0479. Anal. Calcd. for $(C_{21}H_{14}Cl_2) \cdot (CH_2Cl_2)_{1/2}$: C, 68.00; H, 3.98. Found: C, 67.72; H, 3.73.

8s: mp 355-357 °C; ¹H NMR (CDCl₃) δ 7.26 (2H, d, J = 6.84 Hz), 7.23 (1H, d, J = 7.20 Hz), 7.04 (2H, d, J = 7.92 Hz), 6.93 (2H, dd, J = 7.56, 7.56 Hz), 6.92 (1H, dd, J = 7.56, 7.56 Hz), 6.89 (1H, d, J = 6.84 Hz), 6.73 (1H, s), 5.43 (1H, s), 2.60 (3H, s); ¹³C NMR (CDCl₃) δ 147.81, 141.90, 133.04, 129.86, 126.76, 126.09, 125.45, 124.89, 121.64, 121.14, 54.68, 43.40, 18.59; MS (EI) m/e (relative intensity) 340 (M⁺ + 4, 6), 338 (M⁺ + 2, 32), 336 (M⁺, 61), 301 (75), 286 (37), 266 (100), 250 (15), 176 (4), 150 (8), 143 (10), 131 (37), 118 (11); high resolution mass spectrum, exact mass calcd. for $C_{21}H_{14}Cl_2$ (M⁺) 336.0473, found 336.0479. Anal. Calcd. for $(C_{21}H_{14}Cl_2) \cdot (CH_2Cl_2)_{1/8}$: C, 72.94; H, 4.13. Found: C, 73.44; H, 4.29.

1.8-Dichloro-13-dibromomethyl triptycene (9s) and 1.8-dichloro-16-dibromomethyl triptycene (9a): A mixture of 8a and 8s (0.20 g, 0.59 mmol) was dissolved in CCl₄ (60 mL). The solution was flushed with Ar, and N-bromosuccimide (0.21 g, 1.2 mmol) along with a few granules of

dibenzoyl peroxide were added to the reaction flask. The solution was stirred under a high-intensity lamp for 12h. The flask was cooled to 0 °C in an ice/water bath and precipitated succimide was filtered off through a Buchner funnel. The filtrate was rotary evaporated to dryness to yield 9a and 9s as a white solid (0.24 g, 83%): mp > 450 °C; ¹H NMR (CDCl₃) 6 7.46 (2H, m), 7.34 (1H, d, J = 7.20 Hz), 7.28 (3H, m), 7.10 (6H, m), 6.99 (5H, m), 6.93 (1H, s), 6.83 (1H, s), 6.57 (1H, s), 6.47 (1H, s), 5.48 (1H, s); MS (EI) m/e (relative intensity) 494 (M⁺, 8), 414 (90), 350 (10), 336 (100), 117 (30).

1.8.16-tris(methoxycarbonyl)triptycene (17a): Reaction of 13 (1.5 g) with 16, by the general procedure above, yielded 17a and 17s (1.3 g, 62%). Separation by radial chromatography (Rf 0.24 (17a), Rf 0.10 (17s), silica gel, CH₂Cl₂) and subsequent recrystallization from 1:1 CH₂Cl₂: EtOAc

1,8,13-Tris(methoxycarbonyl)triptycene (17s) and

afforded colorless crystals of pure 17a and pure 17s.

17a: mp 256-257 °C; ¹H NMR (CDCl₃) & 8.01 (1H, s), 7.70 (1H, d, J = 7.20 Hz), 7.65 (1H, d, J = 7.92 Hz), 7.61 (4H, d, J = 7.92 Hz), 7.08 (1H, dd, J = 7.56, 7.56 Hz), 7.07 (2H, dd, J = 7.56, 7.56 Hz), 6.95 (1H, s), 4.02 (9H, s); ¹³C NMR (CDCl₃) & 167.32, 147.40, 146.38, 146.05, 145.94, 129.14, 128.15, 127.10, 126.73, 125.40, 125.20, 52.06, 52.02, 50.23, 46.75; IR (KBr) 1740-1720 (br, s, -C=O), 1600 (s, -C=C), 1300-1250 (br, s, -CO₂) cm⁻¹. MS (EI) m/e (relative intensity) 428 (M⁺, 100), 413 (4), 397 (36), 381 (6), 368 (22), 337 (85), 309 (11), 305 (8), 293 (17), 278 (19), 266 (6), 250 (29), 237 (7), 183 (22), 176 (4), 161 (4), 153 (5), 147 (4), 139 (8), 125 (33), 118 (7), 84 (9). Anal. Calcd. for C₂₆H₂₀O₆: C, 72.89; H, 4.71. Found: C, 72.80; H, 4.69.

17s: mp 287-289 °C; 'H NMR (CDCl₃) & 8.69 (1H, s), 7.57 (3H, d,

J = 7.92 Hz), 7.52 (3H, d, J = 7.20 Hz), 7.07 (3H, dd, J = 7.92, 7.92 Hz), 5.53 (1H, s), 4.05 (9H, s); 13 C NMR (CDCl₃) & 167.40, 146.73, 144.72, 127.86, 126.97, 126.92, 125.19, 54.23, 52.02, 43.63; IR (KBr) 1740-1700 (br, s, -C=0), 1600 (s, -C=C), 1310 (s, -CO₂), 1260 (s, -CO₂); MS (EI) m/e (relative intensity) 428 (M⁺, 100), 413 (3), 397 (31), 368 (19), 337 (27), 310 (13), 293 (13), 278 (12), 266 (5), 250 (19), 237 (7), 198 (13), 183 (9), 147 (5), 125 (26), 118 (9). Anal. Calcd. for $C_{24}H_{20}O_4$: C, 72.89; H, 4.71. Found: C, 72.43; H, 4.66.

Triptycene 1,8,13-tricarboxylic acid (7s) and triptycene

1,8,16-tricarboxylic acid (7a): Compound 17a or 17s (2.5 g, 5.8 mmol)

was dissolved in MeOH (625 mL). 10% KOH (125 mL) was added to the
solution which was then refluxed for 12 h. The reaction mixture was

cooled to room temperature, water (200 mL) was added, and the solution

was concentrated by rotary evaporation to half the volume of solvent.

6N HCl was added with stirring until a white precipitate formed. The
solid was collected on a fine glass frit, and dried in vacuo at 60 °C

overnight to yield pure 7a or pure 7s: (2.1 g, 95%).

7a: mp 426-428 °C; ¹H NMR (Me₂SO-d₆) δ 13.12 (3H,s), 7.87 (1H, s), 7.64 (2H, d, J = 7.20 Hz), 7.60 (1H, d, J = 7.20 Hz), 7.57 (1H, d, J = 7.92 Hz), 7.50 (2H, d, J = 7.92 Hz), 7.15 (1H, dd, J = 7.20, 7.20 Hz), 7.13 (2H, dd, J = 7.20, 7.20 Hz), 6.90 (1H, s); ¹³C NMR (Me₂SO-d₆) δ 167.85, 167.81, 146.43, 146.16, 145.68, 145.26, 128.20, 127.91, 127.58, 126.72, 126.45, 125.26, 49.64, 46.19; MS (EI) m/e (relative intensity) 386 (M⁺, 100), 368 (12), 340 (25), 323 (50), 295 (14), 279 (44), 250 (29), 239 (15), 237 (10), 184 (6), 124 (14), 119 (11), 75 (5). Anal. Calcd. for C₂₃H₁₄O₆: C, 71.50; H, 3.65. Found: C, 71.40; H, 3.76.

7s: mp 432-435 °C; ¹H NMR (Me₂SO-d₆) δ 12.91 (3H, s), 8.35 (1H, s),

7.63 (3H, d, J = 7.20 Hz), 7.40 (3H, d, J = 7.92 Hz), 7.11 (3H, d, J = 7.56 Hz), 5.87 (1H, s); 13 C NMR (Me₂SO-d₆) 5 167.85, 146.96, 129.31, 126.62, 125.85, 125.06, 52.58, 43.45; MS (EI) m/e (relative intensity) 386 (M⁺, 24), 324 (21), 279 (10), 250 (10), 239 (8), 84 (100); high resolution mass spectrum, exact mass calcd. for $C_{22}H_{12}O_3$ (M⁺ - (CO₂ + H₂O)) 324.0786, found 324.0775. Anal. Calcd. for $C_{23}H_{14}O_6$: C, 71.50; H, 3.65. Found: C, 70.64; H, 3.72.

Triptycene 1,8,13-tris(carbonylchloride) (18s) and triptycene

1,8,16-tris(carbonylchloride) (18a): Compound 7a or 7s (0.2 g,

0.52 mmol) and SOCl₂ (10 mL) were mixed under Ar, and the slurry was refluxed for 12 h. SOCl₂ was removed under reduced pressure to yield 18a or 18s as a white solid: (0.23 g, 98%).

1.8-Bis(methoxycarbonyl)-13-methyltriptycene (23s) and

1.8-bis(methoxycarbonyl)-16-methyltriptycene (23a): Reaction of 13

(1.5 g) with 2-amino-6-methylbenzoic acid (recrystallized from 95%

BtOH), by the general procedure above, yielded 23a and 23s (1.1 g, 58 %). Separation by semi-preparative HPLC afforded pure 23a and pure 23s as white solids.

23a: mp 215-216 °C; ¹H NMR (CDCl₃) δ 7.90 (1H, s), 7.58 (2H, d, J = 7.92 Hz), 7.50 (2H, d, J = 7.20 Hz), 7.39 (1H, d, J = 7.20 Hz), 7.03 (2H, dd, J = 7.56, 7.56 Hz), 6.92 (1H, dd, J = 7.56, 7.56 Hz), 6.85 (1H, d, J = 7.56 Hz), 5.71 (1H, s), 4.01 (3H, s), 2.50 (3H, s); ¹³C NMR (CDCl₃) δ 167.41, 146.80, 146.35, 143.86, 143.23, 131.69, 128.94, 127.26, 127.03, 126.90, 126.63, 125.22, 124.90, 122.85, 52.02, 50.63, 47.02, 18.35; MS (EI) m/e (relative intensity) 384 (M⁺, 71), 362 (5), 353 (14), 337 (13), 331 (4), 324 (16), 310 (4), 303 (4), 293 (100), 278 (5), 265 (25), 263 (29), 250 (19), 239 (7), 189 (7), 176 (5), 146 (5), 132 (19), 125 (10), 75 (4); HPLC retention

time (CH₂Cl₂) 13.3 min, flow rate 8.0 mL/min. Anal. Calcd. for C₂₅H₂₀O₄: C, 78.11; H, 5.24. Found: C, 78.15; H, 5.26.

23s: mp 231-233 °C; ¹H NMR (CDCl₃) δ 8.32 (1H, s), 7.58 (2H, d, J = 7.92 Hz), 7.49 (2H, d, J = 7.20 Hz), 7.22 (1H, d, J = 7.20 Hz), 7.02 (2H, dd, J = 7.56, 7.56 Hz), 6.90 (1H, dd, J = 7.20, 7.20 Hz), 6.87 (1H, d, J = 7.20 Hz), 5.47 (1H, s), 4.01 (3H, s), 2.68 (3H, s); ¹³C NMR (CDCl₃) δ 167.40, 147.31, 145.98, 145.03, 142.25, 134.04, 127.26, 127.14, 126.84, 126.70, 125.13, 124.93, 121.19, 54.51, 52.00, 42.94, 18.59; MS (EI) m/e (relative intensity) 384 (M⁺, 100), 352 (59), 324 (37), 309 (12), 292 (91), 278 (7), 265 (59), 263 (57), 250 (29), 239 (12), 226 (4), 189 (16), 176 (10), 161 (13), 146 (7), 132 (24), 125 (10), 118 (6), 84 (21), 75 (6); HPLC retention time (CH₂Cl₂) 9.7 min, flow rate 8.0 mL/min. Anal. Calcd. for C₂₅H₂₀O₄: C, 78.11; H, 5.24. Found: C, 77.70; H, 5.20.

1.8.13-Trichlorotriptycene (24s) and 1.8.16-trichlorotriptycene (23a):

Reaction of 2⁵⁵ (1.2 g) with 2-amino-6-chlorobenzoic acid⁷³, by the

general procedure above, yielded 24a and 24s (0.48 g, 27%). This pair

of isomers was not separated.

24a and 24s: mp 355-358 °C (dec.), ¹H NMR (Me₂SO-d₆) 6 7.58 (2H, d, J = 7.92 Hz), 7.55 (3H, d, J = 7.92 Hz), 7.51 (1H, d, J = 7.20 Hz), 7.21 (2H, d, J = 8.64 Hz), 7.20 (1H, d, J = 8.64 Hz), 7.20 (3H, d, J = 7.92 Hz), 7.12 (1H, dd, J = 7.92, 7.92 Hz), 7.12 (3H, dd, J = 7.92, 7.92 Hz), 7.11 (2H, dd, J = 7.92, 7.92 Hz), 6.82 (1H, s), 6.38 (1H, s), 6.17 (1H, s), 5.98 (1H, s); MS (EI) m/e (relative intensity) 360 (M⁺ + 4, 9), 358 (M⁺ + 2, 27), 356 (M⁺, 33), 321 (42), 286 (100), 250 (34), 176 (8), 160 (7), 143 (20), 125 (22), 112 (5); high resolution mass spectrum, exact mass calcd. for $C_{20}H_{11}Cl_3$ (M⁺) 355.9926, found 355.9950. Anal. Calcd. for $(C_{20}H_{11}Cl_3) \cdot (CH_2Cl_2)_{1/8}$: C, 65.63; H, 3.07. Found: C, 65.14; H, 2.98.

1.8-Bis(methoxycarbonyl)-13-chlorotriptycene (25s) and

1.8-bis(methoxycarbonyl)-16-chlorotriptycene (25a): Reaction of 13 (1.5 g) with 2-amino-6-chlorobenzoic acid⁷³, by the general procedure above, yielded 25a and 25s (0.40 g, 20%). Separation by semi-preparative HPLC yielded pure 25a and pure 25s as white solids.

25a: mp 218-219 °C; ¹H NMR (CDCl₃) δ 7.99 (1H, s), 7.62 (2H, d, J = 7.92 Hz), 7.57 (2H, d, J = 7.20 Hz), 7.44 (1H, d, J = 7.20 Hz), 7.08 (1H, d, J = 7.92 Hz), 7.05 (2H, dd, J = 8.28, 8.28 Hz), 6.95 (1H, dd, J = 7.56, 7.56 Hz), 5.97 (1H, s), 4.02 (6H, s); ¹³C NMR (CDCl₃) δ 167.25, 146.61, 146.01, 145.94, 142.59, 129.30, 127.75, 127.23, 127.01, 126.72, 126.04, 125.26, 123.48, 52.07, 50.69, 46.94; MS (EI) m/e (relative intensity) 406 (M⁺ + 2, 38), 404 (M⁺, 100), 373 (61), 368 (11), 344 (54), 337 (45), 312 (83), 301 (6), 293 (13), 286 (57), 278 (41), 273 (6), 266 (34), 249 (67), 238 (34), 223 (12), 210 (9), 186 (12), 175 (30), 169 (11), 142 (13), 138 (21), 124 (37), 118 (29), 111 (11), 85 (9), 83 (78); high resolution mass spectrum, exact mass calcd. for $C_{24}H_{17}O_4Cl$ (M⁺) 404.0815, found 404.0796; HPLC retention time (CH₂Cl₂) 17.3 min, flow rate 6.0 mL/min. Anal. Calcd. for $(C_{24}H_{17}O_4Cl)\cdot(CH_2Cl_2)_{1/4}$: C, 69.74; H, 4.18. Found: C, 69.73; H, 4.33.

25s: mp 204-205 °C; ¹H NMR (CDCl₃) δ 8.41 (1H, s), 7.63 (2H, d, J = 7.56 Hz), 7.52 (2H, d, J = 7.20 Hz), 7.28 (1H, d, J = 7.20 Hz), 7.08 (2H, dd, J = 7.56, 7.56 Hz), 7.07 (1H, d, J = 7.56 Hz), 6.95 (1H, dd, J = 7.56, 7.56 Hz), 5.51 (1H, s), 4.06 (6H, s); ¹³C NMR (CDCl₃) δ 146.81, 144.85, 127.76, 127.31, 127.25, 126.73, 126.69, 126.41, 125.35, 121.86, 54.53, 52.17, 51.90; MS (EI) m/e (relative intensity) 406 (M⁺ + 2, 40), 404 (M⁺, 100), 373 (80), 367 (25), 344 (42), 336 (66), 312 (67), 305 (7), 300 (24), 293 (34), 286 (74), 277 (32), 273 (8), 265 (43), 249 (58), 237 (43), 22 (14),

209 (12), 185 (16), 175 (30), 161 (8), 142 (17), 138 (28), 131 (29), 124 (35), 118 (26), 111 (24), 83 (78), 71 (9); high resolution mass spectrum, exact mass calcd. for $C_{24}H_{17}O_4Cl$ (M⁺) 404.0815, found 404.0796; HPLC retention time (CH₂Cl₂) 18.1 min, flow rate 6.0 mL/min. Anal. Calcd. for $(C_{24}H_{17}O_4Cl)\cdot(CH_2Cl_2)_{1/4}$: C, 68.36; H, 4.14. Found: C, 68.65; H, 4.29.

1.8-Dichloro-13-(methoxycarbonyl)triptycene (26s) and

1.8-dichloro-16-(methoxycarbonyl)triptycene (26): Reaction of 2⁵⁵

(1.2 g) with 16 by the general procedure above, yielded 26a and 26s, and some unreacted 2. Sublimation of the mixture separated the more volatile anthracene from the triptycenes yielded 26a and 26s (0.90 g, 47%). Separation by semi-preparative HPLC yielded pure 26a and pure 26a as white solids.

26a: mp 256-258 °C; ¹H NMR (CDCl₃) δ 7.67 (1H, d, J = 7.92Hz), 7.65 (1H, d, J = 7.92 Hz), 7.36 (2H, d, J = 7.20 Hz), 7.10 (1H, dd, J = 7.56, 7.56 Hz), 7.06 (2H, d, J = 7.20 Hz), 6.95 (2H, dd, J = 7.56, 7.56 Hz), 6.91 (1H, s), 6.45 (1H, s), 3.98 (3H, s); ¹³C NMR (CDCl₃) δ 167.20, 147.07, 146.94, 145.14, 141.84, 129.76, 128.51, 127.29, 126.71, 126.11, 125.78, 125.21, 122.84, 52.10, 50.10, 50.42, 47.10; MS (EI) m/e (relative intensity) 384 (M⁺ + 4, 9), 382 (M⁺ + 2, 51), 380 (M⁺, 96), 349 (22), 345 (8), 320 (33), 313 (89), 286 (100), 278 (12), 266 (16), 250 (63), 224 (6), 211 (6), 176 (20), 156 (9), 143 (13), 139 (16), 125 (61), 112 (11), 84 (13); HPLC retention time (CH₂Cl₂) 7.8 min, flow rate 4.0 mL/min. Anal. Calcd. for $C_{22}H_{14}O_2Cl_2$: C, 69.31; H, 3.70. Found: C, 69.30; H, 4.01.

26s: mp 322-323 °C ¹H NMR (CDCl₃) δ 7.81 (1H, s), 7.69 (1H, d, J = 7.92 Hz), 7.54 (1H, d, J = 7.20 Hz), 7.27 (2H, d, J = 7.92 Hz), 7.10 (1H, dd, J = 7.56, 7.56 Hz), 7.07 (2H, d, J = 7.92 Hz), 6.95 (2H, dd, J = 7.56, 7.56 Hz), 5.48 (1H, s), 4.08 (3H, s); ¹³C NMR (CDCl₃) δ 167.22,

147.47, 146.60, 144.59, 141.42, 130.56, 127.65, 127.43, 126.71, 126.26, 125.42, 122.85, 121.96, 54.52, 52.29, 43.82; MS (EI) m/e (relative intensity) 384 (M⁺ + 4, 8), 382 (M⁺ + 2, 44), 380 (M⁺, 91), 349 (20), 344 (8), 320 (34), 313 (91), 286 (100), 278 (11), 266 (11), 250 (83), 246 (8), 224 (6), 211 (5), 176 (14), 157 (10), 143 (11), 139 (10), 125 (37), 112 (7); HPLC retention time (CH₂Cl₂) 8.1 min, flow rate 4.0 mL/min. Anal. Calcd. for $C_{22}H_{14}O_{2}Cl_{2}$: C, 69.31; H, 3.70. Found: C, 69.05; H, 3.78.

1,8-Dicyano-13-(methoxycarbonyl)triptycene (27s): Reaction of 3 (1.1 g) with 16, by the general procedure above, yielded 27s and some unreacted 3. Sublimation of the mixture separated the anthracene from the triptycene yielded 27s (0.69 g, 38%). The compound was further purified by semi-preparative HPLC. This procedure afforded pure 27s as white crystals: mp 366-369 °C; ¹H NMR (CDCl₃) δ 7.77 (1H, d, J = 7.92 Hz), 7.73 (1H, d, J = 7.92 Hz), 7.69 (2H, d, J = 7.56 Hz), 7.36 (2H, d, J = 7.56 Hz), 7.17 (1H, dd, J = 7.56, 7.56 Hz), 7.16 (2H, dd,J = 7.56, 7.56 Hz), 7.08 (1H, s), 6.32 (1H, s), 4.00 (3H, s); ¹³C NMR (CDCl₃) δ 161.40, 149.38, 147.21, 145.84, 145.63, 143.63, 129.03, 128.98, 128.61, 127.97, 126.65, 125.95, 116.52, 108.79, 52.25, 50.23, 49.47; MS (EI) m/e (relative intensity) 362 (M⁺, 83), 347 (20), 330 (30), 302 (100), 275 (16), 201 (5), 181 (5), 165 (6), 151 (21), 138 (29), 124 m(35), 11(8), 84 (8), 75 (11); high resolution mass spectrum, exact mass calcd. for $C_{24}H_{14}N_{2}O_{2}$ (M⁺) 362.1055, found 362.1055. Anal. Calcd. for $C_{24}H_{14}N_{2}O_{2}$: C, 79.55; H, 3.89; N, 7.73. Found: C, 78.77; H, 4.46; N, 7.39.

G. <u>Preparation of 1,8,13- and 1,8,16-tris[(N-substituted)carboxamido]-</u>
<u>triptycenes</u>

General procedure for the preparation of 1,8,13- and 1,8,16-tris-[(N-substituted)carboxamido]triptycenes:

Method 1: The tris(carbonylchloride) 18a or 18s, (0.23 g, 0.51 mmol) was made in situ and kept under Ar. The appropriate amine (1.5 mmol) in CH₂Cl₂ (20 mL) or CH₃CN (30 mL) was syringed into the reaction flask, followed by Et₃N (0.22 mL, 1.5 mmol). Upon addition of the reagents, some reaction mixtures formed solutions, while others remained as slurries. Each reaction mixture was refluxed 18 h under an inert atmosphere, allowed to cool, and the volume reduced to 15 mL under reduced pressure. A white precipitate was collected on a fine glass frit and washed with water, followed by 10% HCl. The products were dried in vacuo overnight at 60 °C.

Method 2: The tris(carbonylchloride) 18a or 18s, (0.23 g, 0.51 mmol) was made in situ and kept under Ar. The appropriate amine (3.6 mmol) in CH₂Cl₂ (50 mL) or CH₃CN (80 mL) was syringed into the reaction flask. The reaction mixture was refluxed 24 h under inert atmosphere. The cooled reaction mixture was filtered through a fine glass frit, and the solid collected was washed with water, 10% HCl and 95% EtOH. The products were dried in vacuo overnight at 60 °C.

1,8,13-Tris-[(N-4-hydroxyphenyl)carboxamidoltriptycene (19s) and

1,8,16- tris-[(N-4-hydroxyphenyl)carboxamidoltriptycene (19a): Reaction

of 18s or 18a with p-aminophenol in CH₂Cl₂, by the general procedure

above, yielded pure 19a or 19s as a white solid: (0.32 g, 95%).

19s: mp 420-424 °C (dec.); ¹H NMR (Me₂SO-d₆) δ 10.18 (3H, s), 9.29

(3H, s), 7.94 (3H, d, J = 7.20 Hz), 7.50 (1H, s), 7.40 (6H, d, J = 8.64 Hz), 7.29 (3H, d, J = 7.56 Hz), 7.15 (3H, dd, J = 7.56, 7.56 Hz), 6.63 (6H, d, J = 8.28 Hz), 5.93 (1H, s); 13 C NMR (Me₂SO-d₆) δ 165.90, 153.99, 146.44, 141.84, 133.43, 129.93, 125.43, 125.10, 124.61, 123.81, 114.56, 52.72, 43.42; MS (EI) m/e (relative intensity) 659 (M⁺,7), 551 (59), 442 (8), 282 (4), 250 (40), 109 (100), 86 (17), 80 (79); high resolution mass spectrum, exact mass calcd. for C₄₁H₂₉N₃O₆ (M⁺) 659.2056, found 659.2042. Anal. Calcd. for C₄₁H₂₉N₃O₆: C, 74.65; H, 4.43; N, 6.37. Found: C, 73.92; H, 4.55; N, 6.38.

19a: mp 413-416 °C (dec.); ¹H NMR (Me₂SO) δ 10.12 (1H, s), 10.06 (2H, s), 9.30 (1H, s), 9.29 (2H, s), 7.60 (1H, d, J = 8.64 Hz), 7.57 (2H, d, J = 7.56 Hz), 7.49 (6H, d, J = 8.64 Hz), 7.30 (1H, d, J = 7.56 Hz), 7.25 (2H, d, J = 7.56 Hz), 7.13 (1H, dd, J = 6.48, 6.48 Hz), 7.11 (2H, dd, J = 7.20, 7.20 Hz), 6.80 (1H, s), 6.78 (2H, d, J = 8.28 Hz), 6.71 (4H, d, J = 8.28 Hz), 6.30 (1H, s); IR (KBr) 3368-3270 (s, br, -NH amide), 1652 (s, -C=O), 1620 (m, -NH amide) cm⁻¹; MS (EI) m/e (relative intensity) 659 (M⁺, 5), 551 (2), 250 (2), 149 (3), 109 (100), 91 (2), 80 (98).

1,8,16-Tris-[(N-propyl)carboxamido]triptycene (20a): Reaction of 18a with propylamine in CH_2Cl_2 , by the general procedure above, yielded pure 20a as a white solid (0.25 g, 96%): mp 369-402 °C (dec.), ¹H NMR (Me₂SO-d₄) δ 8.48 (2H, t, J = 5.40 Hz), 8.33 (1H, t, J = 5.40 Hz), 7.48 (2H, d, J = 6.84 Hz), 7.38 (1H, d, J = 7.20 Hz), 7.13 (3H, d, J = 7.56 Hz), 7.06 (3H, dd, J = 7.20, 7.20 Hz), 6.63 (1H, s), 6.25 (1H, s), 3.32 (6H, m), 1.62 (6H, m), 0.97 (6H, t, J = 7.20 Hz), 0.95 (3H, t, J = 7.20 Hz); ¹³C NMR (Me₂SO-d₄) δ 167.46, 145.73, 145.27, 143.90, 142.39, 133.11, 132.55, 125.46, 125.34, 124.85, 124.68, 124.10, 123.57, 49.85, 46.72, 41.00, 40.74, 22.41, 22.35, 11.51, 11.43; MS (EI) m/e (relative intensity) 509 (M⁺, 24), 451

(14), 424 (16), 394 (18), 365 (10), 279 (10), 250 (13), 168 (20), 125 (15), 100 (8), 86 (29), 73(100); high resolution mass spectrum, exact mass calcd. for C₃₂H₃₅N₃O₃ (M⁺) 509.2678, found 509.2680. Anal. Calcd. for C₃₂H₃₅N₃O₃: C, 75.41; H, 6.92; N, 8.24. Found: C, 74.66; H, 6.80; N, 8.08.

1,8,16-Tris-[(N-4-methylphenyl)carboxamido]triptycene (21a): Reaction of 18a with p-toluidine in CH₃CN, by the above procedure. yielded pure 21a as a white solid (0.32 g, 97%): mp 371-374 °C (dec.); ¹H NMR (Me₂SO-d₄) & 10.28 (3H, s), 10.17 (3H, s), 7.72 (2H, d, J = 7.92 Hz), 7.59 (2H, d, J = 6.48 Hz), 7.57 (4H, d, J = 7.92 Hz), 7.52 (1H, d, J = 7.20 Hz), 7.33 (1H, d, J = 7.56 Hz), 7.27 (2H, d, J = 9.00 Hz),6.78 (1H, s), 6.29 (1H, s), 3.35 (6H,s), 2.31 (3H,s); 13 C NMR (Me₂SO-d₄) δ 166.19, 166.09, 145.89, 145.36, 144.10, 143.27, 136.72, 136.49, 133.28, 132.59, 132.42, 128.99, 128.73, 126.31, 125.60, 124.81, 124.04, 123.80, 120.52, 119.98, 49.86, 46.68, 20.55, 20.52; MS (EI) m/e (relative intensity) 653 (M⁺, 10), 547 (81), 413 (10), 394 (5), 384 (10), 366 (5), 355 (7), 341 (6), 307 (5), 278 (5), 250 (38), 239 (5), 221 (15), 207 (11), 198 (8), 184 (10), 176 (22), 171 (20), 149 (10), 133 (5), 125 (19), 106 (100), 91 (37), 86 (46), 79 (51), 64 (23); high resolution mass spectrum, exact mass calcd. for $C_{44}H_{35}N_{3}O_{3}$ (M⁺) 653.2678, found 653.2681. Anal. Calcd. for $(C_{44}H_{35}N_{3}O_{3})\cdot(CH_{2}Cl_{2})_{1/4}$: C, 78.74; H, 5.30; N, 6.23. Found: C, 79.07; H, 5.37; N, 6.21.

1.8.16-Tris-[(N-benzene-p-S-xylene)carboxamido]triptycene (22a): Reaction of 18a with p-aminobenzene p-xylene sulfide⁹³ in CH_2Cl_2 , by the general procedure above, yielded 85% of 22a as a white solid. mp 300-304 °C (dec.); ¹H NMR (Me₂SO-d₆) δ 10.40 (1H, s), 10.30 (2H, s), 7.77 (2H, d, J = 8.28 Hz), 7.60 (2H, dd, J = 6.84, 6.84 Hz), 7.53 (1H, d, J = 7.20 Hz), 7.36 (4H, d, J = 8.28 Hz), 7.31 (1H, d, J = 8.28 Hz), 7.20

(12H, m), 7.08 (11H, m), 6.76 (1H,s), 6.29 (1H, s), 4.20-4.15 (6H, br, s), 2.27 (3H, s), 2.25 (3H, s); MS data not available because M^+ > 1000 m/e.

H. Reaction of [Pr.N]2[Fe.S.Cl.] with (HO)2-tripod ligand

In a dry box, 19s (0.15 g, 0.023 mmol) and [Pr₄N]₂[Fe₄S₄(SEt)₄] (0.022 g, 0.023 mmol) were weighed out and placed in a side-arm flask equipped with a serum stopper. Me₂SO-d₄ (1.5 mL) was syringed into the reaction vessel, and the resultant red-brown solution was stirred for 4h, with periodic evacuation of the flask to remove volatile EtSH. An aliquot of solution was transferred to a 5 mm NMR tube via cannulla, and the tube was sealed under Ar. The sample was frozen until the ¹H NMR could be obtained.

A second sample was prepared as outlined above, but allowed to stir for 12 h under dynamic vacuum. After ~4 h, all solvent had evaporated, and another 1.5 mL aliquot of Me₂SO-d₆ was added to the flask. This procedure was repeated one more time before the sample was sealed in an NMR tube.

I. Reaction of [Et₄N]₂[Fe₄S₄Cl₄] with Na₃(O₃-tripod)

1. Preparation of Na₃(O₃-tripod)

A stock solution of NaOMe (0.435 M) was prepared by dissolving Na (1.0 g, 43.5 mmol) in MeOH (100 mL). Compound 19s (0.010 g, 0.015 mmol) was placed in a side-arm flask under Ar and dissolved in DMA (2 mL). NaOMe in MeOH (0.10 mL) was syringed into the solution,

causing an immediate color change to a bright yellow-green. After 6 h, the solvents were removed in vacuo to give a yellow solid of Na₃(O₃-tripod) (0.011 g, 98%): ¹H NMR (Me₂SO-d₆) 6 9.87 (3H, s), 7.69 (1H, s), 7.56 (3H, m), 7.25 (9H, m), 7.13 (3H, m), 6.31 (6H, s), 5.81 (1H, s).

2. Reaction of chloro tetramer with the trisodium salt of (HO) - tripod

The Na₃(O₃-tripod) (0.011 g, 0.015 mmol) isolated by the procedure outlined above, was washed twice with CH₃CN (1 mL) under Ar, and dried overnight to remove excess solvent. A stock solution of iron-sulfur cluster (1.38 · 10⁻² M) was prepared by dissolving [Et₄N]₂[Fe₄S₄Cl₄] (0.05 g) in Me₂SO-d₄ (4.8 mL). Various amounts of iron-sulfur cluster solution were syringed into the flask containing the sodium salt of the ligand. Five reactions were done and the amount of cluster used in each was 0.020, 0.015, 0.011, 0.010 and 0.008 mmol, respectively. The solution was stirred at room temperature for 8 h before an aliquot was removed and sealed in an NMR tube under Ar.

J. Preparation of [Et₄N]₂[S₂MoS₂Fe(OAc)₂]

Tetraethylammonium tetrathiomolybdate (1.0 g, 2.0 mmol) was placed in a side-arm flask and flushed with Ar. CH₃CN (80 mL) was added to dissolve the solid. Ferrous acetate (0.39 g, 2.3 mmol) was transferred in the dry box to a side-arm flask equipped with a serum stopper. CH₃CN (20 mL) was syringed into the flask containing the Fe(OAc)₂ to

form a slurry. The orange tetrathiomolybdate solution was cannulled into the white Fe(OAc)₂ slurry; this resulted in an immediate color change to wine-red. The solution was stirred at room temperature for 2 h and then filtered anaerobically through a fine glass frit. The filtrate volume was reduced to 30 mL under vacuum. Diethyl ether (50 mL) was added to precipitate a red-brown solid of [Et₄N]₂[S₂MoS₂Fe(OAc)₂] (1.0 g, 74 %): Optical spectrum \(\lambda_{max}\)
(\(\epsilon(M^{-1} \cdot cm^{-1})\)) 286 (7795), 310 (10000), 428 (sh), 464 (5270), 508 (sh).
Anal. Calcd. for C₂₀H₄₄N₂O₄S₄FeMo: C, 36.47; H, 7.04; N, 4.25. Found: C, 35.73; H, 6.82; N, 4.00.

IV. CONCLUSIONS

A macrocyclic tridentate ligand ((HO)₃-tripod) based on a symmetrically trisubstituted triptycene with terminal phenoxide substituents has been designed and prepared. Interactions of the ligand with a 4Fe-4S cluster were examined in order to investigate the possibility of the presence of oxygen-ligated iron-sulfur clusters in nitrogenase. En route to preparing this ligand, twenty-one new trisubstituted triptycenes were isolated and characterized by ¹H NMR, ¹³C NMR and IR spectroscopies, as well as by mass spectrometry.

Fifteen of the trisubstituted triptycenes were synthesized from the Diels-Alder cycloadditon of a 1,8-disubstituted anthracene with an ortho-substituted benzyne. The other six trisubstituted compounds were prepared from conversion reactions of preformed triptycenes. The syntheses of the starting materials 1,8-dicyanoanthracene, 1,8-dicyanoanthraquinone and anthracene 1,8-dicarboxylic acid were improved from that of literature procedures. A high yield synthesis of a synthetically useful ortho-substituted benzyne precursor, 2-amino-6-(methoxycarbonyl)benzoic acid, was also developed.

The triptycenes were isolated as mixtures of syn (1,8,13) and anti (1,8,16) trisubstituted triptycenes. These were purified by sublimation and separated by HPLC to afford pure isomeric products. The ratio of syn to anti isomers obtained was found to depend on the electrondonating or withdrawing ability of the substituents on the benzyne and anthracene units.

Complexation of the tridentate ligand to an Fe₄S₄ cubane core was investigated by ¹H NMR spectroscopy. Two methods of ligand exchange reactions were used: (1) the (HO)₃-tripod ligand was reacted with $[Fe_4S_4(SEt)_4]^{2-}$ and (2) the trisodium salt of the (HO)₃-tripod ligand was reacted with $[Fe_4S_4Cl_4]^{2-}$. Proton magnetic resonance spectra show isotropically shifted peaks that are mainly contact in origin and occur through a π delocalization mechanism. The paramagnetically shifted resonances were assigned by comparison of chemical shifts with those reported for previously known iron-sulfur clusters. Evidence of free ligand was observed in the spectra, suggesting that in highly-coordinating solvents the (HO)₃-tripod ligand is labile and is being displaced by solvent. Analysis of the proton resonances indicated that a mixture of tetrameric (Fe₄S₄) and hexameric (Fe₄S₄) forms of the ligated cluster are generated in solution.

The ratio of tetrameric species to hexameric species was altered by changing the ratio of ligand to cluster in the NMR samples. The $(HO)_3$ -tripod ligand binds to form a mixed-ligand $[Fe_4S_4(O_3-\text{tripod})(L)]^{2-}$ (L = SEt, Cl) cluster, but rapidly rearranges to hexameric $[Fe_4S_4(O_3-\text{tripod})_2]^{3-}$ and $[Fe_4S_4(O_3-\text{tripod})(L)_3]^{3-}$ (L = SEt, Cl) complexes. The results presented in this dissertation show that under the reaction conditions used, oxygen ligation stabilizes the hexameric Fe-S species.

In addition to investigating a mixed-ligand cluster as a possible model for P-clusters, an oxygen-ligated model of the FeMo-cofactor was prepared. A linear Mo-Fe-S cluster with acetate ligands,

[Et₄N]₂[S₂MoS₂Fe(OAc)₂], was synthesized by reacting [Et₄N]₂[MoS₄] with Fe(OAc)₂. In solution the oxygen ligands are labile, and

conversion to $[Fe(MoS_*)_2]^{3-}$ was observed. The optical spectrum of the acetate-ligated dimer exhibits characteristic absorbances of an FeS_2MoS_2 core. The ¹H NMR spectrum shows a paramagnetically shifted methyl resonance, and variable temperature studies indicate Curie Law magnetic behavior. Magnetic susceptibility measurements shows simple paramagnetism that follows the Curie Law, in agreement with the NMR data. An effective moment of 4.96 μ_B was observed and is consistent with an S=2 system, and indicates an Fe(II)-Mo(VI) couple. The magnetic properties of this cluster show no major differences from that of the chloro- or phenoxide-ligated dimers. The FeS_2MoS_2 unit may resemble a structural portion of the cofactor, although a simple linear array does not agree with preliminary physical data obtained on the enzyme¹¹. The study of this compound has served to extend the general knowledge of iron-molybdenum-sulfur clusters of this type.



REFERENCES

- Hardy, R. W. F.; Burns, R. C. "Iron-Sulfur Proteins"; Lovenberg,
 W., Ed.; Academic Press: New York, 1973; Vol. 1, pp 65-110.
- 2. Holm. R. H.; Ibers, J. A. "Iron-Sulfur Proteins"; Lovenberg, W., Ed.; Academic Press: New York, 1977; Vol. 3, pp 206-281.
- Orme-Johnson, W. H.; Davis L. C.; Henzl, M. T.; Averill, B. A.;
 Orme-Johnson, N. R.; Munck, E.; Zimmerman, R. "Recent Developments in Nitrogen Fixation"; Newton, W. E., Postgate, J.,
 Rodriquez-Barrueco, J., Eds.; Academic Press: New York, 1977;
 pp 131-178,.
- Orme-Johnson, W. H.; Davis, L. C. "Iron-Sulfur Proteins";
 Lovenberg, W., Ed.; Academic Press: New York, 1977; Vol. 3,
 pp 15-60.
- 5. Shah, V. K.; Brill, W. J. Proc. Natl. Acad. Sci. USA 1977, 74, 5468.
- Wang, G. B.; Kurtz, D. M.; Holm, R. H.; Mortenson, L. E.;
 Upchurch, R. G. J. Am. Chem. Soc. 1979, 101, 3078.
- Zimmerman, R.; Munck, E.; Brill, W.; Shah, V.; Henzl, M.;
 Rawlings, J.; Orme-Johnson, W. H. Biochim. Biophys. Acta 1978,
 537, 185.
- 8. Averill, B. A. Structure and Bonding 1983, 53, 61.
- 9. Orme-Johnson. W. H.; Lindahl, P. A.; Nelson, M. J. "Advances in Inorganic Biochemistry"; Eichhorn, G., Marzilli, L., Eds.; Elseveir Biomedical: New York, 1981; Vol. 4, pp 1-35.

- 10. Lehninger, A. L. "Biochemistry"; Worth: New York, 1975; pp 720-725.
- 11. Coucouvanis, D. Acc. Chem. Res. 1981, 14, 201.
- Cramer, S. P.; Hodgson, K. O.; Gillum, W. O.; Mortenson, L. E.;
 J. Am. Chem. Soc. 1978, 100, 3398.
- Cramer, S. P.; Gillum, W. O.; Hodgson, K. O.; Mortenson, L. E.;
 Stiefel, E. I.; Chisnell, J. R.; Brill. W. J.; Shah, V. K.
 J. Am. Chem. Soc. 1978, 100, 3814.
- Antonio, M. R.; Teo, B.-K.; Orme-Johnson, W. H.; Nelson, M. J.;
 Groh, S.; Lindahl, P. A.; Kauzlarich, S. M.; Averill, B. A.
 J. Am. Chem. Soc. 1982, 104, 4703.
- Rawlings, J.; Shah, V. K.; Chisnell, J. R.; Brill, W. J.;
 Zimmerman, R.; Munck, E.; Orme-Johnson, W. H. J. Biol. Chem.
 1978, 253, 1001.
- 16. Munck, E.; Rhodes, H.; Orme-Johnson, W. H.; Davis, L. C.;
 Brill, W. J.; Shah, V. K. Biochem. Biophys. Acta 1975, 400, 32.
- 17. a.) Huynh, B. H.; Henzl, M. T.; Christner, J. A.; Zimmerman, R.; Orme-Johnson, W. H.; Munck, E. Biochim. Biophys. Acta 1980, 623, 124. b.) Johnson, M. K.; Thomson, A. J.; Robinson, A. E.; Smith, B. E. Biochim. Biophys. Acta 1981, 671, 61.
- 18. Orme-Johnson, W. H.; Lindahl, P. A.; Meade, J.; Warren, W.;
 Nelson, M.; Groh, S.; Orme-Johnson, N. R.; Munck, E.; Hunyh, B.;
 Emptage, M.; Rawlings; Smith, J.; Roberts, J.; Hoffmann, B.;
 Mims, W. B. J. "Current Perspectives in Nitrogen Fixation";
 Gibson, A. H., Newton, W. E., Eds.; Auatralian Academy of
 Science: Canberra, 1981; pp 79-83.

- a.) Tieckelmann, R. H.; Silvis, H. C.; Kent, T. A.; Huynh, B. H.; Waszczak, J. V.; Teo, B.-K.; Averill, B. A. J. Am. Chem. Soc. 1980, 102, 5550.
 b.) Coucouvanis, D.; Simhon, E. O.; Swenson, D.; Baenziger, N. C. J. Chem Soc. Chem. Comm. 1979, 361.
 c.) Coucouvanis, D.; Stremple, P.; Simhon, E. D.; Stremple, P. P. J. Am. Chem. Soc. 1983, 105, 5767.
- a.) Muller, A.; Tolle, H,-G.; Bogge, H. Z. Anorg. Allg. Chem.
 1980, 471, 115. b.) Muller, A.; Jostes, R.; Tolle, H.-G.;
 Trautwein, A.; Bill, E. Inorg. Chim. Acta 1980, 46, L121.
- a.) Silvis, H. C.; Averill, B. A. Inorg. Chim. Acta, 1981, 54,
 L57. b.) Teo. B.-K.; Antonio, M. R.; Tieckelmann, R. H.;
 Silvis, H. C.; Averill, B. A. J. Am. Chem. Soc. 1982, 104, 6126.
- 22. Zhuang, B.; McDonald, J. W.; Newton, W. E. Inorg. Chim. Acta 1983, 77, L221.
- 23. Coucouvanis, D.; Simhon, E. D.; Stremple, P.; Baenziger, N. C. Inorg. Chim. Acta 1981, 53, L135.
- 24. Coucouvanis, D.; Simhon, E. D.; Baenziger, N. C.; Stremple, P.; Swenson, D.; Kostokas, A.; Simopulos, A.; Petrouleas, V.; Papaefthymiou, V. J. Am. Chem. Soc. 1980, 102, 1730.
- 25. Garner, C. D.; Acott, S. R.; Christou, G.; Collison, D.; Mabbs,
 F. E.; Petrouleas, V.; Pickett, C. J. "Nitrogen Fixation: The
 Chemical-Biochemical-Genetic Interface"; Muller, A., Newton, W. E.,
 Eds., Plenum Press: New York, 1983; pp 245-273.
- Coucouvanis, D.; Baenziger, N. C.; Simhon, E. D.; Stremple,
 P.; Swenson, D.; Somopoulos, A.; Kostikas A.; Petrouleas, V.;
 Papaefthymiou, V. J. Am. Chem. Soc. 1980, 102, 1732.
- 27. Tieckelmann, R. H.; Averill, B. A. Inorg. Chim. Acta 1980, 46, L35.

- a.) Coucouvanis, D.; Simhon, E. D.; Baenziger, N. C. J. Am. Chem. Soc. 1980, 102, 6644.
 b.) McDonald, J. W.; Freisen, G. D.;
 Newton, W. E. Inorg. Chim. Acta 1980, 46, L79.
 c.) Friesen, G. D.;
 McDonald, J. W.; Newton, W. E.; Euler, W. B.; Hoffmann, B. M.
 Inorg. Chem., 1983, 22, 2202.
- 29. Dahlstrom, D. L.; Kumar, S.; Zubieta, J. J. Chem. Soc. Chem. Comm. 1981, 411.
- 30. Bose, K. S.; Lamberty, P. E.; Kovacs, J. A.; Sinn, E.; Averill, B. A. Polyhedron 1986, in press.
- 31. a.) Wolff, T. E.; Berg, J. M.; Warrick, C.; Hodgson, K. O.;
 Holm, R. H.; Frankel, R. B. J. Am. Chem. Soc. 1978, 100, 4630.
 b.) Wolff, T. E.; Berg. J. M.; Hodgson, K. O.; Frankel, R. B.;
 Holm, R. H. J. Am. Chem. Soc. 1979, 101, 4140.
- a.) Christou, G.; Garner, C. D.; Mabbs, F. E.; King, T. J.
 J. Chem. Soc. Chem. Comm. 1978, 740. b.) Christou, G.; Garner,
 C. D.; Mabbs, F. E.; Drew, M. G. B. J. Chem. Soc. Chem. Comm.
 1979, 91. c.) Acott, S. R.; Christou, G.; Garner, C. D.; King,
 T. H.; Mabbs, F. E.; Miller, R. M. Inorg. Chim. Acta 1979, 35,
 L337. d.) Christou, G.; Garner, C. D.; Miller, R. M.; Johnson,
 C. E.; Rush, J. D. J. Chem. Soc. Dalton Trans. 1980, 2364.
- 33. Cleland, W. E.; Averill, B. A. Inorg. Chim. Acta 1985, 107, 181.
- Wolff, T. E.; Berg. J.M.; Power, P. P.; Hodgson, K. O.; Holm,
 R. H.; Frankel, R. B. J. Chem. Soc. 1979, 101, 5454.
- a.) Christou, G.; Garner, C. D. J. Chem. Soc. Dalton Trans.
 1980, 2354. b.) Christou, G.; Mascharak, P. K.; Armstrong, W. H.;
 Papaefthymiou, G. C.; Frankel, R. B.; Holm, R. H. J. Am. Chem.
 Soc. 1982, 104, 2820.

- 36. Armstrong, W. H.; Holm, R. H. J. Am. Chem. Soc. 1981, 103, 6246.
- Armstrong, W. H.; Mascharak, P. K.; Holm, R. H. J. Am. Chem.
 Soc. 1982, 104, 4373.
- 38. a.) Palermo, R. E.; Singh, R.; Baskin, J. K.; Holm, R. H.
 J. Am. Chem. Soc. 1984, 106, 2600. b.) Palermo, R. E.;
 Holm, R. H. J. Am. Chem. Soc. 1983, 105, 4310. c.) Mascharak,
 P. K.; Armstrong, W. H.; Mizobe, Y.; Holm, R. H. J. Am. Chem.
 Soc. 1983, 105, 475.
- 39. Coucouvanis, D.; Kanatzidis, M. G. J. Am. Chem. Soc. 1986, 108, 337.
- 40. a.) Laskowski, E. J.; Frankel, R. B.; Gillum, W. O.;
 Papaefthymiou, G. C.; Renaud, J.; Ibers, J. A.; Holm, R. H.
 J. Am. Chem. Soc. 1978, 100, 5322. b.) Laskowski, E. J.;
 Reynolds, J. G.; Frankel, R. B.; Foner, S.; Papaefthymiou, G. C.;
 Holm, R. H. J. Am. Chem. Soc. 1979, 101, 6562. c.) Stepan, D. W.;
 Papaefthymiou, G. C.; Frankel, R. B.; Holm, R. H. Inorg. Chem.
 1983, 22, 1150.
- 41. Berg, J. M.; Hodgson, K. O.; Holm, R. H. J. Am. Chem. Soc. 1979, 101, 4586.
- 42. Hagen, K. S.; Watson, A. D.; Holm, R. H. Inorg. Chem. 1984, 23, 2984.
- 43. Cotton, F. A.; Wilkinson, G. "Advanced Inorganic Chemistry:

 A Comprehensive Text"; John Wiley and Sons: New York 1980;

 pp 759.
- Coucouvanis, D.; Kanatzidis, M. G.; Simhon, E.; Baenziger, N. C.
 J. Am. Chem. Soc. 1985, 107, 1874.

- 45. Kanatzidis, M. G.; Baenziger, N. C.; Coucouvanis, D.; Simopoulos, A.; Kostikas, A. J. Am. Chem. Soc. 1984, 106, 4500.
- 46. Johnson, R. W.; Holm, R. H. J. Am. Chem. Soc. 1978, 100, 5338.
- 47. a.) Cleland, W. E.; Averill, B. A. Inorg. Chim. Acta 1981, 56,
 L9. b.) Cleland, W. E.; Holtman, D. A.; Sabat, M.; Ibers, J. A.;
 DeFotis, G. C.; Averill, B. A. J. Am. Chem. Soc. 1983, 105, 6021.
- 48. Kanatzidis, M. G.; Salifoglou, A.; Coucouvanis, D. J. Am. Chem. Soc. 1985, 107, 3358.
- 49. Kanatzidis, M. G.; Coucouvanis, D.; Simopoulos, A.; Kostikas, A.; Papaefthymiou, V. J. Am. Chem. Soc. 1985, 107, 4925.
- 50. Kanatzidis, M. G.; Ryan, M.; Coucouvanis, D.; Simopoulos, A.; Kostikas, A. Inorg. Chem. 1983, 22, 179.
- Johnson, R. E.; Papaefthymiou, G. C.; Frankel, R. B.; Holm, R. H.
 J. Am. Chem. Soc. 1983, 105, 7280.
- 52. Tieckelmann, R. H. "Possible Synthetic Pathways to Models of Metal Cofactors of Nitrogenase"; Michigan State University;

 Masters Thesis 1978.
- 53. Lamberty, P. E. unpublished results.
- 54. Friedman, L.; Logullo, F. M. J. Org. Chem. 1969, 34, 3089.
- 55. House, H. O.; Koepsell, D.; Jaeger, W. J. Org. Chem 1973, 38, 1167.
- Akiyama, S.; Misumi, S.; Nakagawa, M. Bull. Chem. Soc. Japan
 1960, 33, 1293.
- 57. Skvarchenko, V. R.; Shalaev, V. K.; Klabunovski, E. I. Russ. Chem. Rev. 1978, 43, 951.
- 58. Mori, I.; Kodoaka, T.; Yoshiteri, S.; Misumi, S. Bull. Chem Soc. Japan 1971, 44, 1649.
- 59. Fuson, R. C.; Rabjohn, N. Org. Synth. 1955, 3, 557.

- 60. Berger, G.; Olivier, S. C. J. Rev. Trav. Chim. 1927, 46, 600.
- 61. Sharai, H.; Yashiro, T.; Sato, T. Chem. Pharm. Bull. 1969, 17, 1564.
- 62. Trahanovsky, W. S.; Young, L. B. J. Org. Chem. 1966, 31, 2033.
- 63. Holum, J. R. J. Org. Chem. 1961, 26, 4814.
- 64. Sala, T.; Sargent, M. V. J. Chem. Soc. Chem. Comm. 1978, 253.
- 65. Bartlett, P. D.; Ryan, M. J.; Cohen, S. G. J. Am. Chem. Soc. 1942, 64, 2649.
- 66. Pearson, R. E.; Martin, J. C. J. Am. Chem. Soc. 1963, 85, 3142.
- 67. Corey, E. J. Pure Appl. Chem. 1967, 14, 19.
- 68. Waldmann, H.; Oblath, A. Chem. Ber. 1938, 71, 366.
- 69. Akiyama, S.; Misumi, S.; Nakagawa, M. Bull. Chem. Soc. Japan 1962. 35, 1829.
- 70. Nagai, U.; Abe, E.; Sano, R. Tetrahedron 1974, 30, 25.
- 71. "Handbook of Chemistry and Physics"; Weast, R. C., Ed.; CRC Press: Clevland, Ohio, 1975; 56th ed., p D-151.
- 72. Jencks, W. P.; Salvesen, K. J. Am. Chem. Soc. 1971, 93, 4433.
- 73. Piper, J. R.; Stevens, F. J. J. Org. Chem. 1962, 27, 3134.
- 74. Sauer, J.; Sustmann, R. Angew. Chem. Int. Ed. Engl. 1980, 19, 779.
- 75. Exner, O. "Correlation Analysis in Chemistry"; Chapman, N. B.,

 Shorter, J., Eds.; Plenum Press: New York, 1978; pp 439 540.
- 76. Bromilow, J.; Brownlee, R. T. C.; Lopez, V. O.; Taft, T. W. J. Org. Chem. 1979, 44, 4766.
- 77. Topsom, R. D. Acc. Chem. Res. 1983, 16, 292.
- 78. Kidd, K. J.; Kotowycz, G.; Schaeffer, T. Can. J. Chem. 1967, 45, 2155.

- 79. Silverstein, R. M., Bassler, G. C., Morill, T. C. "Spectroscopic Identification of Organic Compounds", 4th ed.; John Wiley and Sons: New York, 1981; pp 264-265.
- 80. Que, Jr., L.; Bobrik, M. A.; Ibers, T. A.; Holm, R. H. J. Am. Chem. Soc. 1974. 96, 4168.
- 81. Dukes, G. R.; Holm, R. H. J. Am. Chem. Soc. 1975, 97, 528.
- 82. Cleland, W. E. "The Synthesis, Characterization and Reactivity of Iron-Sulfur and Molybdenum-Iron-Sulfur Complexes with Phenoxide Terminal Ligands"; Michigan State University; Ph. D. Dissertation 1984.
- 83. Drago, R. S. "Physical Methods in Chemistry"; W. B. Saunders:
 Philadelphia, 1977; pp 436 463.
- 84. Holm, R. H.; Phillips, W. D.; Averill, B. A.; Mayerle, J. J.;

 Herskovitz, T. J. Am. Chem. Soc. 1974, 96, 2109.
- 85. Horrocks, Jr., W. DeW. "NMR of Paramagnetic Molecules.
 Principles and Applications"; LaMar, G. N., Horrocks, Jr.,
 W. DeW., Holm, R. H., Eds.; Academic Press: New York, 1973;
 pp 127 175.
- 86. Cleland, Jr., W. E.; Averill, B. A. Inorg. Chim. Acta 1985, 106, L17.
- 87. Kanatzidis, M. G.; Hagen, W. R.; Dunham, N. R.; Lester, R. K.; Coucouvanis, D. J. Am. Chem. Soc. 1985, 107, 953.
- 88. Bobrick, M. A.; Hodgson, K. O.; Holm, R. H. Inorg. Chem. 1977

 16, 1851.
- 89. Diemann, E.; Muller, A. Coord. Chem. Rev. 1973, 10, 79.

- 90. Tieckelmann, R. H. "The Synthesis and Characterization of the Molybdenum-Iron-Sulfur Clusters [S₂MoS₂FeL₂]²⁻, [S₂MoS₂FeS₂FeL₂]³⁻ and [S₂MoS₂FeS₂FeS₂MoS₂]^{4-"}; Michigan State University; Ph. D. Dissertation 1981.
- 91. Silvis, H. C. "The Synthesis, Characterization and Reactivity of Molybdenum and Tungsten-Iron-Sulfur Complexes"; Michigan State University; Ph. D. Dissertation 1981.
- 92. Wong, G. B.; Bobrick, M. A.; Holm, R. H. Inorg. Chem. 1978, 17, 1093.
- 93. Frankel, M.; Gertner, D.; Jacobson, H.; Zilkha, A. J. Chem. Soc. 1960, 1390.
- 94. Hardt, V. H. D.; Moller, W. Z. Anorg. Allg. Chem. 1961, 313, 57.
- 95. Golden, R.; Stock, L. M. J. Am. Chem. Soc. 1972, 94, 3080.

